Universitat Autònoma de Barcelona

Development of therapeutic strategies for amyotrophic lateral sclerosis

Maria Puigdomenech Poch

Development of therapeutic strategies for amyotrophic lateral sclerosis

Presented by Maria Puigdomenech Poch

ACADEMIC DISSERTATION

To obtain the Degree of PhD in Neuroscience of the

Universitat Autònoma de Barcelona, 2020

Group of Neuroplasticity and Regeneration

Institut de Neurociències

Departament de Biologia Cel·lular, Fisiologia i Immunologia

Directed by:

Rubèn López Vales

Tutorized by:

Xavier Navarro Acebes

INDEX

Summary

Amyotrophic lateral sclerosis (ALS) is a devasting neurodegenerative disorder with no effective treatment currently available. This neurodegenerative disease is characterized by the progressive loss of both upper and lower motoneuron (MN) which leads to muscle weakness and death. The specific molecular mechanisms underlying MN death are not fully known yet. However, several dysfunctional mechanisms that occur in MNs and the surrounding cells, such as, oxidative stress, inflammation or aggregation of aberrant proteins like superoxide dismutase 1 (SOD1), contribute to this pathology.

In this thesis, we studied the therapeutic potential of two different strategies for ALS disease: (i) to increase the efficiency of antisense oligonucleotides (ASO) technology in silencing mutant SOD1; (ii) to modulate the LPA-LPA_2 axis.

In the first chapter, with the aim to reduce the RNA levels of the mutant *SOD1*, we administrated ASO conjugated to several ligands for serotonin and serotonin/dopamine receptors in order to increase the cellular internalization of the molecule. The results presented here reveal that this approach is able to enhance the silencing of mutant SOD1 as compared to naked ASO. However, single administration of this conjugated ASO failed to ameliorate disease symptomatology in $SOD1^{G93A}$ mice.

Since inflammation is a hallmark of most neurological conditions, including ALS, and LPA contributes to the neuroinflammation after central nervous system injury, in the second chapter of this thesis we studied whether the modulation of the LPA-LPA_2 axis mediates beneficial actions in ALS. Our results reveal that the genetic deletion of LPA_2 delays the onset and progression of ALS disease and prevents muscle atrophy.

Collectively, the results presented here provide novel insight about future therapeutic strategies for ALS.

Abbreviations list

ALS: Amyotrophic lateral sclerosis

AMPA: α-amino-3-hydroxy-5-methly-4-isioxazolepriopionic acid

ASGPR: Asialoglycoprotein

ASO: Antisense oligonucleotides

ATP: Adenosine triphosphate

ATX: Autotaxin

BBB: Blood brain barrier

CAMP: Compound muscle action potential

ChAT: Choline acetyltransferase

CLZ-Alkyl: Clozapine

CNS: Central nervous system

CSF: Cerebrospinal fluid

CST: Corticospinal tract

DAG: Diacylglycerol

DHT: 2,3-Dichlorophenylpiperazine

DHT: Dihydroxytryptamine

DNA: Deoxyribonucleic acid

EAAT2: excitatory amino acid transporter 2

ER: Endoplasmic reticulum

fALS: Familial amyotrophic lateral sclerosis

FDA: Food and drug administration

FF: Fast motor unit

FR: Fast-glycolytic fatigable motor unit

FTD: Frontotemporal dementia

FUS: Fused in sarcoma

GalNac: N-Acetylgalactosamine

GFAP: Glial fibrillary acidic protein

GPCRs: G protein-coupled receptors

i.m: Intramuscular injection

i.p: Intraperitoneal injection

IBA1: Ionized calcium-binding adapter molecule 1

ICV: Intracerebroventricular injection

IT: Intrathecal injection

LPA: Lysophosphatidic acid

LPL: Lysophospholipids

MEP: Motor evoked potentials

MN: Motoneuron

mRNA: Messenger ribonucleic acid

MUNE: Motor unit number estimation

MyHC: Myosin heavy chain

NDS: Donkey serum

NF200: Neurofilament 200

NMJ: Neuromuscular junction

PA: Phosphatidic acid

PB: Phosphate buffer

PC: Phosphatidylcholine

PE: Phosphatidylethanolamine

PET: Positron emission tomography

PFA: Paraformaldehyde

PLA2: Phospholipase A2

PS: Phosphatidylserine

PS: Phosphatidylserine

PS: Phosphorothioate

RNA: Ribonucleic acid

ROS: Reactive oxygen species

RT: Room temperature

S: Slow-oxidative motor unit

sALS: Sporadic amyotrophic lateral sclerosis

SC: Spinal cord

SERT: Serotonin transporter

SMUP: Single motor unit potential

snRNA: Small nuclear RNA

SOD1: Superoxide dismutase one

SSRI: Serotonin reuptake inhibitors

SU: Single motor unit size

TDP43: TAR DNA-binding protein 43

TLR: Toll-like receptor

UPR: Unfolded protein response

WT: Wilde-type

INTRODUCTION

1. RELATIONSHIP BETWEEN THE NERVOUS SYSTEM AND THE MOTOR SYSTEM

Any type of body movement, such as dancing, writing or breathing, either it is voluntary or involuntary, is produced by spatial and temporal patterns of muscular contractions orchestrated by neuronal circuits in the central nervous systems (CNS). All these movements, mostly produced by skeletal muscles are controlled, ultimately, by a specific type of neuron called lower motoneuron (MN). The cell bodies of the lower MN are located in the spinal cord and brainstem and their axons innervate skeletal muscles through the peripheral nerves. Lower MN are controlled directly by neuronal local circuits that coordinate individual muscle groups, and indirectly, by neurons located in the motor cortex and brainstem, that are known as upper MN. This enables and coordinates complex sequences of movements. Upper MN, in turn, are modulated by neural circuits located in basal ganglia and cerebellum which are the responsible to modulate the performance of movement with spatial and temporal precision (Figure 1).
In the field of motor control, we must add the role of the sensory inputs. These include extrinsic information about the state of the environment, as well as, intrinsic information about our body. These data allow the construction of a sensory representation that is the framework in which the motor system plans, coordinates and executes the movements (Kandel, E; 2000).

In summary, this is how the control of the movement works. It is a constant dialogue between the muscle, the sensory inputs and the CNS, in which MNs are the principal characters.

1.1 THE MUSCLE

Gross anatomy and classification of the muscles

The movement is generated by specialized cells called muscle cells. Depending on the structure and control mechanisms, muscles can be classified in three different types: skeletal, cardiac and smooth. Some muscle cells show a regular pattern of alternating light and dark bands that extend across the width of the fiber. These are called striated muscle cells. Striated cells form the type of muscle associated with the skeleton and heart and, therefore, form the skeletal and cardiac muscle, respectively. Not all muscle

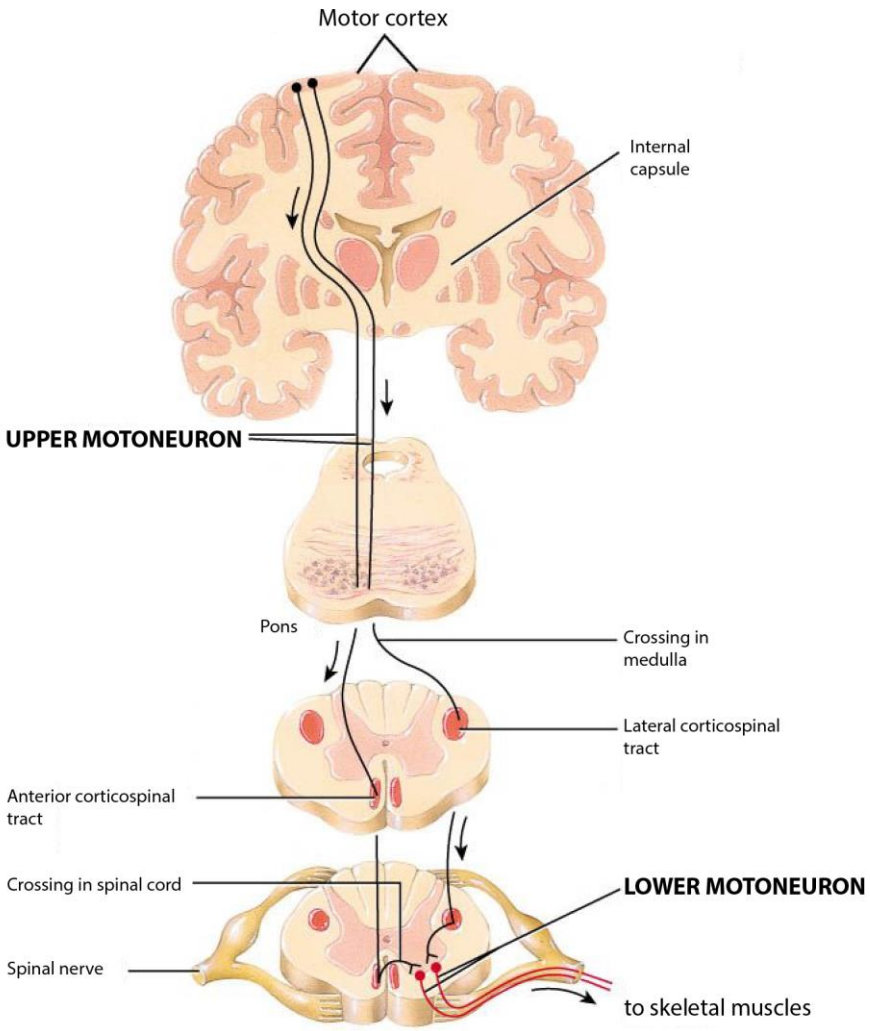

Figure 1. Central nervous system orchestred body movement. Upper motoneuron, in this diagram represented in cerebral cortex, by descending tracts control indirectly the lower motoneuron. Lower motoneurons has their soma in the spinal cord and their axons leave the central nervous system to innervate skeletal muscles.

cells are striated. Indeed, muscle cells surrounding hollow organs and blood vessels lack cross-striations and are known as smooth muscle cells. According to control mechanisms, muscles can be contracted under the voluntary or involuntary control. Contraction of skeletal muscle is initiated by action potentials in lower MN, and is usually under voluntary control. However, smooth and cardiac muscle contraction is involuntary. It is autonomously regulated in some cases, but frequently, it occurs in response to signals from the autonomic nervous system, hormones, and autocrine or paracrine signals (Krause JW, 2005).

The skeletal muscle is the most abundant tissue in the human body represents about the 40% of the total weight (Krause JW, 2005). This type of muscle is characterized by its highly ordered cellular structure that provide to the skeletal muscle its principal properties such strength, flexibility and plasticity (Roman and Gomes, 2018). The unit structure of muscle tissue is the muscle cell or also called a fiber or myofiber because of its elongated shape. Groups of parallel fibers form fascicles and, in turn, groups of fascicles make an entire muscle (Figure 2). In skeletal muscles, there is close relationship between the muscle fibers and the connective tissue, responsible for providing the nourishment of the muscle and the transmission of the force. Thus, each striated muscle is surrounded on the outside by a fibrous structure called fascia a dense lamellar connective tissue, which is anchored by epimysium (Li, 2018). Septa pass from the deep surface of the epimysium to invest each fascicle as the perimysium, delicate extensions of the perimysium wrap each fiber as the endomysium. Although given different names according to its association with different structural units of muscle, the connective tissue is continuous from one part to another (Krause JW, 2005). The connective tissue of perimysium consist of collagen, reticular and elastic fibers and contains vessels, nerves and sensory receptors. Endomysium is composed mainly of reticulin fibers (type III collagen) and rare type I collagen fibers, this shape is the support for a numerous blood capillaries and nerve fibers (Li, 2018).

The diameter of skeletal fibers ranges from 10 to 100 μm and may reach a length of 10 cm or even higher. The size varies from muscle to muscle and even within the same muscle. Longer fibers have the greater diameters and are associated with more powerful muscles. Some special arrangement of the fibers within a muscle has been noted. Indeed, fibers of large diameter tend to be located more centrally. Highlight that the size of the fibers is not static since they may undergo changes depending on their use, leading to hypertrophy (increase in diameter) in response to continued use, or atrophy (decreased in diameter) with disuses (Li, 2018).

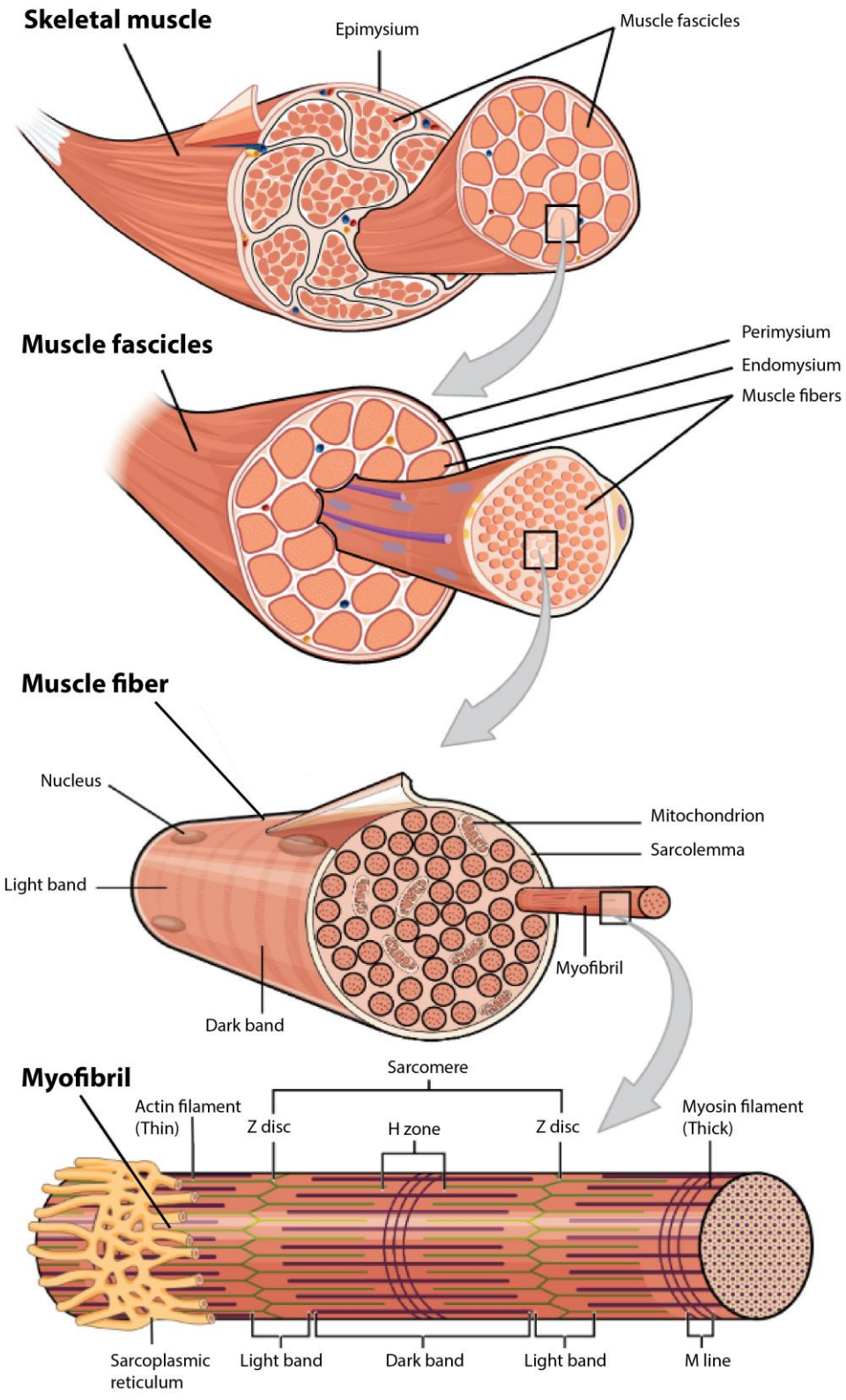

Figure 2. Skeletal muscle gross anatomy and ultrastructure. Skeletal muscle is formed by groups of fascicles. The fascicles, in turn, are formed by groups of parallel fibers, the unit structure of muscle tissue. The fibers are formed by multiple myofibrils, intracellular contractile fibers built from sarcomeres.

Ultrastructure of skeletal muscle

From the ultrastructural point of view the skeletal striated muscle fibers describe all three classical components of a cell: membrane (sarcolemma), cytoplasm (sarcoplasm) and numerous peripheral nuclei. Myofibers are multinucleated cells and may contain up to 100-200 nuclei each fiber, representing the largest cell in the body. Each myofiber contains long, thin and cylindrical rods, called myofibrils which run parallel to the long axis of the muscle fiber occupying most of the intracellular space. As a consequence, cell organelles, like mitochondria and nuclei, are pushed to the periphery of the sarcoplasm (Li, 2018). Myofibrils are intracellular contractile fibers built from sarcomeres joint end to end. One sarcomere unit is delineated on both sides by Z-lines which serve as anchors for perpendicular actin filaments participating in the contraction process. Mid-way between two adjacent z-lines is the M-line. M standing for myosin, this line is an anchor for perpendicular myosin chains that overlap and intercalate in between actin filaments. Contraction of the sarcomere is therefore ruled by an actomyosin mechanism in which myosin heads pull on actin filaments. The cumulative contraction of several sarcomeres accomplishes overall muscles contraction and our ability to move within our environment (Roman and Gomes, 2018).

Classification of skeletal fibers

To deal with divergent activities, muscles are composed of muscle cells with large differences in metabolic profile and contractile properties, found under the influence of hormonal and neural systems. Moreover, it seems that nerve activity plays a major role in the determination of the fiber type. Over time scientist have classified these fibers taking account different characteristics (Li, 2018).

Since the beginning of the nineteenth century, skeletal muscle cells can be distinguished for: (i) their red or white colour, due to high or low concentration of myoglobin, respectively; (ii) fast and slow based on their contractile properties (Li, 2018). In the mid-twentieth century, the combination of histochemical analysis for myofibrillar actomyosin ATPase and for enzymes of energy metabolism gave rise to three main types of skeletal muscle fibers (cells): (i) type I, slow oxidative; (ii) type IIa, fast oxidative and; (iii) type IIb, fast glycolytic (Edstrom and Kugelberg, 1968). However, in the last 40 years the notion of muscle fiber type diversity has rapidly progressed leading to the identification of four major fiber types in adult mammalian skeletal muscles based on *myosin heavy chain* (MyHC) isoforms. Monoclonal antibodies against MyHCs led to the identification of fibers called type 2X (Schiaffino et al., 1989). In rat skeletal muscle, type 2X fibers have the maximal velocity of shortening is intermediate between that of 2A and 2B fibers.

Immunohistochemical and in situ hybridization analyses of muscle sections and biochemical and physiological studies of single fibers confirmed the existence of a spectrum of fiber types with pure or hybrid MyHC composition, according to the following scheme: 1 ↔ 1/2A ↔ 2A ↔ 2A/2X ↔ 2X ↔ 2X/2B ↔ 2B. Nowadays, one knows that these MyHC isoforms are first established by intrinsic myogenic control mechanisms during embryonic development and are later modulated by neuronal (Sieck et al., 1997) and hormonal factors (Larsson et al., 1995). According to a study conducted by Schiaffino, in any muscle, different fiber types coexist (Schiaffino and Reggiani, 2011).

1.2 THE SPINAL CORD

Gross anatomy

The spinal cord (SC) is the part of the central nervous system that controls the voluntary muscles of the limbs and trunk, and which receives sensory information from these regions. It also controls most of the viscera and blood vessels of the thorax, abdomen and pelvis. Anatomically, is the most caudal part of the central nervous system, in humans starts in the base of the brain (after medulla oblongata) and ends in the first lumbar vertebras (Watson et al., 2009).

The spinal cord is a continuous cylinder of central nervous tissue lying within the vertebral canal. Similar to the brain, the SC is protected by the meninges, three membrane layers that envelope the CNS and serves as a physical and functional barrier between the nervous tissue and the surrounding bone. The dura mater is a thick and resistant fibrous layer that strongly adheres to the bone and contains the venous sinuses (Figure 3). The arachnoid layer is a fine fiber network through which the cerebrospinal fluid (CSF) can circulate; it sends protrusions, the arachnoid granulations, into the venous sinus of the dura mater. The pia is a thin and delicate fibrous tissue that is impermeable to fluid. This allows the pia mater to enclose the CSF (Ferry et al., 2014). Forming from these layers are three clinically significant spaces, or potential spaces (sometimes called cavities): the epidural, subdural and subarachnoid spaces, from superficial to deep (Ghannam and Al Kharazi, 2019) . The meninges principal function is cushion the CNS and allow blood vessels to pass through to nourish the tissue.

Over the meninges, the vertebral column follows caudally the skull and is the main responsible to protect the SC. The mammalian vertebral column consist of five morphologically different groups of vertebrae: cervical, thoracic, lumbar, sacral and

coccygeal (Watson et al., 2009). During the development, the vertebral column elongates more rapidly than the SC, so that there is an increasing discrepancy between the anatomical level of SC segments and their corresponding vertebrae (Barson, 1970). The result is that only the cervical segments of the SC are approximately level with their corresponding vertebrae. The cord segments are determined by the pattern of emergence of spinal nerves (Watson et al., 2009). Each cord segment has a pair of dorsal (sensory) and ventral (motor) roots that join to form a mixed spinal nerve just as they leave the vertebral column throught the intervertebral foramin (Catala and Kubis, 2013). Below cervical levels, spinal nerves run increasingly obliquely downwards to their intervertebral foramen. (Watson et al., 2009).

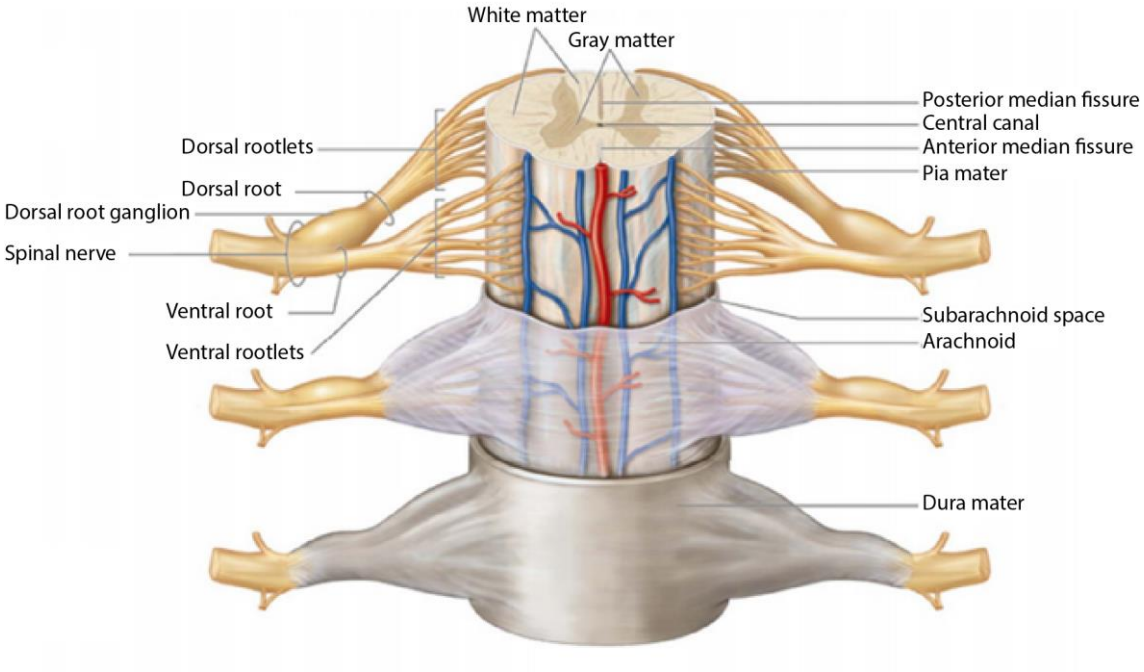

Figure 3. Spinal cord gross anatomy. The spinal cord is a cylinder of central nervous system tissue protected by the meninges and connected to their target organs through the nerves.

Internal organization

The SC consist of longitudinal columns of gray matter, composed principally for neuronal cell bodies, dendrites, axons, glial cells and blood vessels, surrounded by white matter, formed by ascending and descending axons and glia cells (Watson et al., 2009).
A transverse section of SC shows that the gray matter is arranged in the form of butterfly or the capital letter H, depending on the cord level. The dorsally and ventrally projecting arms of the gray matter are called the dorsal and ventral horns (Watson et al., 2009). The cross bar of the H, called the commissural gray matter, encloses the central canal: the remnant of the neural tube central cavity. The central canal is typically a closed space that runs the length of the SC, beginning rostrally from the forth ventricle (Catala and Kubis, 2013).

Gray matter

The neuronal cells of the gray matter are quite heterogeneous, differ considerably in terms of size, shape and density. However, the gray matter does show some intrinsic organization that allows Rexed in 1952 to describe laminae, specific zones of regularity, in the cat SC (Rexed, 1952). Since then, the concept of laminae has been adopted widely for describing the cytoarchitectonic boundaries in the SC in many species. Rexed divided the spinal gray matter into 10 regions, the first nine laminae are arranged from dorsal to ventral. The tenth corresponds a circle of cells surrounding the central canal.

In addition, the laminae are related whit specific functions. The dorsal horn, constituted by laminae I-VI, receive sensory information from primary afferents that innervate skin and deeper tissues of the body. These afferents terminate in the dorsal horn with a distribution pattern that is determined by their sensory modality and the region of the body that they innervate. The incoming information is processed by complex circuits involving excitatory and inhibitory interneurons and is transmitted to projection neurons for relay to several brain areas. In addition nociceptive information is conveyed to the ventral horn and contributes to spinally-mediated nociceptive reflexes (Todd, 2010). Specifically, the laminae I-IV receive mainly information from the cutaneous regions; lamina V receives afferents from the viscera, skin and muscles, and lamina VI is concerned mostly with proprioceptive sensation.

The rest of the laminae, VII to X constitute the ventral horn. Lamina VII contains interneurons that communicate the dorsal ant the ventral horns and mainly act as relay points in the transmission of visceral information. It is also involved in the regulation of

posture and movement. In laminae VII, and to greater extent laminae VIII, are located the lower MN. Laminae VII and IX form the final motor pathway to initiate and modulate motor activity. Finally, lamina X surrounds the central canal and this neurons project to the contralateral side of the SC (Watson et al., 2009).

Motoneuron (MN)

The term MN (lower) is the neuron whose axon innervates muscles. Typically, the axon ramifies into many axon collaterals each of which innervates a single muscle fiber (Barbara and Clarac, 2011). The MNs in the SC belong to two functional groups: somatic and visceral. Somatic MNs innervate skeletal or voluntary muscle, while visceral (autonomic) MNs innervate smooth muscle and glands. Somatic MNs are located in the ventral horn of the gray matter and innervate the striated muscles of the axial skeleton (neck and trunk) and the muscles of the upper and lower limbs. The majority of these MNs are alpha, innervating the extrafusal muscle fibers within skeletal muscle. A smaller proportion of MNs, the gamma, innervate the intrafusal muscle fibers within muscle spindles. A third class of somatic MNs has been described, the beta, which sends axons branches within the muscle to both extrafusal and intrafusal muscle fibers (Watson et al., 2009).

The MNs subtypes are found at all levels of the SC. However, in order to exert their functions in a coordinated manner, they are spatially grouped in a way that reflects both their developmental history and their function in the adulthood. During development, newly postmitotic motor neurons are grouped into motor columns, which stretch along the rostro-caudal extent of the neural tube. In mammals, these are composed of: (i) medial motor column, which projects to epaxial muscles of the dorsal body region; (ii) hypaxial motor column, which projects to hypaxial muscles of the ventral body wall and; (iii) lateral motor columns, which project to the limbs. At thoracic levels, the preganglionic column innervates sympathetic ganglia.

Within a given column, the collective of motor neurons that innervate a single skeletal muscle is defined as a motor pool that contains all types of motor neurons. Within the SC pool organization follow a topological order: more proximal muscles in a limb are innervated by more rostral pools, whereas dorsal and ventral limb muscles are innervated by lateral and medial motor neurons, respectively (Diaz and Morales, 2016).

White matter

The white matter consists mostly of longitudinally running axons that connect the SC to other parts of the CNS, principally supraspinal areas but also other SC levels. The ascending projections transmit information such as pain, temperature, position sense and touch from somatic structures and pressure, pain and visceral information from internal organs to supraspinal structures. Meanwhile descending projections carry commands fort the control of movement and modulate spinal reflex mechanisms and transmission of sensory information. Anatomically, the bundles of axons can be organized in funiculi depending on their location and is due to the horns of the gray matter that white matter is divided into dorsal, lateral and ventral funiculus.

The bundles of axons can be organized in funiculi depending on their location, tracts based on their origin, course and termination and pathway related to their function (Watson et al., 2009).

Descending tracts

The best known of these descending tracts is the corticospinal tract (CST) (Watson et al., 2009). The CST is formed by an uncrossed small bundle located in the anterior region of the SC, known as anterior CST, and a crossed bundle in the dorsolateral aspect of the SC, also known, as the lateral CST (Figure 4). The neuronal origins of the lateral CST are the premotor and primary motor cortex. From here, the bundle decussates at the level of pyramids of the medulla and terminates in a second order neuron (the lower MN) of the contralateral ventral-medial gray matter. It is organized in a somatotopic distribution with the fibers controlling the cervical and upper extremities centrally located and the fibers of the lumbosacral region and lower extremities laterally located. The anterior CST tract does not decussate at the medulla, but instead decussates in the SC through the anterior commissure and is primarily involved in axial and proximal limb motor control (Diaz and Morales, 2016)

Apart from CST, the most prominent descending tracts are those that arise from the red nucleus (rubrospinal), the vestibular nuclei (lateral and medial vestibulospinal) and the hindbrain reticular formation (lateral and medial reticulospinal) (Watson et al., 2009).

Ascending tracts

The most clinically relevant ascending white matter tracts are the posterior and the anterolateral columns. The posterior columns are composed by the cuneate fasciculus that is laterally located and the gracile fasciculus, medially located. As the cuneate

fasciculus carries information from the upper extremities and upper thoracic spine, it is only found in the cervical SC. However, the gracile fasciculus carrying information from the lower and midthoracic spine is found along the entire cord length. The posterior column axons originate in the ipsilateral dorsal root ganglion neurons and ascend to synapse in the gracile and cuneate nuclei of the medulla, respectively. This column conveys proprioceptive, tactile, and vibratory information from the ipsilateral side of the body.

The anterolateral column are collectively referred as the central pain pathway, that contain multiple ascending fibers which the spinothalamic tract is the most important. Other ascending white matter pathway is the spinocerebellar tract, their function is to provide primarily unconscious proprioception (Diaz and Morales, 2016)

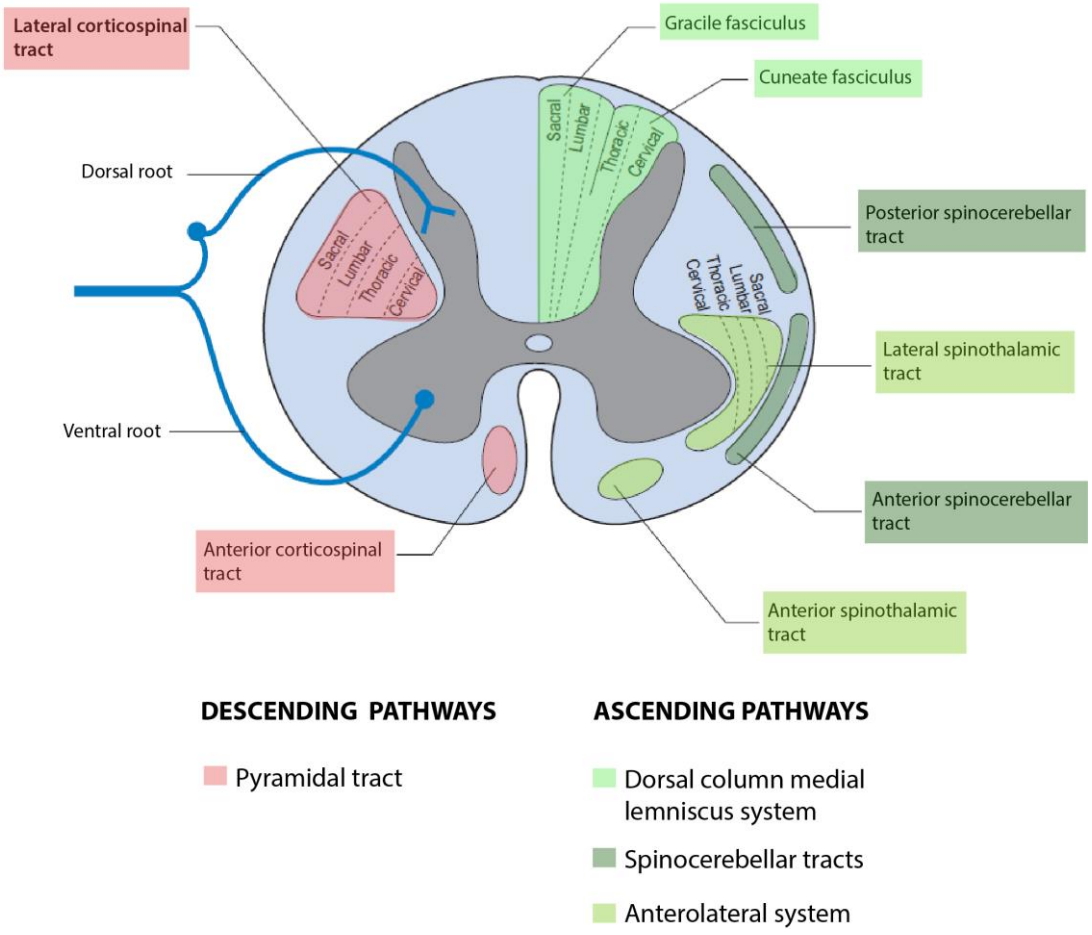

Figure 4. Spinal cord internal organization. The spinal cord is organized in the gray matter, in the diagram with H form, organized on Rexed laminae and the white matter organized on pathways. In the right of the image there is represented the major ascending tracts and, in the left, the descending tracts (Adapted from Harvey, 2008)**.**

1.3 THE MOTOR UNIT

For years the scientist have wondered the relationship between MN and muscle fibers (Barbara and Clarac, 2011). How can an electric impulse traveling through the nerve cause a muscle contraction? Nowadays we know that the answer to this question is a very specific synapses, called neuromuscular junction (NMJ).

The MN axon leave the SC wrapped in a myelin sheath that is lost when arrive to the target muscle. In there, the axon enters the muscle and begin to divide into tens or hundreds of terminal branches, until the nerve reaches the muscle forming the NMJ. The NMJ is a specialized synapse between the motor nerve terminal and the muscle fiber. It's designed to convert the electric impulses from the nerve terminal into muscle contraction by means of neurotransmitter (acetylcholine) release (Hughes et al., 2006). The NMJ is a complex structure that undergoes remodelling during development (Ma et al., 2002) and aging (Deschenes, 2011) and in response to denervation (Nishizawa et al., 2006). At NMJ, the motor nerve terminal is separated from the post-synaptic muscle membrane by a synaptic space containing basal lamina with synapses-specific glycoproteins. On the postsynaptic side, the muscle membrane is highly folded. Acetylcholine receptors are found on the crests of the junctional folds opposing the vesicles release sites on the presynaptic terminal, whereas the voltage-gated sodium channels responsible for action potential generation are densest in the depths of the folds (Hirsch, 2007; Floeter, 2010).

The description of the NMJ elucidated the close relationship between the muscle and the MN, but the identification of the motor unit concept answer the question of how the CNS controls motor output. Charles Sherrington and Edward Liddell were the first physiologist to describe the motor unit concept, they were studding the mechanisms of reflex inhibition in a decerebrate cat when they release that force occurred in discrete steps when muscle contracted. They postulated that each step was produced by the all-or-none action of a single motor neuron upon the muscle fibers it innervated (Liddell and Sherrington, 1925). Since then a motor unit comprises the entire MN and the muscles fibers innervated by the axon (Floeter, 2010) (Figure 5).

The motor unit is composed of a MN and a bunch of muscle fibers with similar, if not identical, structural and functional properties. To form a muscle, many (from tens to hundreds) motor units are assembled together, and each brings its own specific and distinct contribution. Since muscle fibers in a single motor unit are of the same fiber type,

one can apply the fiber designation to the motor unit and refer to (i) slow-oxidative motor units (S; composed by type I fibers); (ii) fast-oxidative-glycolytic resistance motor units (FR, composed by type IIa fibers); (iii) fast-glycolytic fatigable motor units (FF; composed type IIb fibers), and (iv) fast motor units formed by type IIX fibers which show intermediate features of FR and FF. Most skeletal muscles are composed of all four motor unit types interspersed with each other. No muscle has only a single fiber type. Depending on the proportions of the fiber types present, muscles can differ considerably in their maximal contraction speed, strength, and fatigability. For example, the muscles of the back, which must be able to maintain their activity for long periods of time without fatigue while supporting an upright posture, contain large numbers of slow-oxidative fibers. In contrast, muscles in the arms that are called upon to produce large amounts of tension over a short time period, as when a boxer throws a punch, have a greater proportion of fast-glycolytic fibers. Leg muscles used for fast running over intermediate distances typically have a high proportion of fast-oxidative-glycolytic fibers have a greater proportion of fast-glycolytic fibers (Radák, 2018).

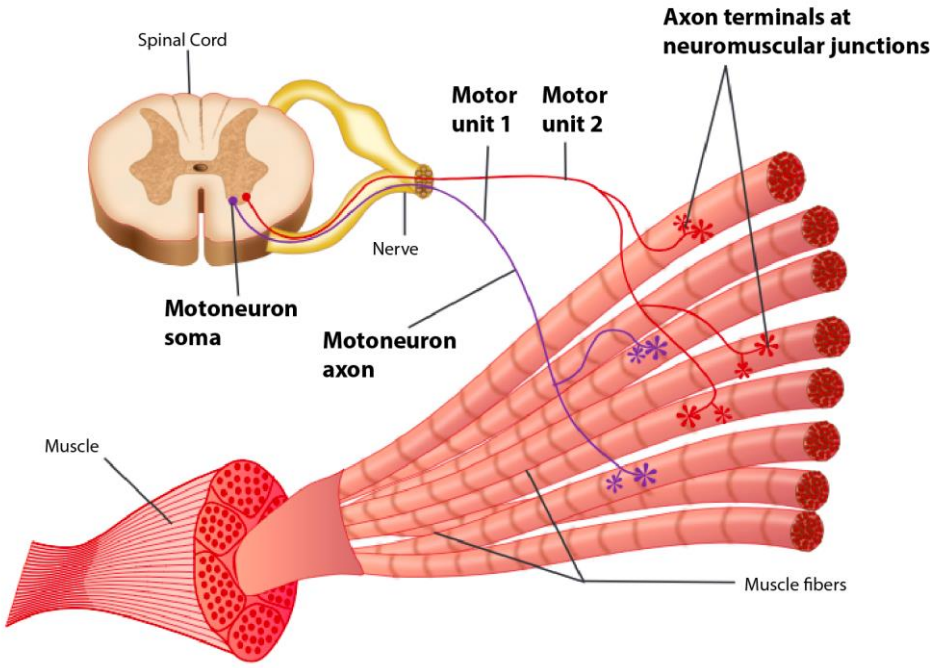

Figure 5. The motor unit. The axon of a motoneuron leave the spinal cord, near the muscle ramified and innervate several muscle fibers, forming a motor unit. The neuromuscular junction is the specialized synapses between the motor nerve terminal and the muscle (Extracted from Carlson, 2013).

2. AMYOTROPHIC LATERAL SCLEROSIS

The name of this disease it is due to Jean-Martin Charcot who, between 1860-1875, was able to link the disease to its pathology and describe the amyotrophic lateral sclerosis (ALS) as a distinct clinical entity. The word amyotrophic is derived from Greek, with "a" meaning no or negative, “myo” meaning muscle, and “trophic” meaning nourishment. Therefore, amyotrophic means "no muscle nourishment ". Lateral refers to the column of the spinal cord where some of the affected motor neurons are located, and sclerosis describes the hardening or scaring that occurs as motor neuron degeneration and death occurs. He identified the sclerosis in the lateral columns of the SC and gray matter as the primary pathology, whereas the amyotrophy was the secondary phenomenon. His choice of the term amyotrophic lateral sclerosis actually reflects this point of view, where sclerosis somehow induced muscle atrophy (Goetz, 2000).

2.1 ALS DESCRIPTION

Epidemiology

The ALS is considered a rare disease. The annual incidence of this pathology in the general European populations ranges from 1 to 3 cases per 100.000 individuals, higher among men (~60%) than women (~40%). Recently a systematic review published that the overall pooled worldwide ALS incidence was 1,75 per 100.000 person for year (Marin et al., 2017). The incidence, however, differs based on ancestral origins, being lower in Asia than in Europe (Marin et al., 2017)**.** ALS diagnosis usually happens between the ages of 40 and 60. Most people get a diagnosis in their mid-50s (Logroscino et al., 2010).

Diagnostic criteria

ALS presents clinically with painless and progressive muscle weakness and atrophy leading to paralysis and eventually to death, usually from respiratory failure. Loss upper MN results in spasticity, hyperreflexia and Hoffman sign. Occasionally the Babinski sign may be present as well. Loss of lower MN results in fasciculations, muscle cramps and muscle atrophy. The clinical hallmark of ALS is the involvement of both upper and lower MN, but no definitive test for the diagnosis is available. The diagnosis relies predominately on the clinical evaluation and is supported by electrophysiological studies, neuroimaging and multiple blood and CSF tests used to exclude other possible diagnoses (Salameh et al., 2015).

According to the Awaji-Shima criteria, the last revision of the El Escorial criteria, diagnosis of ALS depends on identification of upper and lower MN signs within body regions defined as bulbar, cervical, thoracic and lumbar (Al-Chalabi et al., 2016). The Awaji-Shima criteria incorporated a recommendation to use electrophysiological data in the diagnosis of ALS. Specifically, neurophysiological features of lower MN dysfunction, including acute changes such as fibrillation potentials and chronic neurogenic changes markers of unstable motor units (Carvalho and Swash, 2009).

Establishing a diagnosis in the early phases of the disease when symptoms are mild and clinical signs are equivocal may prove challenging. For that reason the diagnostic have an average of delay of 11 to 12 months and at least one incorrect diagnosis in 30 to 50% of cases, there is clearly room for improvement in the diagnostic process (Paganoni et al., 2014). Effort to reduce the diagnostic delay is becoming increasingly important because the administration of treatments in the early stages can be crucial for the progression of the disease.

Clinical presentations and prognosis

ALS present specific phenotypes depending on the site onset of the disease. Its identification has important implications for patients, particularly with regards to prognosis and survival. Approximately 30% of ALS patients present bulbar-onset disease, which is characterized by progressive dysarthria, followed by dysphagia and often associated with emotional lability. Limb-onset disease accounts for 60% of cases and it is usually asymmetrical in presentation of the symptoms, since they can first develop in the upper or lower limbs (Hardiman et al., 2017).

The rate of disease progression among patients is highly variable. The median survival time from disease diagnosis to death ranges from 20 to 48 months, but 10-20% of ALS patients have a survival longer than 10 years (Chiò et al., 2009). Older age symptoms onset, early respiratory muscle dysfunction and bulbar-onset disease are associated with reduce survival, whereas limb-onset disease, younger age at presentation, and longer diagnostic delay are predictors of prolonged survival (Kiernan et al., 2011). With the aim to predict the disease progression, mathematical models have been developed using the information of prognostic factor (Knibb et al., 2016; Elamin et al., 2015; Hothorn and Jung, 2014). Nevertheless, they are quite inefficient and consequently, it is currently very difficult to predict the survival of ALS patients when they are diagnosed.

Symptoms

Spasticity**:** Classically, spasticity has been characterized as velocity-dependent muscle resistance to passive movement resulting from hyperexcitability of the stretch reflex (Lance, 1980) (Figure 6). It has been hypothesized that spasticity may occur due to the loss of upper MN, alterations of intraspinal motor circuitry and/or degeneration of brainstem serotonin neurons (Trompetto et al., 2014; Chang and Martin, 2011; El Oussini et al., 2017). The most commonly used drugs are baclofen and tizanidine, both of which are muscle relaxants (Hardiman et al., 2017).

Hypersalivation: Medically called sialorrhea is more commonly observed in patients with bulbar onset disease and during late disease stages. This can be treated with anti-cholinergic drugs and if pharmacological treatment is inefficient, injections of botulinum toxin A, B or irradiation into salivary glands is recommended (Hardiman et al., 2017). Hypersalivation is caused mostly by a decreased ability to swallow secretions (not by increased saliva production) mainly due to progressive weakness of facial muscles and tongue spasticity (Banfi et al., 2015).

Muscle cramps: Muscle cramps are sustained, painful contractions of muscle and are prevalent in patients with and without medical conditions (Katzberg, 2015). The relationship between the pathophysiology of ALS and cramps is unknown, but neuronal hyperexcitability and the consequence motor unit instability has emerged as a possible central feature. Muscle cramps are the main cause of pain in approximately one-quarter of patients with ALS. Common treatments for muscle cramps include quinine, sulphate, levetiracetam and mexiletine (Stephens et al., 2017).

Pain: Pain is reported by most of the patients with ALS. It occurs at all stages of the disease and can be an onset symptom preceding motor dysfunction. Pain is correlated with a deterioration in patient's quality of life and increased prevalence of depression. Given the multifactorial nature of pain in patients with ALS, different treatments have been suggested, ranging from non-steroidal anti-inflammatory drugs, drugs for neuropathic pain, opioids and cannabinoids, to physical therapy strategies and preventive assistive devices (Chiò et al., 2017).

Dysphagia: The difficulty in swallowing emerges in more than 80% of patients during the advanced phases of the disease. In ALS, dysphagia is related to tongue atrophy, dysfunction in the closure of the soft palate and of the larynx due to the nuclear or supranuclear lesion of the cranial nerves (IX, X, XII) and diaphragm dysfunction (Onesti et al., 2017). Several strategies can reduce the effects of dysphagia in patients, including dietary changes and exercises. However a weight loss of >5% and unsafe swallow are generally considered the criteria to initiate the enteral nutrition by the insertion of a gastrostomy tube (Hardiman et al., 2017).

Dysarthria**:** speech disorder occurs in more than 80% of ALS patients. Initially, dysarthria may be intermittent, presenting as a slight slurring with fatigue or a hoarse voice quality at the end of the day. These intermittent episodes progress as muscles of the lips, tongue and pharynx become weak, slow and limited, resulting in a decreasing intelligibility (Sterling et al., 2010). Loss of communications prevents ALS patients from participating in several activities and leads to social isolation, that significantly reduces their quality of life. Speech therapy can delay the progression of this symptom and communication techniques based on brain-computer interfaces have been developed to enhance the quality of live in the most advances phases of the disease (Linse et al., 2018).

Mood alterations: Depression has been reported in up to 50% of patients with ALS. In general, treated with selective serotonin reuptake inhibitors (SSRI) or tricyclic antidepressants (Thakore and Pioro, 2016).

Cognitive impairment**:** Cognitive impairment, in particular frontotemporal dementia (FTD), is one of the most disabling symptoms in patients with ALS. No pharmacological therapy is effective for the treatment of FTD. However, some symptoms of FTD can be treated; for example, SSRI might help to control the loss of inhibition, overeating and compulsive behaviour, and antipsychotics can reduce restlessness (Hardiman et al., 2017).

Respiratory insufficiency: Nearly all ALS patients develop respiratory symptoms at some point during the disease and respiratory insufficiency is the commonest cause of death. The pathophysiology of this symptom is complex and includes weakness and atrophy of

respiratory muscles and also disfunction in the cortical and brainstem areas involved in the respiratory function (Ahmed et al., 2015). Non-invasive ventilation is the preferred treatment for the symptoms of respiratory failure and can significantly prolong survival and improves the quality of live in patients with ALS (Bourke et al., 2006).

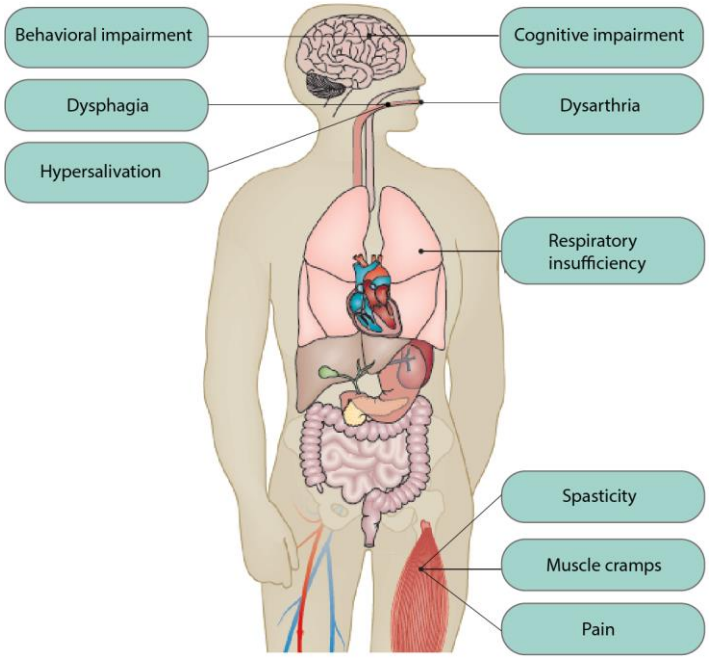

Figure 6. Symptoms of ALS. Motor manifestations are the main clinical manifestations of amyotrophic lateral sclerosis, however the patients also present non-motor symptoms such cognitive impairment (Adapted from Hardiman et al., 2017).

Treatment

Almost 150 years have elapsed since Charcot described ALS, and even the knowledge of the disease is better, nowadays ALS is still an incurable disease with a devastating prognostic. There are only two drugs available in the market for the treatment of ALS. The first approved for the food and drug administration (FDA) was Riluzole, described as an inhibitor of glutamate release, that increase the survival of patients by 3 months (Bensimon et al., 1994). The mechanism of action of Riluzole is still unclear, but it has been speculated to reduce glutamatergic neurotransmission by blocking voltage gate sodium channels on presynaptic neurons (Bensimon et al., 1994). More recently, the FDA of United States approved a second compound named Edaravone, which is thought to act as an antioxidant agent. Edaravone has shown to slow disease progression but only in a highly selected cohort of Japanese patients with early onset and rapidly

progressing disease (Abe et al., 2017). Although the European Medicines Agencies was assessing the approval of the use of Edaravone for the treatment ALS patients in Europe, last May, Mitsubishi Tanabe Pharma GmbH officially notified the Committee for Medicinal Products for Human Use it's wishes to withdraw its application for a marketing authorisation for Radicava (Edaravone) for the treatment of ALS patients.

Molecular genetics

Related to genetics causes, ALS cases are classically subdivided in sporadic forms (sALS) and familial forms (fALS) due to inheritable, mostly autosomal dominant, genetic mutations. The sporadic form constitutes the large majority of cases (90-95%), while the remaining 5-10% are hereditary, the familiar form (Talbott et al., 2016) . This definition is not univocal: the classification of affected individuals may depend on the knowledge of the family history, the technique used to detect mutation and on how penetrant is the disease gene. Thus, it is not surprising that some gene mutations causing fALS are also found in a significant proportion of apparently sporadic cases (Bozzo et al., 2017). For example, it is now evident that 1-3% approximately of sALS cases reflect missense mutations in superoxide dismutase one (*SOD1)* (Gamez et al., 2006) and another 5% or more are caused by intronic expansion in *C9ORF72* (Cooper-Knock et al., 2012). Pathogenic mutations in other ALS gens, also have been identified in the sALS population (Taylor et al., 2016).

Although more than 100 genes confer a major risk of ALS, evidences suggests roles of oligogenic inheritance, in which a phenotypic trait is determined by more than one gene, and of genetic pleiotropy, in which a single gene has multiple phenotypic manifestations (Hardiman et al., 2017). However, four genes account for up to 70% of all cases of familial ALS, namely, *C9ORF72*, *TARDBP* (encoding TAR DNA-binding protein 43, TDP43), *SOD1* and *FUS* (encoding RNA-binding protein FUS). However, the penetrance is different for each gene, mutation or codon. For *SOD1,* some mutations have a higher penetrance (D90A-homozygous and A4V patients) respect others with low penetrance (D90A-heterozygous and N19S patients). Mutations in the *FUS* gene seems to have quite a high penetrance, while those of *TARDBP* probably vary according to the involved codon. Data on *C9ORF72* hexanucleotide expansion show an age-dependent penetrance, of 50% at 60 years and almost a full penetrance at 80 years (Chiò et al., 2014; Andersen, 2006)

2.2 ANIMAL MODELS

The first animal model of ALS was developed after the description of superoxide dismutase 1 (SOD1) mutations in fALS. In 1994 Gurney and colleagues generated a transgenic mouse that constitutively expressed high levels of human mutated SOD1. These animals expressed the protein containing the same mutation described in fALS patients (G93A), a substitution of glycine to alanine at position 93 (Gurney et al., 1994). Since then, more than twenty other SOD1 models have been created to evaluate the mechanisms involved in this pathology since they recapitulate many features described in ALS human patients. The advances in our understanding of the genetic basis have lead to the creation of other models of this disease beyond the SOD1 mice, focused on *TDP43*, *FUS, UBQLN2, VCP*… At least 12 different genes related to ALS have been used to develop rodent models (Van Damme et al., 2017). Furthermore, the genetic engineering technologies of CRISPR/Cas9 provide a new tool to assess these mutations in the context of specific populations (Lutz, 2018). Beyond the rodent model, the researchers are modelling certain aspects of ALS in a range of model systems including *in vitro* biochemical systems, cell culture systems, invertebrates and non-mammalian vertebrates and more recently human patient-derived stem cell models (Van Damme et al., 2017).

The use of these models has increased the knowledge of the mechanisms involved in the pathophysiology of ALS and opened a new avenue to identify novel therapeutic targets for its treatment.

SOD1^{G93A} mice model

Transgenic SOD1^{G93A} mice are the principal mice model used in ALS research, followed by SOD1^{G37R}, because replicates the most relevant phenotypical and histopathological features of the human disease. SOD1^{G93A} transgenic mice develop hindlimb tremor and weakness around 3 months of age, detected by locomotor deficits, the motor clinical signs progress to hyper-reflexia, paralysis and premature death after 4 months. Neuromuscular junctions degenerate, pathologically, around 47 days after birth. Has been reported that proximal axonal loss is prominent by 80 days coinciding with motor impairment and a sever 50% dropout of lower MN at 100 days. SC are also characterised by substantial astrocytosis and microgliosis around disease onset (Turner and Talbot, 2008) Besides, this experimental model present also upper MN degeneration (Marcuzzo et al., 2011). Several lines of transgenic SOD1^{G93A} mice were originally obtained and depending on the transgene copies it is called low or high copy line. In this thesis we

refer to SOD1^{G93A} at the transgenic mice with a high copy number and is predicted to present 25 copies (Turner and Talbot, 2008).

SOD1 involvement in ALS

It was Rosen and their colleagues, which in 1993 identified missense mutations in the gene for the protein SOD1 in patients of fALS, they define for the first time a possible genetic cause of this pathology. SOD1 is homodimer ubiquitously expressed cytosolic metalloenzyme that catalyses the dismutation of the superoxide radicals to molecular oxygen and hydrogen peroxide. Given his dominant inherited role in ALS and the potential role of free radical toxicity in neurodegenerative disease, firstly *SOD1* mutation pathogenesis has been related whit a loss of dismutase activity (Rosen et al., 1993a).

However, posterior studies have extensively shown the involvement of mutated SOD1 in a toxic gain of function, rather than a loss of activity. *SOD1* knockout mice revealed no signs of motor neuron pathology (Reaume et al., 1996). Furthermore, transgenic mice expressing mutations in crucial residues essentials for SOD1 dismutase activity, develop motor neuron disease whit fibrillar inclusions (Wang et al., 2002). In the same line have been described some missense variants that cause *SOD1* ALS and retain full enzymatic activity (Hayward et al., 2002a). Additionally overexpression of mutant protein causes disease in a dose dependent manner, higher expression levels cause earlier onset (Wong et al., 1995).

Several evidences support the gain of toxic function hypothesis:

-Phenotypically, SOD1-related ALS is manifested in the accumulation of amyloid aggregates of misfolded SOD1(Bruijn et al., 2004). Cytoplasmic inclusions in MN and non- neuronal cells were found in SOD1-mediated disease animal models and human patients (Pickles et al., 2016).

-Have been found small granular inclusions positive for SOD1 in SC of sALS (Forsberg et al., 2010).

- Overexpression of wild-type human SOD1 leads to substantial late loss of neurons in the SC ventral horns in mice and it co-expression whit mutant SOD1 exacerbates the disease (Jaarsma et al., 2000).

Mutations identified in the fALS patients may cause SOD1 misfolding by promoting SOD1 demetallation and reducing the stabilizing intrasubunit disulphide bond, thereby lowering the stability of SOD1 monomers or destabilizing the dimer interface. These

mutations may also interfere with SOD1 binding to the copper chaperone for SOD1, which normally recognizes newly synthesized SOD1 and activates it. Thus, in the course of structural transformation, the global stability of SOD1 progressively decrease, such that the misfolded SOD1 eventually precipitates to form amyloid aggregates. The noxious species that arise during this process are yet unidentified, but the soluble monomers and the low-molecular weight SOD1 oligomers that form along the aggregation pathway appear to be particularly attractive candidates. Furthermore SOD1 toxicity may result from the ability of misfolded SOD1 to form aberrant interactions with numerous cellular proteins and interfere with their normal functions (Banerjee et al., 2016)

Nowadays it is accepted that the toxicity of mutant SOD1 is a consequence of one or more acquired adverse properties, a gain of toxic function, but it remains unknown how misfolded SOD1 causes motor neuron death. Soluble misfolded SOD1 species exert several downstream pathophysiological effects including induction of endoplasmic reticulum (ER) stress, defective axonal transport, alteration of motor neuron excitability and mitochondria dysfunction in SOD1 mediate ALS disease models (Pickles et al., 2016).

2.3 ALS PATHOPHYSIOLOGY

The identification of genetic causes in ALS patients allowed us to develop different animal models to study the pathophysiology of ALS disease. Nevertheless, the exact molecular pathway causing MN degeneration in ALS is unknown. However, as it occurs in other neurodegenerative diseases; ALS is probably the result of multiple pathogenic cellular mechanism (Figure 7). The question is which of them are causative and which are consequence of upstream disturbance.

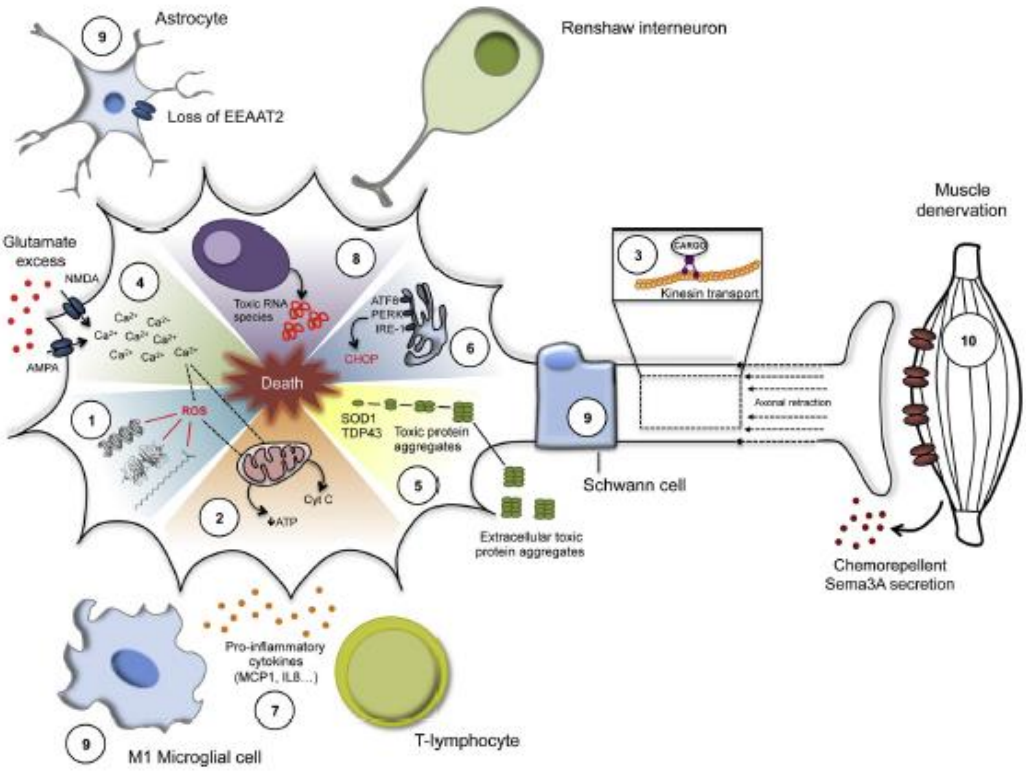

Figure 7. Main pathophysiological mechanisms contributing to motoneuron degeneration of amyotrophic lateral sclerosis. (1) Oxidative stress, (2) mitochondrial dysfunction, (3) impaired axonal transport, (4) excitotoxicity, (5) protein aggregation, (6) endoplasmic reticulum stress, (7) neuroinflammation, (8) abnormal RNA processing, (9) non-neuronal cells and target muscle contribution (Extracted from Mancuso and Navarro, 2015).

Oxidative stress

Oxidative stress results from the imbalance between the production of reactive oxygen species (ROS) and the biological system capacity to remove ROS or repair ROS-induced damage. Evidence for a role of oxidative stress in the pathogenesis of ALS comes from analysis of post-mortem tissues from patients showing a widespread accumulation of oxidative damage to proteins, lipids and deoxyribonucleic acid (DNA) (Ferrante et al., 1997a). Oxidative damage has been also documented in rodent models of the disease (Ferrante et al., 1997b).

Lipids, proteins and DNA are susceptible to oxidative stress, as well as, messenger ribonucleic acid (mRNA). However, studies in SOD1^{G93A} mice demonstrate the significantly increase in lipid, protein and DNA oxidation during the symptomatic stage of the disease. In contrast, mRNA oxidation is reported to occur as early as 45 days of age,

to increase progressively with age and then to drop when MNs begin to degenerate. mRNA oxidation is, therefore, an early event that occurs at pre-symptomatic stage primarily in MNs and oligodendrocytes (Chang et al., 2008)

Mitochondrial dysfunction

Mitochondria are the cellular organelle in charge of adenosine triphosphate (ATP) production, calcium homeostasis maintenance, phospholipid biogenesis and intrinsic apoptosis regulation. Accordingly, dysfunction of this organelle compromises cell metabolism and survival, preferably, in neurons (Smith et al., 2017).

Numerous studies reported mitochondria dysfunction in both ALS patients and animal models in early stages of the disease, suggesting that they may actively contribute to disease progression (Mancuso and Navarro, 2015). Although mutated SOD1 aggregates has been related with the impairment of mitochondria protein import and the interference with anti-apoptotic elements; many others genes identified in ALS patients have been related to mitochondrial functions (Smith et al., 2017).

In addition, the involvement of mitochondria in ALS pathogenesis have been related to dysfunction in bioenergetics, inefficient calcium buffering, induction of mitochondrial apoptosis and defects in mitochondrial transport and morphology (Carrì et al., 2017).

Impairment of axonal transport

Neurons are polarized cells that require mechanisms to direct axonal and dendritical transport. As the cellular metabolism is focused on the cell body, proteins and organelles needed in other parts of the neurons must be delivered correctly to specific compartments. Furthermore, neurons must send signals along long distances, taking in to account that axons of human MN can reach 1 meter long (Mancuso and Navarro, 2015).

It has been reported from ALS patients accumulation of neurofilaments in MN cell bodies (Hirano et al., 1984) and abnormalities of organelle axonal trafficking (Breuer et al., 1987). Impairment of axonal transport was also confirmed in $SOD1^{G93A}$ mice (De Vos et al., 2007). Moreover, mutations in proteins that are essential for axonal transport, such as the dynactin genes (*DCTN*) (Bilsland et al., 2010), profilin (*PFN1*) (Wu et al., 2012)

and tubulin (*TUBA4A*) (Smith et al., 2014) among others, have been identified in sALS, fALS and ALS-FTD families.

The impairment of axonal transport also compromises the correct signal transmission between the MN and the muscle. The loss of viable mitochondria at sites of high energy demand, such the synapse in MN, may result in devastating consequences leading to muscle denervation. Mitochondria transport abnormalities could significantly contribute to dying-back hypothesis, because the distal regions of MN may not be appropriately supplied with healthy and functional mitochondria, while damaged mitochondria may not be correctly turned over (Granatiero and Manfredi, 2019). Indeed, in mutant SOD1 mice deficits in bidirectional transport of mitochondria are described at the pre-symptomatic disease stage suggesting that these alterations may play an early causative role in NMJ degeneration (Bilsland et al., 2010).

Excitotoxicity

Glutamate is the main excitatory neurotransmitter in the CNS. It exerts is effect through the activation of several types of ionotropic and metabotropic receptors. The excitotoxicity results from the excessive activation of glutamate receptors and may be due to the failure in the neurotransmitter clearance from the synaptic cleft or the increased postsynaptic sensitivity to glutamate. This enhanced activation induces massive calcium influx that damages the cell through the activation of calcium-dependent proteases, lipases and nucleases (Mancuso and Navarro, 2015).

The role of excitotoxicity in ALS physiopathology have been observed also in humans. Although there is some discrepancy in the literature, it has been reported that around 40% of ALS patients have increased levels of glutamate in the CSF (Spreux-Varoquaux et al., 2002) and one of the treatments available for the ALS is Riluzole, an anti-glutamatergic agent.

ALS-vulnerable spinal and brainstem MNs are very sensitive to toxicity induced by calcium entry. It has been proved that they have a lower calcium buffering capacity respect ALS resistant MN (Alexianu et al., 1994). Furthermore, this MNs have α-amino-3-hydroxy-5-methly-4-isioxazolepriopionic acid (AMPA) receptors, which are more calcium permeable (Kawahara et al., 2004). In addition, the excitatory amino acid transporter 2 (EAAT2), an astroglial protein that is the main synaptic glutamate reuptake transporter, is impaired in ALS, reducing the glutamate clearance at the synaptic cleft

(Bristol and Rothstein, 1996). These observations support the crucial contribution of the excitotoxicity to ALS disease progression.

Protein aggregation

Most neurodegenerative disease, including ALS, have been related with the presence of protein aggregates as a pathological hallmark. The aggregates usually consist of fibers containing misfolded protein. There is partial but not perfect overlap among the cells in which abnormal proteins are deposited and the cells that degenerate. Some theories postulated that protein aggregates represent an end stage of a molecular cascade of several steps, and that earlier steps in the cascade may be more directly tied to pathogenesis than the aggregates themselves (Ross and Poirier, 2004). However, it remains unknown whether aggregate formation is responsible to cellular toxicity and ALS pathogenesis, or by contrary, it may represent an innocuous or even a protective reaction of the cell to reduce intracellular concentrations of toxic proteins (Mancuso and Navarro, 2015).

The phosphorylated TDP-43 is a major component of theses cytoplasmic protein aggregates and detectable in about 95% of sporadic ALS patients (Oberstadt et al., 2018). Other types of protein aggregates might be observed in specific ALS patients, such as, neurofilamentous hyaline conglomerate inclusions (Schmidt et al., 1987), accumulation of misfolded SOD1 (Shibata et al., 1994), cytoplasm inclusions of FUS (Vance et al., 2013) and ubiquilin 2 (Brettschneider et al., 2012).

Endoplasmic reticulum stress

Accumulation of misfolded proteins, similar to other insults, promotes ER stress response. In the presence of high levels of misfolded proteins in the ER, an intracellular signalling pathway called unfolded protein response (UPR) induces a set of transcriptional and translational events that restore ER homeostasis. However, if ER stress persist chronically at high levels, a terminal UPR program ensures that cells commit to self-destruction. Chronic ER stress and defects in UPR signalling are contributors of several human diseases, including ALS (Oakes and Papa, 2015).

SC samples of humans patients with sporadic ALS show upregulation of UPR indicators (Atkin et al., 2008) suggesting the implication of ER stress in the pathology. In fact, it has

been reported increased UPR in vulnerable MN of SOD1 mice, which are coupled with microglia activation, axonal degeneration and disease progression (Saxena et al., 2009).

Abnormal RNA processing

The implication of impaired ribonucleic acid (RNA) processing as important contributor to the pathophysiology of the ALS was linked after the identification of positive inclusions for ubiquinated TDP-43 in ALS patients (Neumann et al., 2006). TDP-43 is a regulatory protein, whose function is to bind to mRNA transcripts to support their localization, translation and stability, while also play an important role in transcription, alternative splicing and nuclear export (Barton et al., 2019).

Genetic studies discovered in ALS patients several mutations in genes involved in maintaining RNA homeostasis, including *TARDBP* (encoding TDP-43), FUS RNA-binding protein, *C9orf72* and other proteins to a lesser extent (Walsh et al., 2015).

The binding of regulatory proteins to mRNAs, as well as, the accrual of various translation factors, forms an RNA granule. Dysregulation of RNA granule formation has been implicated in neurodegenerative disease. Their involvement ranges from an impaired ability of the RNA granule to sufficiently aid in localization, translation and stability of the mRNAs, to the formation of stress granules, all of which have been implicated in ALS and can initiate a cascade of downstream events predicted to play a role in neuronal decline (Barton et al., 2019).

Changes in ionic conductance

Peripheral axons can be studied applying axonal excitability techniques that provide *in vivo* assessment of axonal membrane excitability and ion channel function (Park et al., 2017). The use of this technics in ALS patients, demonstrated aberrant ionic conductance (Bostock et al., 1995), particularly increased Na^+ and decreased axonal K^+ conductance, a profile that may underline neurodegeneration and contribute to symptoms such as fasciculations and cramps.

Reduction in axonal K^+ conductance would decrease hyperpolarizing tendency while and increase in persistent Na^+ conductance would increase depolarizing. Together, these chances could underline the axon membrane hyperexcitability typical of ALS. Fasciculations reflect ectopic activity in motor axons, in ALS has been linked whit reduction in K^+ conductance (Vucic and Kiernan, 2006). Previous studies documented

ectopic activity arising from the NMJ following presynaptic block of K^+ (Dodson et al., 2003).

In addition, an increase in persistent Na^+ conductance may further contribute to the hyperexcitability of motor axons in ALS, leading to the almost inevitable symptoms of cramps and fasciculations (Vucic and Kiernan, 2006).

Alteration in the neuromuscular junction

The vertebrate NMJ is a “tripartite” synapse, composed by the presynaptic MN, the postsynaptic muscle and the synapse-associated glial cells (terminal Schwann cells, TSCs). Thus, the NMJ is a specialized cholinergic synapse that permits the transmission of action potentials from MNs to muscle. Consequently, impairment of NMJ function results in muscle weakness or paralysis (Campanari et al., 2016).

Several studies report the early functional abnormalities on skeletal muscle pathology in humans sALS (Echaniz-Laguna et al., 2006), fALS (Corti et al., 2009) an mice model of ALS (Derave et al., 2003a). Nevertheless, these abnormalities in skeletal muscle have usually been interpreted as a secondary phenomenon consequence to disease process (Mancuso and Navarro, 2015; Wong and Martin, 2010).

However, in recent years, the “dying-back” hypothesis has obtained much attention in the context of ALS pathophysiology. According to this hypothesis, NMJ show pathological changes, at very early stages of the disease, prior to MN degeneration and the onset of clinical symptoms. Specifically, it proposes that ALS is a distal axonopathy, whereby changes first occur distally at the NMJ itself and progress proximally toward the cell body (Moloney et al., 2014).

To prove this theory Fischer and colleagues performed a comprehensive spatiotemporal analysis of disease progression in $SOD1^{G93A}$ mice, and observed denervation at NMJ by day 47, followed by severe loss of motor axons from ventral root between days 47 and 80, and loss of MNα cell bodies from the lumbar SC after day 80 (Fischer et al., 2004). Furthermore, data from electrophysiological test shows presymptomatic changes in the neuromuscular integrity that could predicted clinical onset and survival in ALS mouse (Mancuso et al., 2014a). Indeed, neuromuscular denervation appears to occur independently to the activation of the cell death pathway in MNs: ALS mice in which MN death is completely abolished by deletion of Bax still develop ALS disease (Gould, 2006). These studies support the idea that neuromuscular denervation and symptom manifestation in ALS can occur regardless of motor neuron survival (Moloney et al.,

2014). Moreover, Wong and colleagues developed a transgenic mouse with muscle restricted overexpression of mutated SOD1 to evaluate the contribution of muscle in MN death. They found that skeletal muscle abnormalities can promote MN degeneration and loss (Wong and Martin, 2010). Currently, it is unknown whether muscle damage is a cause or consequence of MN death in ALS, however the contribution of muscle cells to ALS pathophysiology is clear.

Further analyses revealed that NMJ contribution to ALS pathology might be mediated by "non-guidance" molecules such as galectin-1, secreted from terminal Schwann cells (TSC), and amyloid precursor protein, expressed by damaged muscles fibers that directly promote synapse degradation. Other axon guidance molecules that negatively alter cytoskeletal proteins dynamics and are upregulated in ALS mice, such as semaphorin3A (SEMA3A), expressed by TSCS; NOGO-A, are also expressed by muscle fibers and contribute to ALS (Moloney et al., 2014). Indeed, the differential vulnerability of specific MN populations in ALS could be explained by the distinct pattern expression of these molecules and they involvement in NMJ disintegration. In fact, SEMA3A is produced in TSCs of a particular subset of NMJ, corresponding to the fast-fatigable motor units, those formed by the most vulnerable MN in ALS (De Winter et al., 2006).

Neuroinflammation

ALS, similar to other neurodegenerative diseases, such as Parkinson's disease or Huntington's disease, is characterized by the selective death of certain groups of neurons. Although ALS disease is due to degeneration and death of MNs, several evidences demonstrate non-neuronal cells contribution to MN degeneration and ALS disease progression (Boillée et al., 2006a). The initial evidence that damage within more than one cell types was required, came from the absence of disease when the mutant SOD1 was expressed only in MNs (Lino et al., 2002).

Activation of glial cells located in the vicinity of degenerating neurons is observed in almost all neurodegenerative disease. Many studies have characterised the activation of microglia and astrocytes, and the appearance of lymphocytes in post-mortem tissue of ALS patients (Philips and Robberecht, 2011; Kawamata et al., 1992). The role of glia in ALS pathogenesis gain importance by evidence provided by Cre-Lox recombinase technology. This technic allows to decrease mutant SOD1 levels in specific cell type when the Cre-Lox system is controlled by a selective promoter. For instance, mutant SOD1 can be exclusively removed from microglia and peripheral macrophages in SOD1 mice by crossing a mutant SOD1-lox mouse with a Cre transgene mouse under the

control of the CD11b promoter. The used of these transgenic mice revealed that gene deletion of the mutant SOD1 specifically in microglia and peripheral macrophages markedly slowed ALS disease progression and increased survival in 99 days (Yamanaka et al., 2006). Further works using other examples of genetic and chimeric mouse models elucidated an active role of glial cells in ALS and other neurodegenerative diseases, leaving behind the paradigm that glia cells activation is a secondary phenomenon consequence of neurodegeneration. Since then, the term “neuroinflammation” has been used to describe the key phenomenon involved in the glia-mediated pathology of these diseases (Komine and Yamanaka, 2015) Figure 8).

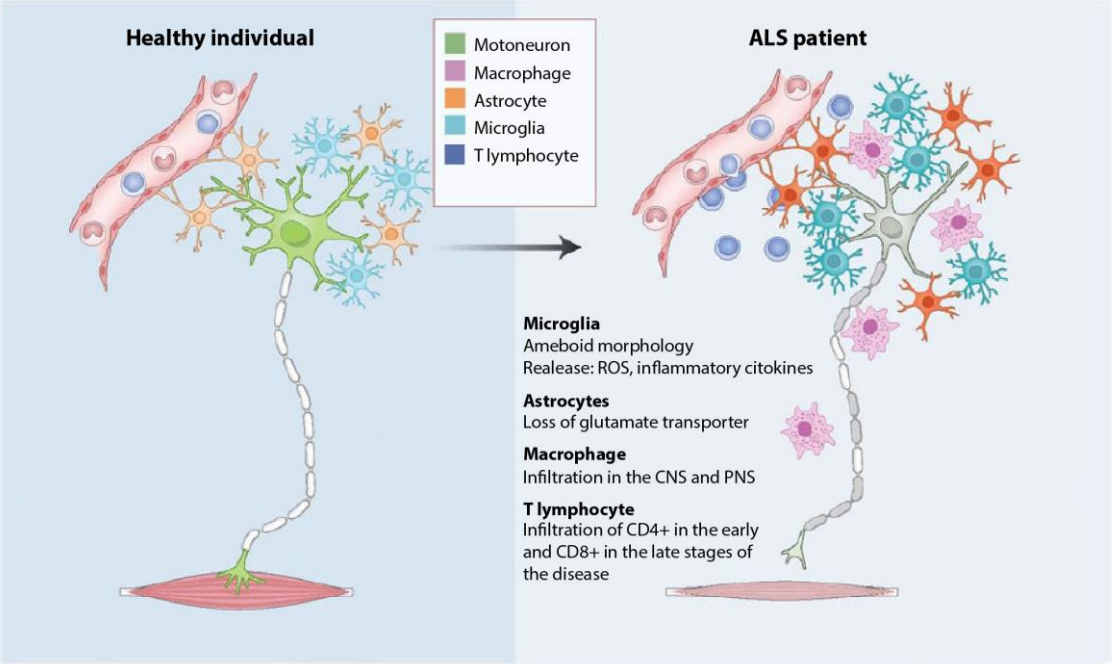

Figure 8. ALS and neuroinflammation. Cross-talk between motoneurons, astrocytes and immune cells (including microglia, macrophages and T lymphocytes) in a healthy individual (left) and an amyotrophic lateral sclerosis patient (right) (Adapted from Rizzo et al., 2014)**.**

Microglia

Microglia are considered the first line of immune defence in the brain and SC. They derived from the hematopoietic cell lineage, their progenitor cells develop in the embryonic yolk sac and then migrate into the CNS during embryogenesis (Ginhoux et al., 2010). At present, many researchers agree that under normal conditions, monocytes and macrophages are not likely to infiltrate into the CNS and become microglia, except when the blood brain barrier (BBB) is damaged. Microglia use their dynamic

arborizations of cellular process to survey continuously the surrounding environment and respond to danger signals. As innate immune cells, microglia react to many types of damage, including microbial infection, microhaemorrhage of blood vessels, immunoglobulin-antigen complexes and misfolded proteins (Komine and Yamanaka, 2015; Liu and Wang, 2017). It has been reported that in ALS, injured MNs and astrocytes release misfolded proteins, which in turn, activate microglia through CD14, toll-like receptor (TLR) 2, TLR4 and scavanger receptor dependent pathways (Roberts et al., 2013). Once activated, microglia change their morphology from ramified to amoeboid form, migrate to the damaged cells and clear the debris of the dead cells by phagocytosis. Through such processes, microglia realease ROS, proinflammatory cytokines, complements and other molecules than can lead to MN toxicity (Komine and Yamanaka, 2015).

Microgliosis has been defined as a hallmark of ALS pathology in humans and animals models. In the brain of living ALS patients, the positron emission tomography (PET) showed microglia activation, with a significant correlation between intensiy of microglia activation in the motor cortex and the severity of clinical deficits (Turner et al., 2004). As reported above, studies in SOD1 mutated transgenic mice have revealed that the replacement of SOD1 mutated microglia with wildtype microglia, as well as, the reduction of the amounts of mutant protein, extend the lifespan of the animals (Boillée et al., 2006b; Beers et al., 2006). Similarly, selective deletion of NF-κB, a transcription factors involved in initiating inflammation, in microglial cells also confers protection against ALS disease (Frakes et al., 2014) further supporting the contribution of microglia to ALS pathogenesis.

Astrocytes

Astrocytes derived from the ectodermal tissue of the developing embryo, particularly the neural tube and crest. These cells are ubiquitous throughout all regions of the CNS. Astrocytes participate in many functions including maintenance of the BBB, ion homeostasis, uptake and turnover of neurotransmitters and formation of synapses (Singh and Joshi, 2017). One of the most important functions of astrocytes is the clearance of glutamate from the synaptic cleft through glutamate transporters (Liu and Wang, 2017). As reported before, excess glutamate in the synaptic cleft results in increased influx of calcium, excessive neuronal firing and may promote neuronal death by glutamate-mediated excitotoxicity (Komine and Yamanaka, 2015). Furthermore other mechanisms have been linked with astrocytes-mediated toxicity by secreting inflammatory mediators such as prostaglandins, leukotrienes, nitric oxide and NADPH

oxidase 2 (NOX2) (Hensley et al., 2006). In sporadic and familiar ALS patients, as well as SOD1 mutant mice, there is loss of glutamate transporter EAAT2/GLT-1. This may lead to less efficient uptake of glutamate by astrocytes and, thus, exacerbate MN degeneration (Rothstein et al., 1995; Howland et al., 2002). Interestingly, selective silencing or blockage of SOD1 mutated gene in astrocytes or transplantation of healthy astrocytes, attenuated astrocyte-mediated toxicity and MN loss, delayed disease progression and prolonged the lifespan of mice, suggesting the pathological role of astrocytes in ALS (Wang et al., 2011; Lepore et al., 2008).

T Lymphocytes

T cells develop in thymus from precursor cells that migrate there from the hematopoietic tissues via the blood. T lymphocytes are the responsible to initiate an adaptative immune response, after the activation by the antigen presenting cells. Once activated, some of the T cells migrate to the site of lesion where they help other phagocytic cells to restore homeostasis in the damage tissue. Other activated T cells remain in the lymphoid organ and help B cells respond to the antigens (Alberts et al., 2002). T lymphocytes can be divided into two major categories, CD4+ and CD8+, which can be identified by their surface expression of either CD4 or CD8 molecules. On one hand, CD4+ T cells acts as "helpers" cells providing signals that induce B cells or CD8+ T cells to proliferate in response to an antigen. CD4+ cells can be divided also into several subtypes defined by specific cytokines produced and functions performed, including Th_1, Th_2, Th_9, Th_{17}, Th_{FH}, and Th_{REG} cells. On the other hand, CD8+ T cells, become cytotoxic T lymphocytes when activated. They initiate a local response that include a lytic attack on target cells and the production of cytokines that can attract inflammatory cells to the local site (Wherry and Masopust, 2016).

The presence of T lymphocytes in SC of ALS patients suggest the involvement of adaptative immunity in ALS (Engelhardt et al., 1993). The studies in $SOD1^{G93A}$ mice reveal the presence of CD4+ T cells in lumbar SC at early stages of the disease, while at end stages both CD4+ and CD8+ T cells are present (Bowerman et al., 2013). To address the role of CD4+ T cells, researchers have used mice model with genetic removal of CD4+ T cells or functional ablation of total T cells. These experiments revealed that the lack of CD4 T cells results in acceleration of ALS progression and increased gliosis (Chiu et al., 2008). In contrast, reconstruction of T cells prolonged survival of SOD1 mutated mice and inhibited the activation of the cytotoxic profile of the microglia (Beers et al., 2008).

It has been also reported alterations in other populations of T cells such as Th_{17} and Th_{REG} in ALS (Beers et al., 2017). However, further research is needed to elucidate their role in the pathophysiology of the ALS.

Monocytes/Macrophages

Monocytes and macrophages are members of innate immunity. Monocytes are bone marrow derived leukocytes that are found in the blood and spleen. They are characterized by their ability to recognize danger signals via pattern recognition receptors. Among their physiological functions, they include the phagocytosis and presentation of antigens, secretion of chemokines and proliferation in response to infection and injury. Once monocytes are recruited to tissues, they differentiate into macrophages and dendritic cells. Macrophages are generally considered terminally differentiated cells that phagocytose pathogens and toxins, secrete chemokines to recruit other immune cells and migrate to local lymph node to present processed antigens (Chiu and Bharat, 2016).

ALS patients have decreased monocyte counts in the peripheral blood. Although some studies suggest that monocytes can enter in the SC of ALS mice and patients (Mantovani et al., 2009). However, studies employing chimeric mice created through parabiosis, a surgical technique in which the vascular systems of two genetically distinct mice are joined, demonstrated that monocytes do not appreciably accumulate within the healthy CNS, and in SOD1 mice (Ajami et al., 2007). Highlight that macrophages do infiltrate in the peripheral nerves of ALS, and their accumulation correlates with disease progression (Chiu et al., 2009). Interestingly, a recent study from our laboratory revealed that macrophages in the peripheral nerve contributes to the course of ALS pathology by accelerating muscle denervation and MN degeneration in a positive feedback loop (Martínez-Muriana et al., 2016).

3.ANTISENSE OLIGONUCLEOTIDE

3.1 GENE THERAPY

The aim of the gene therapy is the modulation of gene expression to treat or prevent diseases. It consists in the administration of a recombinant nucleic acid that can regulate, repair, replace, add or delete a specific genetic sequence. Since its discovery, medicine has been studied this technique for the treatment of several disease, including cancer, cardiovascular disease, ocular disease and neurological disorders (Wirth et al., 2013).

The progression in the field of gene therapy have developed strategies to modify the transfer of genetic information at different levels. Theoretically, each step since DNA transcription until its translation to a protein, is susceptible to intervention by means of gene therapy. The study of the mechanisms involved in the gene expression open a new world where the RNA play an important function in the central dogma of biology (Figure 9) .

While protein-coding sequences have been extensively studied in mammals, this account only for a small fraction of the genome (<2%). In contrast, there is increasing evidence that much (~85%) of the genome is transcribed in to non-coding RNA leading to several species of RNAs that has been described associated whit specific function in translating information from the genetic code to protein products (van Zundert and Brown, 2017a). Small nuclear RNAs (snRNAs) were found to play key roles in the splicing process, microRNAs control translation of targeted mRNAs. The role of RNA has become an interestingly target for therapeutic approaches.

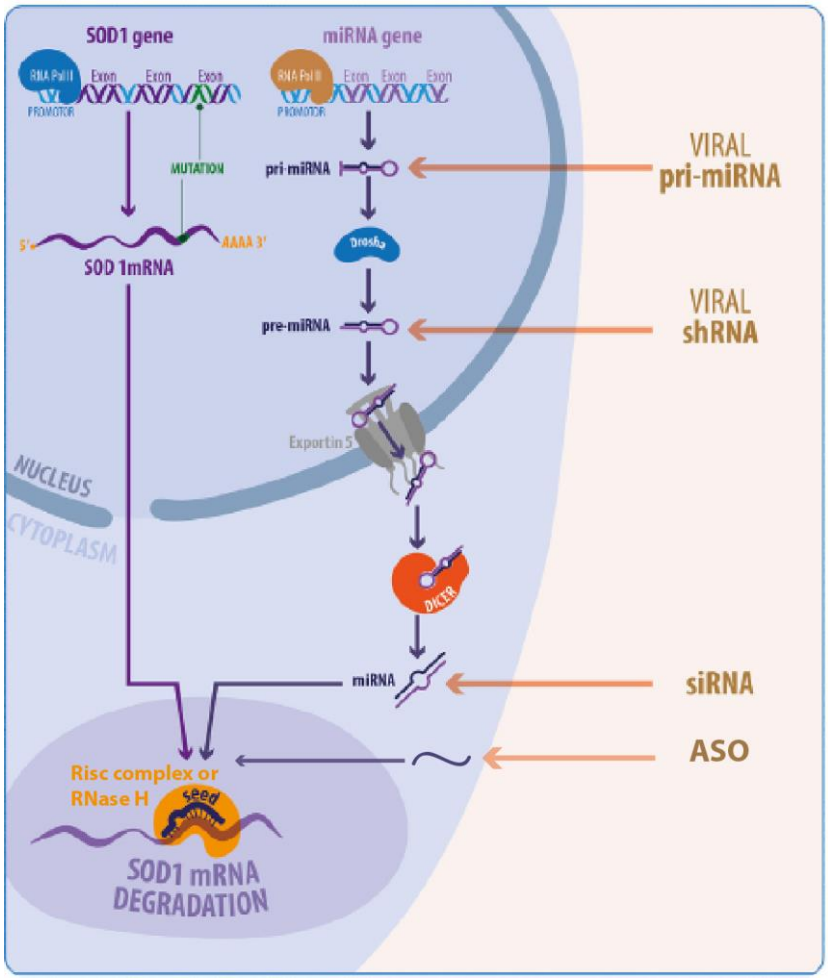

Figure 9. RNA silencing. Endogenous miRNAs biogenesis and use of artificial RNAi approaches to silence SOD1 (Adapted from van Zundert and Brown, 2017)**.**

3.2 ASO STRUCTURE AND CHEMICAL MODIFICATIONS

Antisense oligonucleotides (ASOs) are short, single-stranded whit specific sequence of about 8 to 50 nucleotides, that binds to target RNA and modulate its function. ASOs binds to the target RNA by the well characterized base paring mechanisms first defined by Watson and Crick. This mechanism includes specific hydrogen bonding interactions between bases on the drug and the target RNA strand.

The ASO sequence is designed to be complementary to target RNA, giving a remarkable advantage to this technic; its high accuracy (Bennett and Swayze, 2010). Numerous experiments have demonstrated that ASO exhibit exquisite specificity, capable to distinguishing a single nucleotide mismatch (Monias et al., 1992).

Once the ASO bind to the specific RNA, this can exercise different types of antisense mechanism depending on the chemistry, the design of the oligonucleotide, the site of

union with the RNA, the space inside the cell where they interact and auxiliary factors associated whit the RNA (Bennett and Swayze, 2010).

Unmodified DNA and RNA sequences are unstable molecules in biological systems, due to the ubiquitously expressed nucleases that cleave the phosphodiester linkage. Besides, they are weakly bound to plasma proteins and rapidly filtered by the kidney and excreted. In order to solve this limitation, extensive research has focused on efforts to find chemistry modifications that increased nuclease resistance and maintained or improved affinity to the target and cleavage machinery (Bennett and Swayze, 2010) (Figure 10).

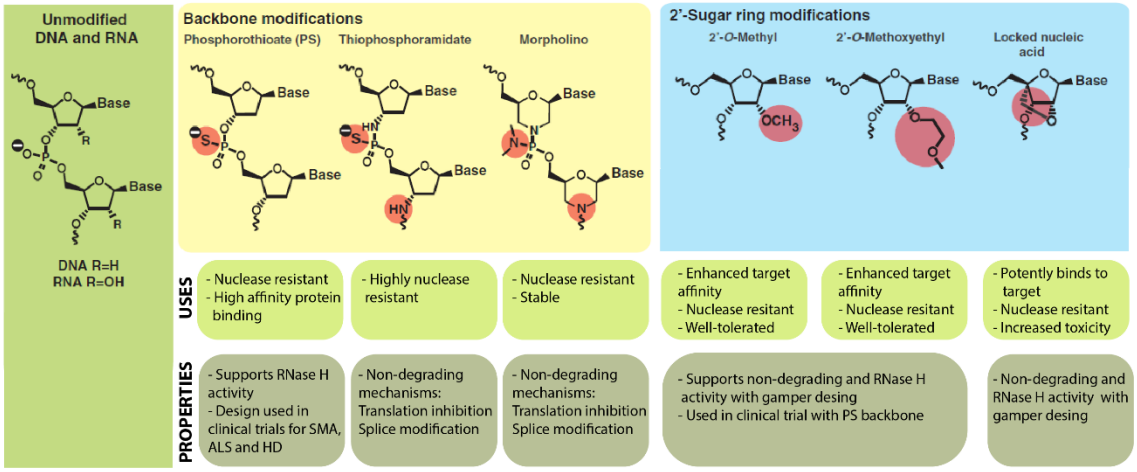

Figure 10. Antisense oligonucleotide chemical structures. The unmodified DNA/RNA base pair need chemical modifications to guarantee their integrity in the biological fluids. Thus has been described different backbone modifications that can be applied and several 2'-sugar modifications that can be used. Deviation from the original unmodified base pair are highlighted in red. Below, there is described the uses and properties of each modification (Adapted from DeVos and Miller, 2013**;** Schoch and Miller, 2017)**.**

One of the first and most commonly used modifications is to replace the singly bonded oxygen group of the phosphate backbone by a sulphur ion, creating a phosphorothioate (PS) linkage. These modifications endow the ASO with enhanced stability and protection against nucleases degradation, increased binding to plasma protein to maintain stable concentrations in serum, better cellular uptake, and the ability to recruit RNase H enzyme for target degradation (Schoch and Miller, 2017). RNase H is a family of enzymes present in all mammalian cells that mediates the cleavage of the RNA in an RNA-DNA heteroduplex. RNase H recognizes and RNA-DNA heteroduplex, cleaving the RNA strand but not the ASO, since the PS backbone protects the ASO against degradation

(Liang et al., 2017). Therefore, the ASO is able to bind to additional target mRNA, enabling sustained mRNA and, in turn, protein reduction (Bennett and Swayze, 2010).

A major disadvantage to the PS backbone is the potential inflammatory response generated at high concentrations (Hartmann et al., 1996). An alternative to PS backbone is the modifications in the 2´position of ribose sugar, that stabilize the ASO minimizing the activation an immune response. An example is the addition of either 2´- O -methyl or 2'-O-methoxyethyl in the 2´position of ribose sugar. These modifications are reported to reduce pro-inflammatory response and to be well tolerated compared to unmodified motifs (Geary et al., 2015). Although 2'-sugar modifications enhance binding to the mRNA target, almost all significantly reduce or even completely obstruct RNase H from cleaving the target RNA. One of the most popular strategies used to solve this limitation has been to adopt the "gamper" design (Figure 11), whereby regions of 2'-modified residues flank a longer central unmodified region. These 2'-modified "wings" further increase binding affinity and nucleases resistance while still allowing the center gap region to recruit RNase H (DeVos and Miller, 2013).

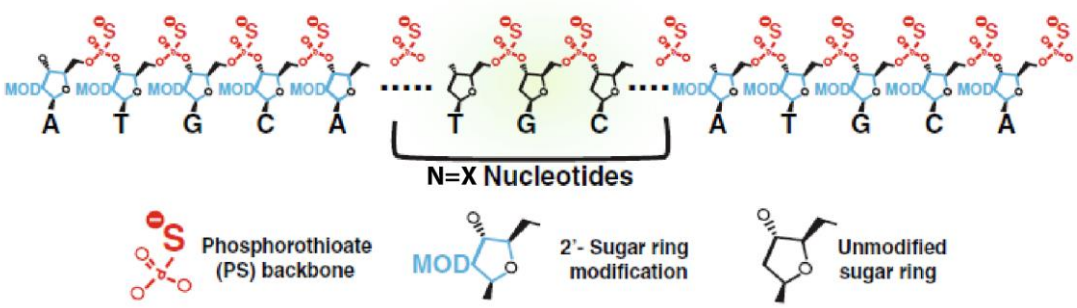

Figure 11. Antisense oligonucleotide "gamper" design. The "gamper" design was described to increase ASO efficiency. The phosphorothioate backbone is used along the entire length of the ASO to provide nuclease resistance, while the 2'-sugar modification is used exclusively on the first and last 5 nucleotides. This provides increased target RNA binding affinity on the outer portions of the ASO, while still allowing RNase H cleavage at the central region (Adapted from DeVos and Miller, 2013)**.**

3.3 ASO, MECHANISM OF ACTION

Antisense drugs do not cross the intact BBB. However, delivery of the antisense drugs in the CSF, by means of intrathecal injection (IT) or intracerebroventricular injection (ICV), results in broad distribution into SC and brain tissue. It has been reported in mice and nonhuman primates models of spinal muscular atrophy, that single bolus injection into the CSF results in better distribution in the CNS than slow infusion. Furthermore,

they still observe maximal effects 6 months after treatment discontinuation (Rigo et al., 2014).

ASOs must cross a lipid bilayer to access the compartment(s) necessary to bind target mRNA and elicit a pharmacological response. The cellular uptake process can be divided broadly into three steps: adsorption, internalization and intracellular trafficking (Figure 12).

- Adsorption: Adsorption of the ASOs to the cell surface by means of different cell surface proteins, including receptors. This interaction can be directly or via ligands conjugated to ASOs.
- Internalization: Cell surface proteins can direct the internalization of associated ASOs via clathrin- or caveolin-dependent endocytic pathways. Theoretically the internalization could be via non- conventional endocytic pathways, including micropinocytosis.
- Trafficking: Inside the cell the ASO can follow two distinct routes: (i) one that is productive, meaning that the ASO is delivered in an effective compartment where it can interact with the target RNA and; (ii) another non-productive in which the ASO is accumulated in a compartment where it cannot perform the therapeutic effect. Internalized ASOs can traffic from early endosomes to late endosomes and finally to lysosomes. ASOs must escape from endosomal organelles to reach the cytosol and nucleus to act on target RNAs. It has been shown that some proteins (AP2M1 and ANXA2) may facilitate ASO productive transport, whereas other proteins (VPS28, TG101) may direct ASO to non-productive pathways (Crooke et al., 2017).

Specific uptake pathways for ASOs have been identified, but it has also been shown that different cell types have differing ASO-binding abilities. Most cells in tissue culture take up ASOs without transfection reagents or electroporation. However, ASOs are active in only a fraction of cell lines when taken up in this way. This leads to the hypothesis that most internalization ASOs are taken up by pathways that do not lead to ASO accumulation at sites where they can bind RNA and influence gene expression (non-productive uptake). It is also possible that cell surface proteins, which are differentially expressed in different cell types, could contribute to the routing of ASOs into productive or no productive pathways (Crooke et al., 2017).

Once inside the cell, depending on their chemical configuration single-stranded ASO, modulate RNA function by several mechanisms including degradation of the target RNA by the enzyme RNase H or modulate RNA intermediate metabolism such as splicing. In

the context of ALS RNase-mediated degradation is particularly advantageous to reduce the levels of abnormal accumulation of toxic protein, in this case, for example the mutated SOD1 (Schoch and Miller, 2017).

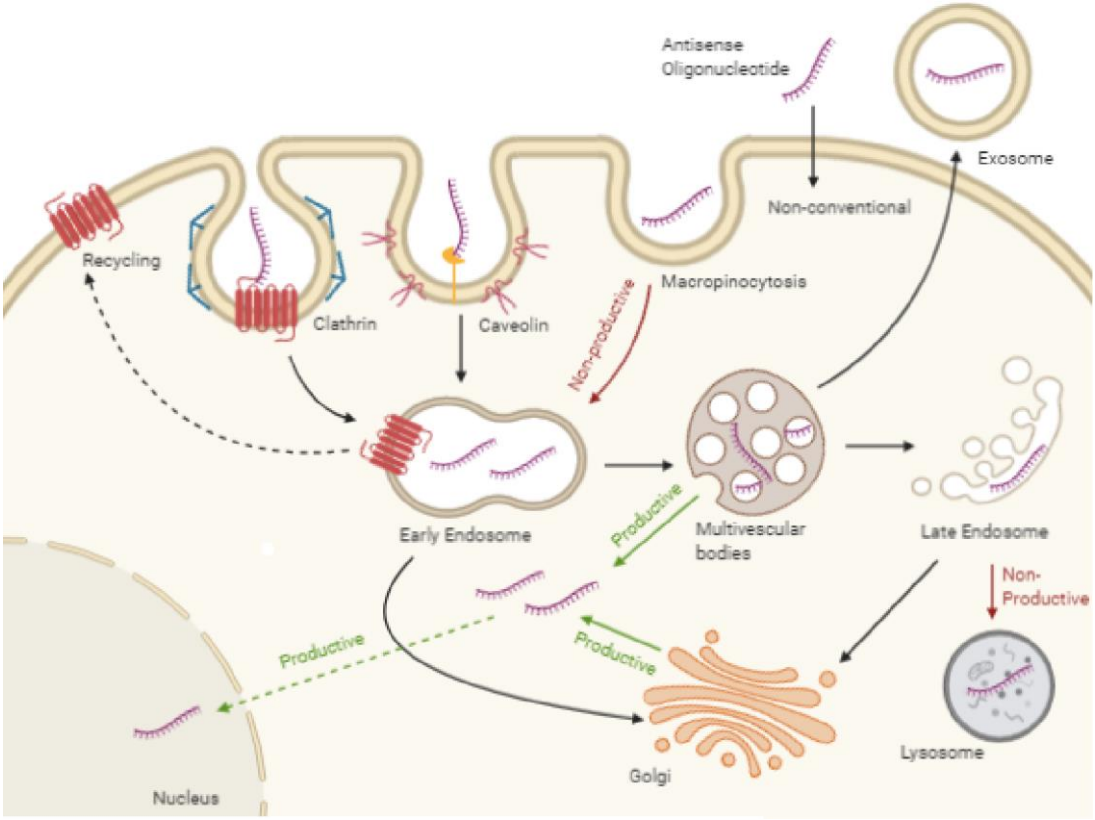

Figure 12. Pathway of ASO uptake and intracellular trafficking. (Created by BioRender modified from Juliano, 2016; Crooke et al., 2017)

The major current obstacles that ASO therapies have presented so far are, among others, is the low efficiency of their uptake by cells and the difficulty to selectively deliver ASO to specific cell types. This is partially solved by administering a high concentration of ASO to increase the internalization into cells. However, increasing ASO amounts also elevate their toxic effects and potential costs of the therapy. The toxic effects are especially relevant for treating CNS conditions due to the low capability of the CNS replace dead cells. Part of these obstacles have been overcome by conjugating ASO with antibodies and other molecules, such as small peptides or chemical ligands. ASOs conjugated with N-Acetylgalactosamine (GalNac) were initially designed to target the ASO into hepatocytes. GalNac-conjugated ASO enter cells via the interaction of the GalNac moiety with the Asialoglycoprotein (ASGPR) receptor. Conjugated ASOs are

internalized with the ASPGR via clathrin-mediated endocytosis (Prakash et al., 2014). Recent studies have revealed that sertraline-conjugated ASO against serotonin transporter (SERT) are internalized in serotonergic neurons and have potent antidepressant potential (Ferrés-Coy et al., 2016). Similarly, intranasal delivery of ASO against α-synuclein conjugated with the monoamine reuptake inhibitor indatraline, has shown selectively reduce α-synuclein expression in the brainstem monoamine nuclei of mice (Alarcón-Arís et al., 2018). Conjugated ASO dissociates from the receptor in early endosome. Then, the receptor is recycled back to the plasma membrane and the ASO reaches the cytosol to act on target RNAs.

3.4 ASO THERAPY FOR ALS

Targeting SOD1

Approximately 10% of familial ALS cases are caused by mutations in SOD1 altering its function (Rotunno and Bosco, 2013). Phase I clinical testing of the first-in-human SOD1 ASO, intended to lower SOD1 expression, demonstrated that the drug was well tolerated when infused into the CSF, but abundance of the mutant SOD1 protein in CSF was reduced by only 12% (Miller et al., 2013a). A reformulated version of the drug designated IONIS-SOD1Rx (BIIB067) is presently undergoing phase 1 clinical trials by Ionis Pharmaceuticals and Biogen.

Targeting ATXN2

ATXN2 as a target for ALS: Although mutations in several genes cause ALS, a number of studies point to ATXN2 as a therapeutic target for ALS. Over the past decade, it has become well established that intermediate CAG repeat expansions in the ATXN2 gene increase the risk of ALS (Elden et al., 2010). Intertwined with this discovery was the finding that reducing ATXN2 expression improved transactive response DNA binding protein 43 (TDP-43) toxicity in both yeast and flies (Elden et al., 2010). When endogenous Atxn2 was reduced in TDP-43 transgenic mice by crossing with Atxn2 knockout mice, survival was significantly improved, TDP-43–positive stress granules were eliminated in motor neurons, and gait scores improved (Becker et al., 2017). Similarly, the survival of TDP-43 transgenic mice was improved by treating with an ASO targeting the Atxn2 gene. The effect of targeting ATXN2 on TDP-43 aggregations might be explained by related effects on STAU1.

Targeting C9ORF72

GGGGCC repeat expansions in the C9ORF72 gene are causative of ALS and FTD (DeJesus-Hernandez et al., 2011). C9ORF72 repeat expansions result in loss of expression of the normal C9ORF72 gene and gain of C9ORF72 mRNA aggregates and repeat associated non-AUG (RAN) translation products. Mice with expanded C9ORF72 treated by intracerebroventricular injection with ASOs that interfere with translation of GGGGCC expanded C9ORF72 had reduced mRNA foci and RAN translation products, associated with improved anxiety and cognitive function phenotypes (Jiang et al., 2016). With proof of concept established, Ionis Pharmaceuticals and Biogen have undertaken a phase 1 clinical trial of an ASO therapeutic targeting C9ORF72 for ALS.

4. LYSOPHOSPHATIDIC ACID

Lysophosphatidic acid (LPA) is a simple phospholipid that has been shown to act as a potent lipid-signalling molecule (Chun et al., 2013). All LPA molecules consist of a glycerol backbone connected to a phosphate head group and are commonly ester-linked to an acyl chain of varied length and saturation. These various chemical forms of LPA are derived from multiple sources, such as membrane lipids, that signal through defined G protein-coupled receptors (GPCRs) to produce a wide number of physiological responses (Kano et al., 2008). Currently 6 GPCRs have been identified which we can classified, according to their homology, in two subgroups. The first subgroup comprise the first three members: LPA_1, LPA_2 and LPA_3. The three receptors form part of the endothelial differentiation gene family. And the second subgroup include the LPA_4, LPA_5 and LPA_6, they belong to the P2Y purinergic receptor family (Yung et al., 2014). Each receptor can couple to one or more of four heterotrimeric Gα proteins ($G_{12/13}$, $G_{q/11}$, $G_{i/o}$ and G_S) resulting in the activation of a wide range of downstream signalling pathways and resulting in diverse physiological and pathophysiological effects documented for LPA signalling (Chun et al., 2013). Recognition of the ligand, generally refers to 1-or 2-acyl-sn-glycerol 3-phosphate, by each receptor seems to be quite different, as LPA species with various fatty acids at either the sn-1 or sn-2 position of the hydroxy residue active each receptor quite differently (Kano et al., 2008). LPA species with both saturated fatty acids (16:0,18:0) and unsaturated fatty acids (16:1, 18:1, 18:2; 20:4) have been detected in various biological samples including serum, plasma (Sano et al., 2002), saliva (Sugiura et al., 2002) and others. These LPA species exhibit differential biological activities, as a result of differentially activating the LPA receptors.

4.1 LPA METABOLISM

LPA is produced from phospholipids, in both intracellularly and extracellularly compartment. The first one is thought to be structural or an intermediated for phospholipid biosynthesis, on the other hand the extracellular production pool it seems the main source of LPA signalling molecule (Chun et al., 2013) (Figure 13). There are two major pathways for LPA production:

Extracellular production

In this pathway the LPA formation derived from phospholipids, specifically phosphatidylcholine (PC), phosphatidylserine (PS) and phosphatidylethanolamine (PE) the first step is the removal of a fatty acid chain to form the respective lysophospholipids (LPLs). Has been described at least two mechanisms to obtain the LPLs. In activated platelets, LPLs are mediated by secretory-type phospholipase A2 (PLA2) and phosphatidylserine (PS) specific PLA1 (PS-PLA1). In plasma, LPLs is synthesized by lecithin-cholesterol acyltransferase and PLA1- like enzymes. Subsequently, the head group of the LPLs generated (choline, ethanolamine or serine) are cleaved by the autotaxin (ATX), a plasma enzyme, to form LPA (Aoki et al., 2008).

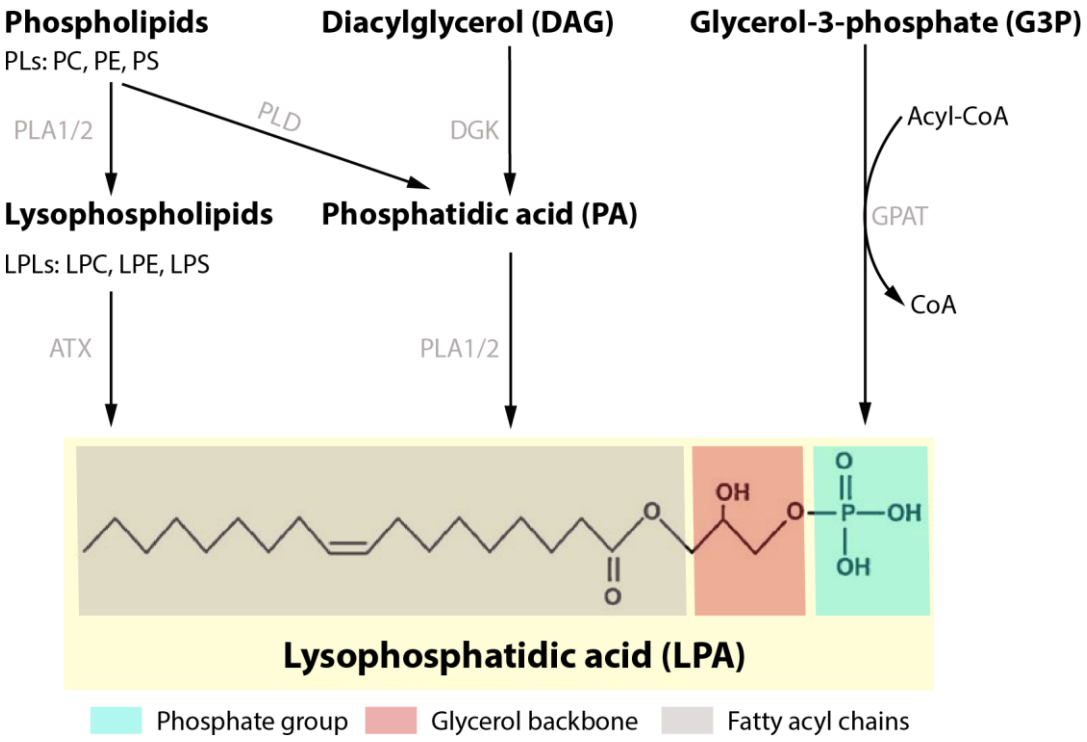

Figure 13. Lysophosphatidic acid synthesis (Modified from Choi and Chun, 2013)

Intracellular production

This other pathway source is the diacylglycerol (DAG), phospholipase D or diacylglycerol kinase promote its breakdown to produce phosphatidic acid (PA). Then PLA1 or PLA2 mediated LPA formation. Because PA is probably located in the cell membrane, this reaction may occur in cells or on the plasma membrane (Aoki et al., 2008).

LPA has a short half-life in the circulation of about 3 minutes (Albers et al., 2010). However, LPA can be transported in plasma bound to albumin (Pagès. et al., 2001). LPA turnover is regulated by ATX activity and LPA degradation. That can be mediated by several mechanisms: lipid phosphate phosphohydrolase type 1, which hydrolyse LPA into monoacylglycerol in the outer leaflet of the cell membrane; LPA-acyltransferase which transfer and acyl chain to LPA converting it into PA in the inner leaflet of the cell membrane (Valdés-Rives and González-Arenas, 2017)

4.2 LPA RECEPTORS

As previously mentioned, LPA signals thought LPA_{1-6} receptors codified by the genes *LPAR1-LPAR6* (humans) and Lpar 1- Lpar 6 (mice). All these receptors are rhodopsin-like, with seven transmembrane domain that range from 39 to 42kDa and differ in their tissue distribution and downstream effectors (Yung et al., 2014) (Figure 14)**.**

LPA_1 was the first receptor to be identified, in 1996 by Hecht et al. (Hecht et al., 1996), to date is the best studied. LPA_1 shares among 50-60% aminoacid sequence identity whit LPA_2 and LPA_3, they belong to the endothelial differentiation gene family (Bandoh et al., 1999). Differently, LPA_4 was the first identified receptor to show a dissimilar amino acid sequence from the others. LPA_4 (Noguchi et al., 2003), LPA_5 (Lee et al., 2006) and LPA_6 (Yanagida et al., 2009) were identified in thought unbiased screening approaches that led to the deorphanization receptors from the P2Y purinergic family.

The involvement of the LPA signalling in several physiological and pathological situations (Table 1) have been possible studied thanks to the development of mice null for each specific receptor. Of the five LPA receptor-null mouse lines that have been reported ($LPA_{1-5}^{-/-}$), $LPA_1^{-/-}$ mice are the only ones to demonstrate obvious neurodevelopment defects and a 50% perinatal lethality (Chun et al., 2013). Have been reported defects in suckling behaviour, which could explain the reduce body size of this line (Contos et al., 2000).

	Expression	Physiology	Pathophysiology
LPA1	Brain, uterus, testis, lung, small intestine, heart, stomach, kindey, spleen, thymus, placenta, skeletal muscle (mice and humans)	Neurodevelopment, astrocytic proliferation, oligodendrocyte regulation, regulation immune cells	Neuropathic pain, obesity, fibrosis, cancer, demyelination, axon repulsion,
LPA2	Testis, leukocytes (human) Kidney, uterus, testis (mice)	Cell survival and migration, nervous system development and function, regulation immune cells	Protumorogenic, demyelination, neuronal death
LPA3	Heart, testis, prostate, pancreas, lung, ovary, brain (humans) Testis, prostate, pancreas, lung, ovary brain (mice)	Embryo implantation	Protumorogenic,
LPA4	Heart thymus, bone marrow (mice)	Cell aggregation and adhesion, inhibits cell migration, osteogenesis	Protumorogenic,
LPA5	Spleen, heart, platelets, gastrointestinal lymphocytes, dorsal root ganglion (mice)	Neurite retraction, stress fiber formation, intestinal water absortion	Neuropathic pain
LPA6			Hypotrichosis

Table 1 : Summary of the LPA receptors highly expression tissues in humans and mice. Overview of some related physiology and pathophysiology features related whit the LPA-LPA receptors signalling.

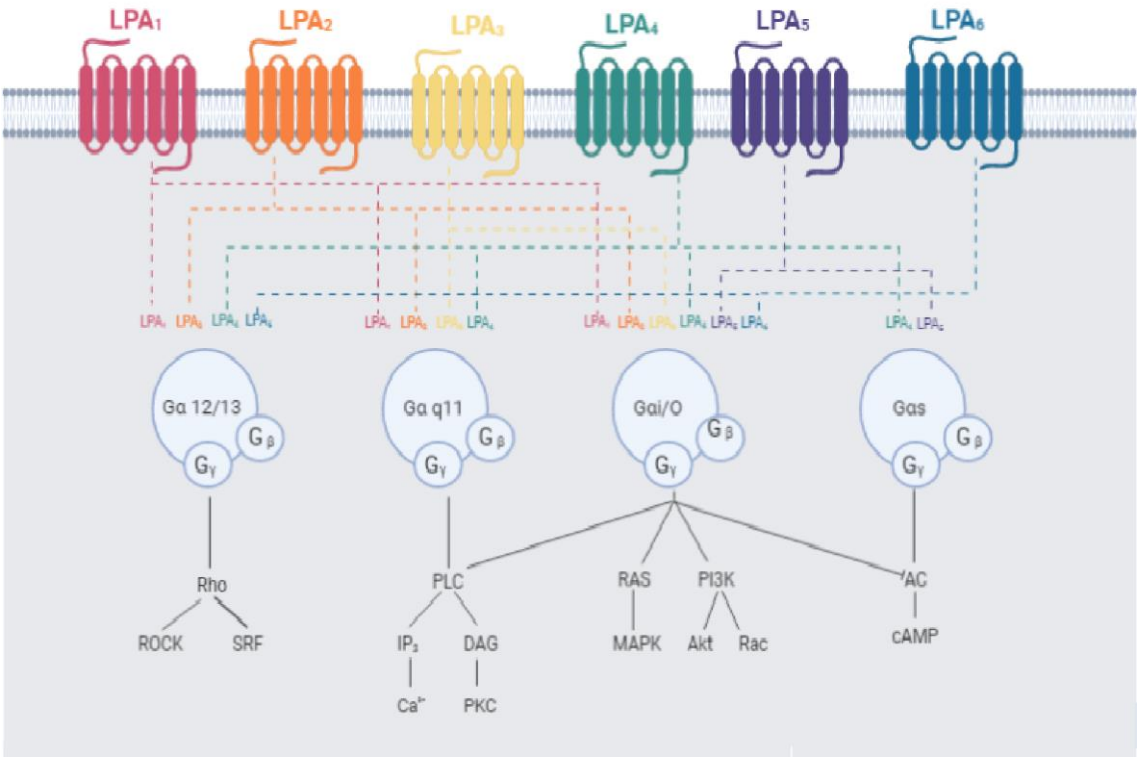

Figure 14. LPA receptors signaling. LPA is the ligand of six receptors (LPA_{1-6}), each interact with different G proteins and for instance initiate distinct signalling cascade in the cell (Created by BioRender modified from Choi and Chun, 2013)**.**

4.3 LPA AND CNS

The discovery of the LPA_1 role in the nervous system development has served as a template and encouragement for the researches to investigate the paper of LPA in CNS and in other tissues. Since then a variety of specific response at cellular and tissue levels have been identified, as well their involvement in some CNS disease. Below will offer and overview of LPA signalling in CNS cell types.

Neurons

In vitro studies using primary neurons and neuronal cell lines related LPA effects to morphological changes involving growth cone collapse and neurite retraction. In vivo studies LPA-induced neurite retraction is accompanied by the formation of F-actin filament, but the explicit participation of the LPA receptors in this mechanism is still unknown (Fukushima et al., 2002). LPA signalling has also been related to neurotoxic and neuroprotective effect. Classically LPA_1 signalling is associated whit neuron survival

role, since LPA_1 null mice present apoptotic cell death in the brain (Fukushima et al., 2002). Recently, López-Serrano *et al*. reported neuronal loss, specially MN, and demyelination after microglia LPA_2 signalling after SC injury (López-Serrano et al., 2019). In addition LPA are linked to neuronal excitability, synapse formation and synapse transmission (Choi and Chun, 2013).

Astrocytes

Many of the *in vitro* effects of LPA in astrocytes are related to LPA_1 signalling that promote astrogliosis, by means of affecting the proliferation, migration, morphology and activation of this type cells (Choi and Chun, 2013). Astrocytes are responsible of neuronal differentiation, that have been related to LPA signalling. LPA-primed astrocytes secrete soluble factors to increase neuronal differentiation (E Spohr et al., 2011). LPA has also consequence on neuron health, LPA signalling decrease glutamate and glucose uptake and increase lipid peroxidation in astrocytes, exacerbating neurotoxicity and reducing energy supply (E Spohr et al., 2011). Finally, astrocytes secrete several cytokines and neurotrophic factors, suggesting a double role in the CNS, pro-inflammatory and neuroprotective (Tabuchi et al., 2000).

Oligodendrocytes

LPA effect on oligodendrocytes seems to depend on the degree of maturation of these cells. This type cell express LPA_1 in a pattern that correlates temporally and spatially with maturation and myelination. In vitro studies show cellular responsiveness to LPA including process retraction and cell rounding, depending on the maturity of oligodendrocytes. As well, LPA stimulates process formation, and increase the number of differentiating, but not mature, oligodendrocytes (Noguchi et al., 2009).

Microglia

LPA signalling in microglia was reported to regulate proliferation, membrane ruffling and hyperpolarization, metabolic changes, migration, chemokines and growth factor upregulation (Choi and Chun, 2013). Furthermore, *de novo* synthesis of LPA in activated microglia could be one of the factors for the pathogenesis of neuropathic pain (Ma et al., 2010). Microglia seems express a range LPA receptors including LPA_{1-3}. However, there are some controversies regarding the LPA receptor expression on microglia cells, since

there are several microglia cell types *in vitro*. This make difficult the description of mechanism mediated by LPA receptors axis *in vivo*. Studies from our laboratory have reveal that microglia express LPA_1 and LPA_2 in vitro but also in vivo conditions, and that microglial cells becomes cytotoxic upon LPA_1 and LPA_2 activation (Santos-Nogueira et al., 2015; López-Serrano et al., 2019).

The description of biological functions mediated by LPA signalling on CNS cell types have led to translational research to identify pathological mechanism in CNS diseases and present new therapeutic targets to validate future treatments. In 2012 a clear the therapeutic potential of LPA axis modulation was reported, the administration of B3, an antibody that is able to bind to LPA and prevent them from interacting with their receptors, promoted functional recovery after a SC hemisection in mice (Goldshmit et al., 2012). However, it has to be highlighted that this antibody not only interacts with LPA, but also to other LPLs. Recent studies using selective LPA receptor antagonist and KO mice that LPA contributes to the physiopathology of spinal cord injury, brain stroke and brain injury, via activation of LPA_1 and/or LPA_2. Indeed, the detrimental actions of LPA are not mediated directly on oligodendrocytes or neurons. In fact, LPA activates LPA1 and LPA2 receptors found in microglia, which in turn, stimulate the secretion of different cytotoxic factors (Santos-Nogueira et al., 2015; López-Serrano et al., 2019) . Indeed, we found that activation of microglia LPA2 led to secretion of purines that mediate oligodendrocyte cell death by stimulation P2X7 receptor in oligodendrocytes (López-Serrano et al., 2019). However, whether LPA signalling mediates detrimental actions in ALS is currently unknown.

Hypothesis and objectives

Hypothesis and objectives

The main goal of this thesis is to develop new therapeutic strategies for the treatment of ALS. In the first chapter, we hypothesized that the conjugation of ASO to facilitate their internalization into cells will enhance *SOD1* silencing of transcripts, relative to naked ASO, and will result in greater therapeutic effects in a mouse model of ALS. In the second chapter, we hypothesized that LPA contributes detrimentally to the course of ALS and that modulation of the LPA-LPA_2 axis will slow the progression of the disease.

To address these general aims, the thesis has been divided in two chapters with the following specific objectives:

Chapter I: Administration of conjugated ASO against *SOD1* to ameliorate the clinical signs of ALS in $SOD1^{G93A}$ mice.

- To assess the internalization of the conjugated ASO in a motoneuron like cell line.
- To study the internalization of the conjugated ASO in neurons and glial cells in the spinal cord of C57Bl/6 and $SOD1^{G93A}$ mice.
- To compare the efficacy of the conjugated ASO in silencing *SOD1* transcripts in the spinal cord and brain of $SOD1^{G93A}$ mice
- To evaluate the therapeutic potential of the conjugated ASO in $SOD1^{G93A}$ mice.

Chapter II: Contribution of the LPA-LPA_2 axis in the physiopathology of ALS

- To evaluate theLPA levels in the cerebrospinal fluid of ALS patients.
- To study the expression of the LPA receptors, LPA_1 and LPA_2, in spinal cord necropsies from ALS patients.
- To assess the dynamics in the expression LPA_2, in the spinal cord, nerve and skeletal muscles of $SOD1^{G93A}$ mice.
- To evaluate the contribution of LPA_2 to neurological deficits in $SOD1^{G93A}$ mice.
- To assess the role of LPA_2 in the survival of lower motoneuron in ALS mice.
- To study the contribution of LPA_2 to microgliosis and astrogliosis in the spinal cord of $SOD1^{G93A}$ mice.

- To study the involvement of LPA_2 in the degeneration of motor axons and myelin in ALS mice.
- To evaluate the contribution of LPA_2 to muscle atrophy in $SOD1^{G93A}$ mice.

MATERIAL AND METHODS

All the experimental procedures were approved by the Universitat Autònoma de Barcelona Animal Experimentation Ethical Committee (CEEAH 1188R3-DMAH 3131)/ (2969) and followed the European Communities Council Directive 2010/63/EU, the methods for each procedure were carried out in accordance with the approved guidelines.

MICE

All mice used in the studies were housed in the Universitat Autònoma de Barcelona animal facilities, in standard cages and feed *ad limitum* with a light-dark cycle of 12h.

The ALS mouse model used for the experiments is the transgenic mouse $SOD1^{G93A}$ (B6-Tg [SOD1-G93A]1Gur), based on the mutations described in the protein SOD1 in ALS patients, that express the mutant SOD1 in heterozygosis (Gurney et al., 1994). This experimental model replicates the most relevant phenotypical and histopathological features of the human disease (Turner and Talbot, 2008). To evaluate the role of the LPA_2 in the pathophysiology of ALS, we used the mice lacking LPA_2 in homozygous provided by Jerold Chun, from the Scripps Research Institute (La Jolla, CA, EEUU). LPA_2 knockout mice were crossed with $SOD1^{G93A}$ mice,

GENOTYPING

To stablish the genotype of the mice, DNA was extracted from a sample of the mouse tail using DNA mouse tail kit from Danagen Genomic and the target allele amplified by PCR. In brief, tail tissue was digested in 0.1 mg/mL proteinase K solution and diluted in lysis buffer at 55 ºC overnight. After digestion, proteins were eliminated using a protein buffer and centrifugation during 3 min at 16000 g. Supernatants were then mixed with 2-propanol (Panreac) to precipitate DNA. After a centrifugation of 3 min at 1600g the pellets were washed with ethanol 70%. Finally, DNA pellets were completely dried at room temperature before DNA solubilisation by adding 50µl of DNA hydration solution at 65ºC for 1 hour. Allele amplification was performed by PCR reaction, using the Taq DNA polymerase kit (Invitrogen) and PCR products were analysed by standard electrophoresis in 2% agarose gels. Since the expression of $SOD1^{G93A}$ is heterogeneous we also amplified the IL-2 as a control (Table 2).

Table 2. Description primers use for genotyping

	Forward primer	Reverse primer	Mutation primer
LPA_2	5'-AGTGTGCTGGTA TTGCTGACCA-3'	5'-CTCTCGGTAGCG GGGATGG-3'	5'-CAGCTGGGGCTC GACTAGAGGAT-3'
hSOD1	5′-CATCAGCCCTAA TCCATCTGA-3′	5′-CGCGACTAACAA TCAAAGTGA-3'	
IL-2	5'-CTAGGCCACAGA ATTGAAAGATCT-3'	5'-GTAGGTGGAAAT TCTAGCATCATCC-3'	

HUMAN SAMPLES

Human samples from ALS patients and healthy controls were gently provided by the Institute of Neuropathology HUB-ICO-IDIBELL Biobank following the guidelines of Spanish legislation and the local ethics committee. Briefly transversal sections of the spinal cord from human ALS patients and controls were post-mortem removed and kept at -80ºC or fixed by immersion in 4% buffered formalin. The study included 14 ALS patients (6 men and 8 women) and 11 control patients (6 men and 5 women). The ALS patients can be classified by their onset: spinal (2 patients), bulbar (4 patients), and respiratory (1 patient), the rest onset wasn't known (7 patients). All data is summarized in the table 1.

Table 1. Controls and ALS patients data

Group	Autopsy nº	Age	Gender	PM delay	RIN	Onset
Controls	A06/047	59	M	12 h 05 min	6,40	-
	A07/067	47	M	04 h 55 min	5,60	-
	A07/082	64	F	11 h 20 min	6,20	-
	A07/084	46	M	15 h 00 min	5,90	-
	A07/114	56	M	07 h 10 min	6,10	-
	A07/162	71	F	08 h 30 min	5,90	-
	A08/042	64	F	05 h 00 min	7,00	-
	A08/070	79	F	06 h 25 min	6,70	-
	A09/120	75	M	07 h 30 min	4,90	-
	A09/137	55	M	09 h 45 min	5,30	-
	A14/003	51	F	04 h 00 min	6,30	-
	A07/010	56	M	10 h 50 min	7,10	N/A
	A07/013	70	M	03 h 00 min	7,30	Resp
	A07/071	77	M	04 h 30 min	7,40	N/A
	A07/072	56	F	03 h 45 min	8,20	N/A

ALS	A07/121	59	M	03 h 15 min	7,50	N/A
	A07/139	63	F	13 h 50 min	6,80	Bulb
	A09/012	59	F	14 h 15 min	6,40	N/A
	A11/054	64	M	16 h 30 min	6,30	N/A
	A12/020	57	F	04 h 00 min	6,20	Bulbar
	A12/040	75	F	04 h 05 min	6,80	Bulbar
	A12/083	79	F	02 h 10 min	7,00	N/A
	A13/003	57	F	10 h 00 min	6,50	Bulbar
	A15/029	46	M	07 h 00 min	7,00	Spinal
	A15/033	69	F	17 h 00 min	6,40	Spinal

ASO

The ASO used were designed and manufactured by nLife therapeutics. Some of the ASO were tagged to a fluorochrome, Alexa 488, to allow the tracking of the molecule both in vitro and in vivo. The specific dose, administration and ASO use for each approach is described in the Table 3.

The sequence was designed to allow specific complementary match with the human SOD1 RNA. Furthermore, the chemistry of the synthetic nucleotides was modified to avoid their degradation in the biological fluids, increase the interaction to the RNase H and prevent the inflammatory response (Table 4). Specifically, the phosphate backbones were replaced to phosphorothiate because increase the ASO affinity to the RNA target and protect from nuclease degradation. With the purpose to prevent an immune response the 2' ribose sugar was modified (2'-O-MOE), because was been reported that confer less toxicity than unmodified designs. (Schoch and Miller, 2017)

Table 3. Description of ASOs

Approach	Ligand	Sequence	Tag	Dose	Admin.
Internalization	Three	Missense	A-488	5µg	*In vitro*
Internalization	Three	Missense	A-488	50µg	IT/ICV
Internalization	DCPP	CCGTCGCCCTTCAGCACGCA	A-488	50µg	ICV
Internalization	-------	CCGTCGCCCTTCAGCACGCA	A-488	50µg	ICV
Therapeutic	DHT DCPP	CCGTCGCCCTTCAGCACGCA		20 nmols	ICV

Table 4. Chemistry of the ASOs

Sequence	5'-Ligand(C10)sCmsCmsGmsUmsCmsdGs(5MdC)s(5MdC)s(5MDc) sdTsdT(5MdC)sdAsdGs(5MdC)sAmsCmsGmsCmsAm-3'
dA, dG, dT, Dc	DNA nucleotide
Am, Gm,Um,Cm	2'-O-MOE- nucleotide
s	phosphorothiate
C10	carboxymodifier
5MdC	5-Methyl-dC

NSC-34 CELLS

The NSC-34 cell line is a hybrid cell line, produced by the fusion of MN-enriched embryonic mouse spinal cord cells with mouse neuroblastoma (Cashman et al., 1992). This cell line, which is considered to express many properties of MN, was used to evaluate the internalization of the ASO *in vitro*. NSC-34 cells were cultured in Dulbecco's modified Eagle's medium high-glucose (DMEM, Biochrom, Berlin) supplemented with 10% fetal bovine serum and 1x penicillin/streptomycin solution (Sigma-Aldrich) on collagen coated plates (Thermo Fisher, Waltham, MA, USA) in a humidified incubator at 37ºC under 5% CO_2. After 4 days of cell culture without changing the medium, cells were differentiated. Conjugated missense ASO tagged to the Alexa-488 fluorochrome, was added to the cells and at 24 hours, the cultures were fixe in 1% paraphomaldehyde (PFA) and processed for immunocytochemistry.

ASO ADMINISTRATION

Intrathecal administration (IT)

ASO were administrated intrathecally to C57Bl/6 and $SOD1^{G93A}$ mice. Mice were anaesthesized by intramuscular injection (i.m) of a mixture of ketamine (90 mg/kg) (Imagen, Merial) and xylazine (10mg/kg) (Rompun, Bayer) anaesthesia). Then the lumbar back was shaved and disinfected to perform an incision of the skin and muscle until the exposition of the vertebra column. Once localized the vertebra L5 and L6, the 4 µl of the ASO were slowly administrated in the CSF using a 33-gauge needle coupled to a 10µl Hamilton syringe (removable needle Hamilton, 701). Correct access to the intrathecal space was confirmed by animal tail flick. After the administration the needle was maintained in the place 3 min after the injection to avoid liquid reflux. Finally, the

wound was closed and disinfected, and the mice were kept in a warm environment until complete recovery from anaesthesia. Buprenorphine (0.01mg/kg i.p) (Buprex, Indivior) was administrated intraperitoneal to preventively avoid animal pain twice a day for 3 days.

Intracerebroventricular administration (ICV)

For the administration of the ASO in the cerebral ventricle, the animals were anesthetized with ketamine (90 mg/kg i.m.) (Imagen, Merial) and xylazine (10mg/kg i.m.) (Rompun, Bayer). The head of the rodent was shaved and disinfected and was placed in the stereotaxic, making sure that the cranium did not moved. A skin incision was performed to expose the cranium and hydrogen peroxide (H_2O_2 at 25% in water) was applied in the surface of the skull to expose the Bregma and Lambda. Once the stereotaxic coordinates (0.2mm posterior to bregma, 1.0 mm lateral right to the midline) were located the cranium was perforated and the needle was placed 2 mm ventral to the surface. 4 µl of the molecule were administrated using a 33-gauge needle coupled to a 10µl Hamilton syringe (removable needle Hamilton, 701). Injections were made at a perfusion speed of 1 µl/min by an automatic injector, the needle was maintained inside the brain 2 min after each injection to avoid liquid reflux. Finally, the wound was closed and disinfected, and the mice were kept in a warm environment until complete recovery from anaesthesia. Buprenorphine (0.01mg/kg i.p) (Buprex, Indivior) was administrated intraperitoneal to preventively avoid animal pain twice a day for 3 days.

FUNCTIONAL TESTS

$SOD1^{G93A}$ mice develop a rapidly progressive MN degeneration, which leads to locomotor deficits that can be evaluated using several functional tests. One of the widely used is the rotarod test, due to their high sensitivity and accuracy to determine the onset of the disease. Rotarod test asseses a complex motor task that allow the researcher the detection of abnormalities in balance, coordination and strength (Miana-Mena et al., 2005). Rotarod consists in a horitzonal rotating cylinder placed above a cage. Mice were placed onto the cylinder rotaing at a consant speed of 14 rpm. The time for which each animal could reamin on the rotating cylinder was mesaured. Each animal was given three trails and the longest latency without falling was recorded. 180 seconds was chosen as the arbitary cutt-off time. Animals were trained were trained during the first week of

evaluation (8 weeks of age) to obtain the baseline levels. Then rotarod test was performed weekly from 8 to 20 or 22 weeks of age.

ELECTROPHYSIOLOGICAL TESTS

ALS is characterized by the progressive loss of both, upper and lower MNs which can be evaluated using electrophysiological tests. Motor conduction studies are fundamental for the assessment of disease progression and allow a time follow-up of the same animal, furthermore enable the assessment of the whole neural pathway from brain to periphery (Mancuso et al., 2014). Since $SOD1^{G93A}$ mice develop ALS with a lumbar onset that rapidly spreads to upper levels, the record of hindlimb compound muscle action potential (CMAP) asses the loss of spinal MNs.

CMAPs

To evoke CMAP, peripheral nerves are percutaneously stimulated through a pair of needle electrodes. The impulse conducted by alpha-motor axons causes synaptic transmission at the NMJ and the production of an action potential in the membrane of the skeletal muscle fibers, that can be recorded with electrodes placed on the muscle. The compound muscle action potential (CMAP) represents the summation of the action potentials of all the excited muscle fibers that respond to the nerve stimulation.

In all electrophysiologicaly tests animals were anesthetized with pentobarbital sodium and placed prone over a heating pad that maintain body temperature. Therefore, pulses were delivered by means of single pulses of 0.02 ms duration (Grass S88) through a pair of needle electrodes; the cathode inserted deep into the sciatic nerve notch and the anode near the first, subcutaneously. Recording microneedles were inserted superficially in the muscle, reference and ground electrodes were inserted at the third toe and the base of the paw, respectively. The recording needles were placed using a magnifier lens and guided by anatomical landmarks, to ensure reproducibility of needle location on all animals. CMAPs were recorded from gastrocnemius *medialis*, tibialis *anterior* and plantar *interossei* muscles. Signals were band pass filtered (3 Hz to 3kHz), amplified x100 for gastrocnemius and tibialis (P511AC amplifiers, Grass), and digitized with Power Lab recording system (PowerLab16SP, ADInstruments) at 20kHz. To asses CMPAs, the M wave was studied. We evaluated the amplitude from baseline to the maximal negative peak and the latency from stimulus to the onset of the first negative peak and to the end of the wave.

MUNEs

Following denervation, compensatory changes can occur (*i.e*. collateral sprouting) to maintain the neuromuscular integrity. These phenomena can be studied by means of motor unit number estimation (MUNE) technique that provide relevant information about the integrity of the MN and its functional counterpart, the motor unit (Arnold et al., 2015). MUNE was made using the incremental technique (Shefner et al., 2006). Electrodes were placed in the same place as for the CMAP registers and the amplitude for the M wave was recorded. For the MUNE assessment the protocol used consist in the incremental technique. Starting from subthreshold intensity the sciatic nerves was stimulated with single pulses of gradually increased intensity until the first response appeared, representing the first motor unit recruited. With the next stimuli, quantal increases in the response were recorded. The data can be represented as the frequency distribution of the single motor unit size (SU); as the mean of consistent increases (increments >100μV), single motor unit potential (SMUP) and finally MUNE that results from the CMAP maximal amplitude divided by the average SMUP.

SURVIVAL

The ALS experimental model, $SOD1^{G93A}$, developed tremor and weakness in the first stages of the disease, followed by paralysis and premature death. For these in the end stages of the disease, since week 22 of age, mice $SOD1^{G93A}$ were evaluated daily until their euthanasia, by overdose of pentobarbital sodium (Dolethal, Vetoquinol), in the endpoint. The endpoint was performed in the age in which the mice was not able to right itself within 30 seconds of being placed on its side.

SCIATIC NERVE INJURY

$LPA_2^{-/-}$ mice and wild type littermates were deeply anesthetized with ketamine (90 mg/kg i.m.) (Imagen, Merial) and xylazine (10mg/kg i.m.) (Rompun, Bayer). The right paw was shaved and disinfected after skin and muscle incision to expose the sciatic nerve. Once localized, the sciatic nerve was cut, above the trifurcation and ligated to avoid the reinnervation. The wound was closed and disinfected, and the mice were kept in a warm environment until complete recovery from anaesthesia. Buprenorphine (0.01mg/kg i.p) (Buprex, Indivior) was administrated intraperitoneal twice a day for 3 days.

REAL TIME PCR ASSAY (qPCR)

Mice were perfused transcardially with sterile saline, depending on the experiment the specific tissue was harvested and immediately frozen in liquid nitrogen. The samples were maintained at -80ºC until use. To RNA isolation, tissue was homogenized with QIAzol lysis reagent (Qiagen) using a tissue rupture, then RNA was extracted using RNeasy Lipid Tissue kit (Qiagen), according the manufacturer's protocol.

1µg of RNA isolated from these samples, as well as, from human spinal cord of ALS and control patients, was primed with random primers (Promega) and reverse transcribed using the Omniscript RT kit (Qiagen). Quantitative PCRs (qPCRs), reactions were prepared using either Brilliant II Ultra-Fast SYBR Green qPCR Master Mix (Table 3) or TaqMan's master mix kit (Table 4) depending on the primers. The resulting analysis was achieved using a MyiQ Single-Color Real-Time PCR detection System (Bio-Rad). Gene data was analysed using the 2-ΔΔCt method using GAPDH as housekeeping.

Table 3. SYBR-Green gene specific primers

Gene	Forward primer	Reverse primer
Lpa₂	5'-TGTCCTGGCCTA TGAGAAGTTCT-3'	5'-TTGTCGCGGTAG GAGTAGATGA-3'
Gapdh	5'-TCAACAGCAACT CCCACTCTTCCA-3'	5'ACCCTGTTGCTG TAGCCGTATTCA-3'
hSOD1	5'-AGGTGTGGGGAA GCATTAAA-3'	5'-ACATTGCCAAGT CTCCAAC-3'

Table 4. Taqman gene specific primers

Gene	
LPA₂	PN4448892
LPA₁	PN4453320
GAPDH	Hs02786624

HISTOLOGY

Mice were euthanized at different time points, with and overdose of pentobarbital sodium (Dolethal, Vetoquinol) and transcardially perfused with 4% paraformaldehyde (PFA) in 0.1 M phosphate buffer (PB). Specific tissues were harvested, spinal cord were post-fixed in 4% PFA for 2 hours and cryoprotected with 30% sucrose in 0.1M PB at 4ºC for minimum 48h, gastrocnemius muscle were direct cryoprotected and ventral root ganglion were cryoprotected into 3% glutaraldehyde, 3% PFA in PB. The spinal cord and muscle were fast-frozen at -20ºC in a cryoembedding compound (Tissue-Tek OCT, Sakura) and cut on a cryostat (Leica), serially picked up in gelatine coated slides. Samples were kept a -20ºC until use. For the ventral root ganglion briefly, the samples were immersed in 2% osmium tetroxide in PB for 2h, dehydrated through ethanol series and embedded in epon resin. Semithin sections (0.5 µm thick) were cut by an ultramicrotome. Samples were kept at room temperature (RT) until use. Processed samples were further stained using different approaches.

Immunostaining

Slides were placed in a hotplate at 37ºC for 30 minutes, to increase the retainment of the samples in the slide during washes. Samples were then rehydrated in PBS for 5 min and blocked with blocking buffer of 5% normal donkey serum (NDS) in 0.3% triton-PBS for 1h at room temperature (RT). Afterwards, sections were incubated overnight at 4ºC with primary antibodies (Table 3) diluted in the blocking buffer. Sections were then washed in 0.3% triton-PBS and further incubated for 1h at RT with the specific secondary antibodies tagged to an alexa-594 or alexa-488 fluorochrome (1:200, Invitrogen). After several washings in 0.3% triton-PBS and PBS, slides were incubated for 1 min in a solution containing DAPI (1µg/mL, Sigma). Finally, samples were washed in PB, dehydrated in a serial battery of ethanol and mounted in DPX (Fluka).

Table 5. Immunostaining antibodies

Epitope	Dilution	Manufacturer
ChAT	1:50	Millipore
TPPP	1:400	Millipore
Iba1	1:500	Abcam
GFAP	1:500	Millipore
NF200	1:1000	Millipore

Synaptophysin	1:500	Abcam
α-bungarotoxin	1:2003.	Life technologies

Cresyl Violet

Frozen transversal sections of spinal cord L4 and L5 were placed in a hotplate for 30 min. Serially cut slides were rehydrated in water for 1 min and stained for 2h with an acidified solution of 3.1mM cresyl violet at RT. Following incubation, sections were then washed and dehydrated in 70%, 96% and 100% ethanol series for 1 min each and mounted in DPX (Fluka) mounting medium.

Hematoxylin and eosin staining

Cryostat transversal sections of gastrocnemius muscle were hydrated in water, immersed in hematoxylin (Fluka, Sigma) for 6 min, and washed in water followed by 1% HCl in ethanol solution for 20 sec. Then, sections were rewashed with water and stained with Eosin (Merck, Millipore) for 5 min. Sections were dehydrated with series of graded ethanol rinses and mounted with DPX (Fluka).

Blue toluidine

Semithin sections of the ventral root ganglion were dried in a hotplate during 30 min and then stained with 1% Borax (Sigma) and 1% Toluidine Blue (Fluka) in distillate water for 1 minute in the hotplate and then cleaned with distillate water.

HISTOLOGY QUANTIFICATION

For histopathological analysis, samples were visualized with Olympus BX51 microscope and the images were captured with Olympus DP50 digital camera. For each analyses a different quantification was performed.

Immunoreactivity: Either GFAP or Iba1 immunoreactivity was measured by quantifying the integrated density of the immunostaining at the ventral horns of L4-L5 segments using Image J software. The integrated density represents the area above the threshold for the mean density minus the background. Both quantification images and representative images were taken at 40X magnification.

MN sparing: Slices from the L4-L5 lumbar segments were stained with cresyl violet to visualize the lumbar MNs. The number of MNs were manually quantified in both ventral horns, counting only those neurons that were within the laminae IX, with soma larger than 20μm, shaped in a polygonal fashion and with a preeminent nucleolus. Representative images were taken at 20X magnification.

Axonal preservation: The number of myelinated fibers in L4 dorsal root stained with blue toluidine was counted in images taken with a light microscope (BX51) attached to a digital camera (DP50, Olympus) at 100X magnification that represented at least 30% of the root cross-section area. The cross-section area was measured at 4x to estimate the total number of myelinated fibers. An axon was considered preserved if it remain the myelin sheath.

Muscle fiber area: Transversal sections of gastrocnemius muscle were stained with hematoxylin and eosin. Three images were randomly toked under light microscopy at 20X magnification and the cross-section area of the muscles fibers were calculated using the Image J software.

NMJ denervation: Transversal sections of gastrocnemius muscle were immunolabeled with synaptophysin, neurofilament 200 and α-bungarotoxin. The proportion of fully occupied endplates was determined by classifying each endplate as either full occupied (when presynaptic terminals overly the endplate) or vacant (no presynaptic label in contact with the endplate). Representative images were performed whit confocal microscope (LSM 700) at 40X magnification, shown as maximum projections images.

STADISTICAL ANALYSIS

Data are shown as mean ± standard error of the mean SEM. Results of the rotarod test, and the CMAP were analysed using repeated measures two-way ANOVA with post-hoc Bonferroni's for multiple comparisons. Data from the disease onset and the survival were analysed whit the Mantel-Cox test. Quantification of gene expression, preserved MNs, GFAP and Iba1 immunoreactivity, axonal sparing, muscle cross-section area, MUNEs and MEPs were analysed by using one-way ANOVA with post-hoc Bonferroni's for multiple comparisons. The comparison of the mean onset and mean survival were analysed using t-test. Statistical significance was considered at $p<0.05$.

RESULTS

CHAPTER I:

Administration of conjugated ASO against *SOD1* to ameliorate the clinical signs of ALS in SOD1^{G93A} mice

Motoneuron internalize conjugated-ASO in vitro

A sequence of 20 nucleotide RNA strand with 3′dTdT overhangs with no homology to mouse genome were chemically conjugated by means of carboxymodifier, in the 5′-end strand to three different synthetic ligands dihydroxytryptamine (DHT), clozapine (CLZ-Alkyl) and 2,3-Dichlorophenylpiperazine (DCPP). These molecules are ligands for 5HT2A, 5HT2A/D2, 5HT1A/D2, respectively. These neurotransmitter receptors are broadly expressed in the membrane of neurons and glial cells of the CNS (Paterson and Darnall, 2009; Perrin et al., 2011) and thus, these modifications were intended to improve the internalization in neuronal and glial cells. These molecules were also fluorescent tagged with Alexa 488 in order to allow their trackability.

First, we assessed whether these conjugated missense ASO were able to internalize into NSC-34 cells, a MN-like cell line (Cashman et al., 1992b). With this purpose, we incubated NSC-34 cells with a dose of 5µg of the conjugated-missense ASO. After 24 hours incubation, we assessed the localization of the ASO and found that that these three chemically-conjugated missense ASO were found in the cytoplasm of NSC-34 cells (Fig. 1), indicating their efficient internalization within this MN-like cell.

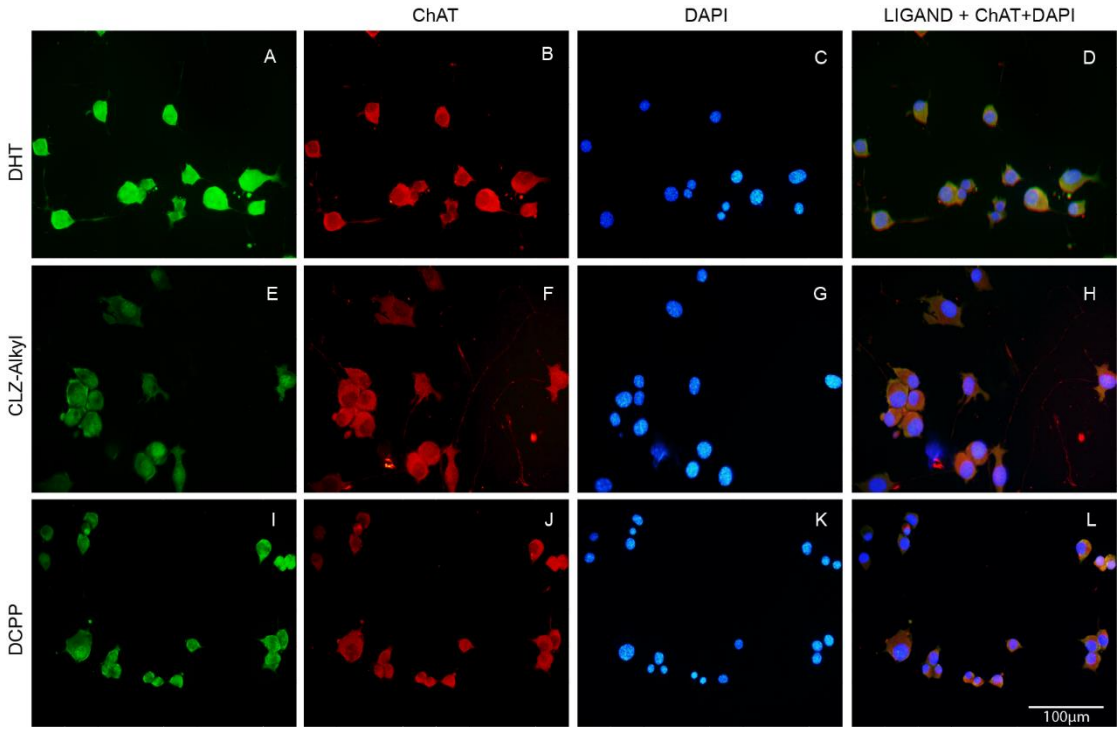

Figure 1. Motoneuron-like cells internalize conjugated-missense ASO *in vitro*. (**A, E, I**) Representative images of NSC-34 cells showing the presence of the three-chemically conjugated missense ASO within the cells. (**B, F, J**) Immunolabeling against choline acetyltransferase confirmed that these cells were motoneurons. (**C, G, K**) Images of the cells stained with DAPI to

show the cell nucleus. (**D, H, L**) Merged images demonstrating the internalization of the three molecules in the motoneurons. n=3 per group

Neurons and glial cells uptake the conjugated-ASO *in vivo*

We next assessed whether these conjugated missense ASO were also taken up by neurons and/or glial cells *in vivo*. Thus, we administrated 40 nmoles of the conjugated missense ASO intrathecally in C57Bl/6 mice and 24 hours later, SC were harvested to detect the presence of the ASO by epifluorescence microscopy (Fig. 2A). SC tissue sections of the lumbar section revealed the presence of the three compounds, mostly, in the gray matter. The ASO were observed in the cytoplasm of cells that had neuronal morphology (Fig. 2B).

Immunofluorescence against ChAT demonstrated that MN, the neuronal population susceptible to undergo cell death in ALS, internalized these three conjugated missense ASO (Fig. 3A). However, most of the neurons in the spinal cord were able to uptake the ASO. This internalization was not selective of neuronal cells, since we also observed the presence of the missense ASO in the cytoplasm of other cell types that were negative for ChAT and had glial morphology. Double immunofluorescence against Iba1, GFAP and TPPP, which labels microglia, astrocytes and oligodendrocytes, respectively, revealed that microglia cells (Fig. 3B), as well as, astrocytes (Fig. 3C) were able to uptake the missense ASO, but oligodendrocytes did not (Fig 3D).

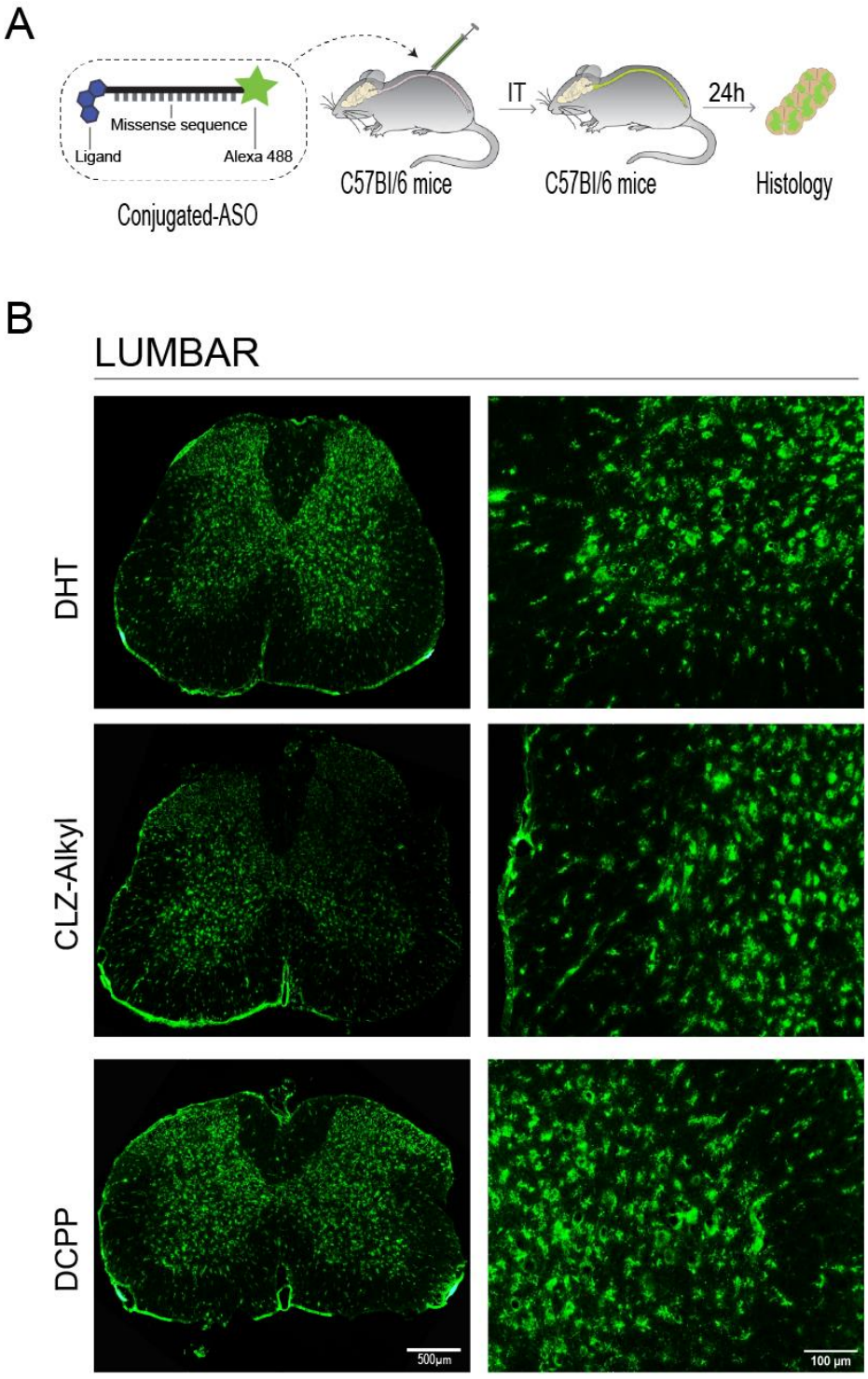

Figure 2. Distribution of the three chemically-conjugated missense ASO in the spinal cord at 24 hours after their intrathecal delivery. (A) Schematic figure of the procedure performed. (**B**) Representative cross tissue sections of the lumbar spinal cord showing the presence of the three chemically-conjugated missense ASO in the cytoplasm of cells located, preferably, in the gray matter. (n=4 per group).

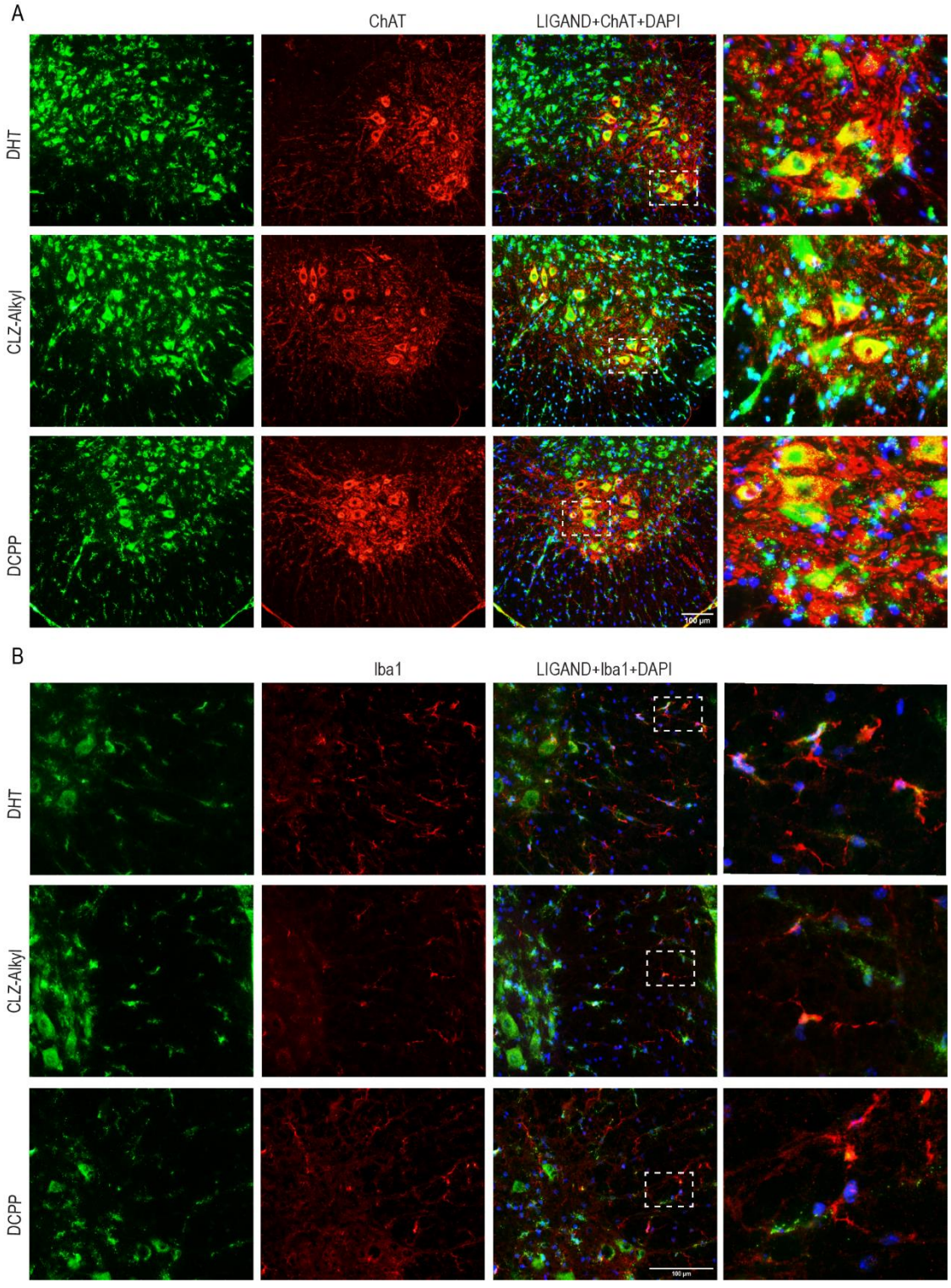
A
ChAT
LIGAND+ChAT+DAPI
DHT
CLZ-Alkyl
DCPP
100 µm
B
Iba1
LIGAND+Iba1+DAPI
DHT
CLZ-Alkyl
DCPP
100 µm

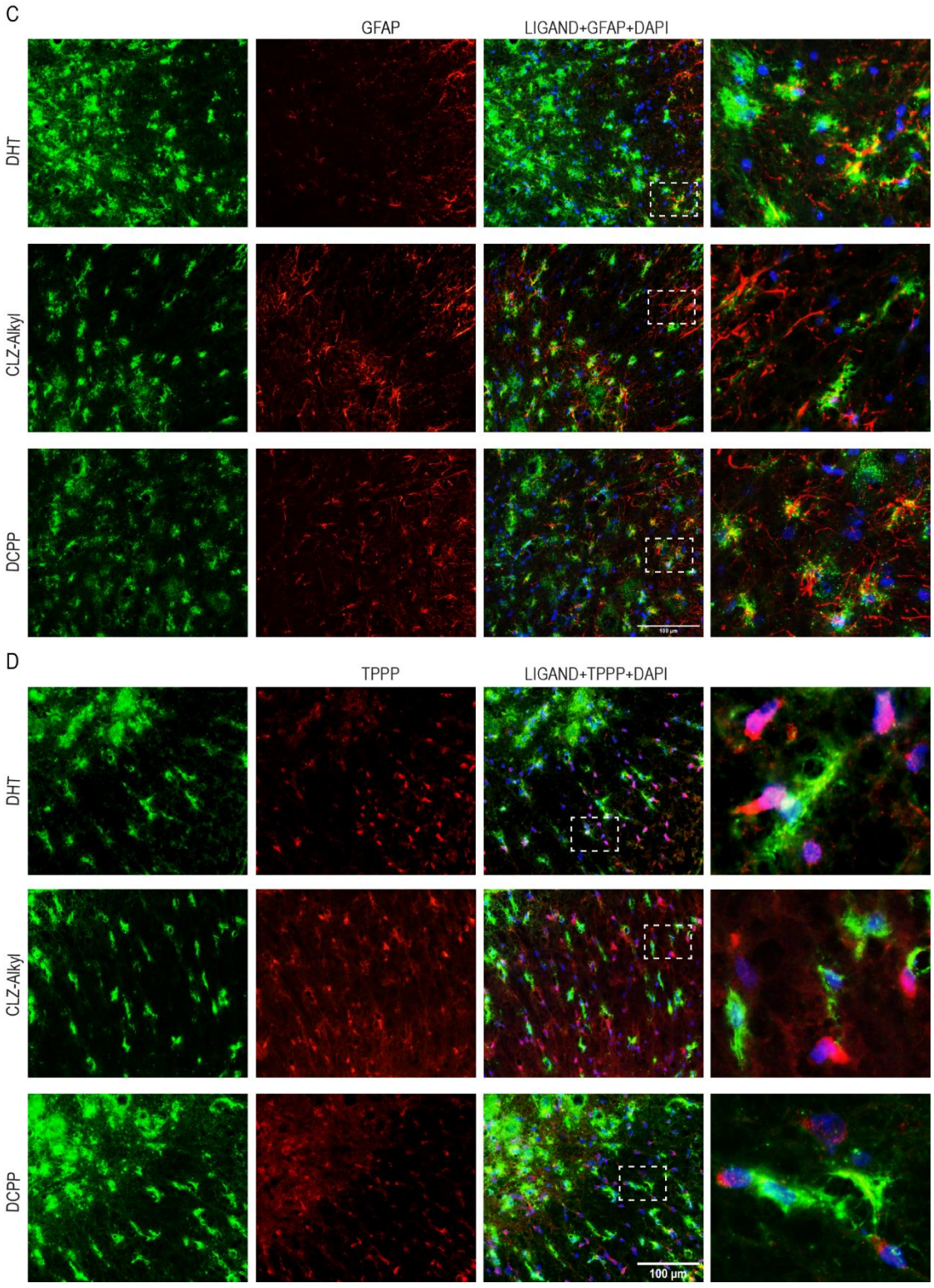

Figure 3. Neurons, microglia and astrocytes internalized the conjugated ASO conjugated. **(A-D)** Micrographs of the ventral horn of the spinal cord in the lumbar region at 24 hours after intrathecal administration of the ASO conjugated. Immunofluoresce against ChAT **(A)**, Iba1 **(B)**, GFAP **(C)** and TPPP **(D)** was performed to identify the cellular uptake of the ASO. Note in the merged images that the three conjugated ASO was found within motoneurons (and other neuronal cells), microglia, astrocytes but not oligodendrocytes. (n=4 per group).

We also observed that the distribution of the missense ASO was not homogenous along the SC after their intrathecal delivery, since they became accumulated in adjacent regions to the injection site but poorly diffused into distant regions, such as the cervical spinal cord (Fig 4). Indeed, in the cervical region, these molecules were mainly found at the meninges but their presence within the cells of the spinal cord parenchyma was scarce (Fig 4).

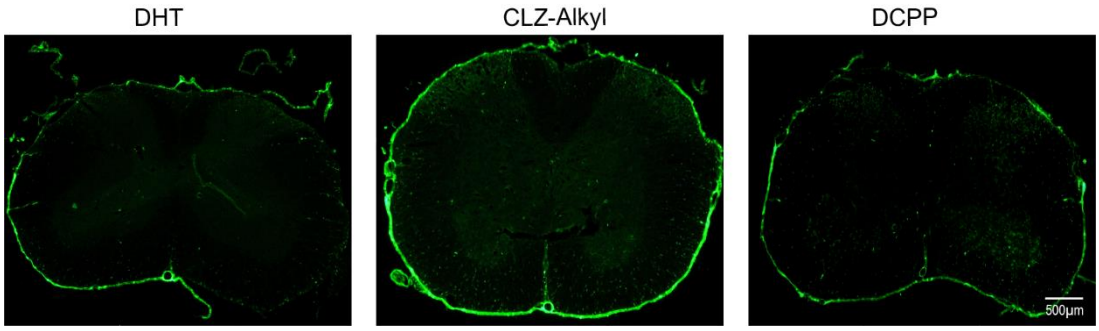

Figure 4. Distribution of the conjugated ASO in the cervical spinal cord at 24 hours following intrathecal administration. Representative images from cross tissue sections of the cervical of the spinal cord revealing the absence/limited of the conjugated ASO within the spinal cord parenchyma at 24 hours following intrathecal administration (n=4 per group).

To solve this limitation, we next assessed whether the distribution of the conjugated missense ASO was improved within the CNS by doing intracerebroventricular (ICV) administration. These experiments demonstrated this delivery route enhanced the distribution of the missense ASO along the whole CNS, and the ASO were detected in the cytoplasm of cells resembling neurons and glial cells, preferably in the gray matter of the SC, in the cervical and lumbar region (Fig. 5). Based on these results, ICV administration was chosen for the delivery of the conjugated-ASO in the following experiments of the study.

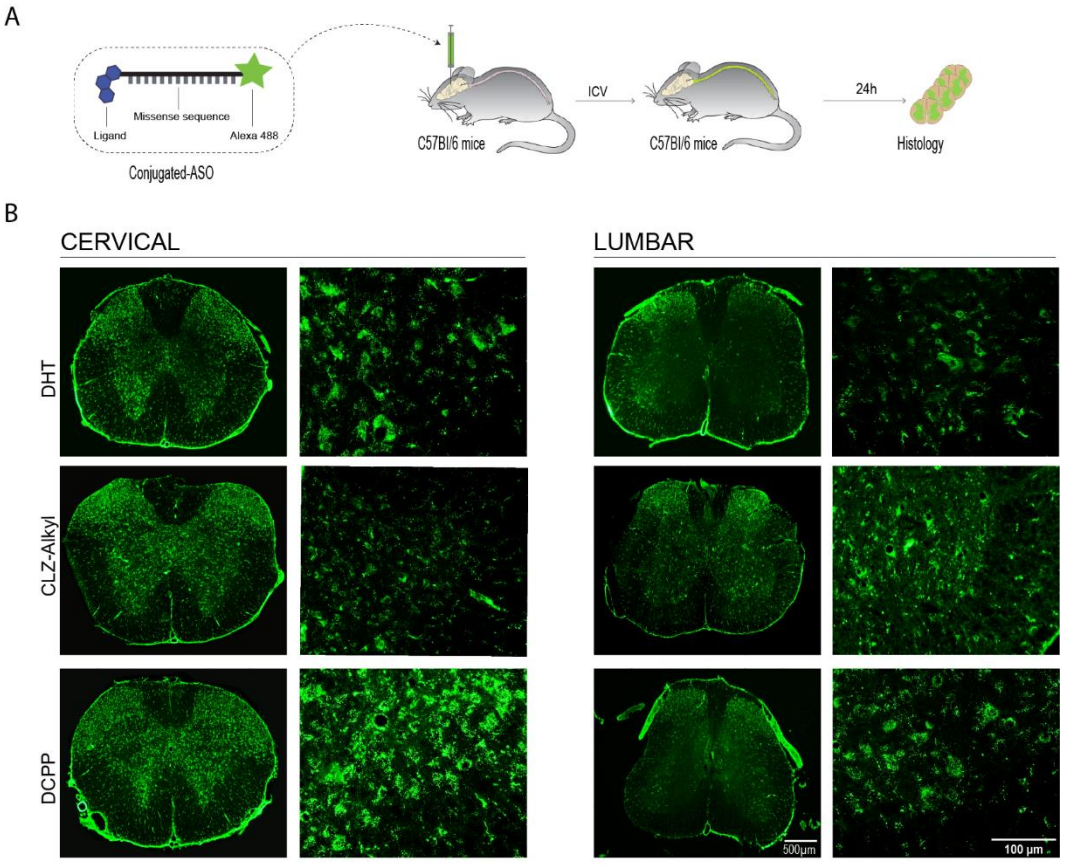

Figure 5. **Distribution of the conjugated ASO in the spinal cord at 24 hours following intraventricular injection**. **(A)** Schematic figure of the procedure performed. **(B)** Representative images of cross tissue sections of the spinal cord at cervical and lumbar region. Note the presence of the three conjugated ASO within the spinal cord parenchyma of these two regions and their efficient internalization in the cells, preferentially, of the gray matter (n=4 per ligand DHT, n=4 per ligand CLZ-Alkyl n=3 per ligand DCPP).

We next assessed whether our chemically-conjugated missense ASO were degraded or remained within the cells in the CNS. For this reason, the three-fluorescent conjugated-ASO were administrated ICV in C57Bl/6 mice and 1 week later we assessed their presence in the SC tissue (Fig 6A). These experiments showed the missense ASO were detected in the cytoplasm of cells located in the cervical and lumbar regions of the SC. The biodistribution of the conjugated-ASO was very similar to that observed at 1 day after delivery, since they were found within neuronal and glial cells, preferably, in the gray matter of the SC (Fig 6B). These experiment demonstrated that the conjugated missense ASO persisted within the CNS cells for at least 1 week.

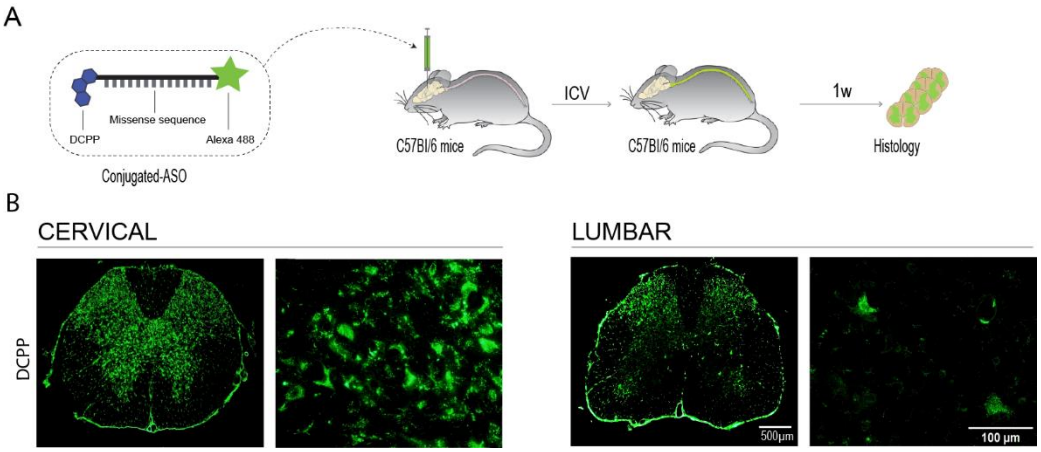

Figure 6. Durability of the conjugated ASO in the spinal cord. (A) Schematic figure of the procedure performed. **(B)** Representative images of cross tissue sections of the spinal cord at cervical and lumbar region demonstrating that the presence of the conjugated missense ASO within the cells at 1 week after intraventricular administration (n=3).

Once we demonstrated the efficient internalization of the three compounds in neurons and glial cells of C57Bl/6 mice in vivo, we next studied whether these conjugated missense ASO were able to internalize within CNS cells of SOD1^{G93A} mice, a mouse model of ALS,. For this purpose, we administrated the three compounds in SOD1^{G93A} mice at 110 days of age, corresponding to the onset of the pathological signs of the disease (Fig 7A). Histological analysis of the spinal cord revealed that the missense ASO were detected in the cytoplasm of cells resembling neurons and glial cells, preferably, in the gray matter (Fig 7B). Indeed, the distribution of the conjugated missense ASO in the SC of SOD1^{G93A} has the same pattern of internalization to that observed in C57Bl/6 mice. These experiments revealed that the conjugated-ASO are efficiently internalized by CNS cells of SOD1^{G93A} mice, our disease animal model of interest.

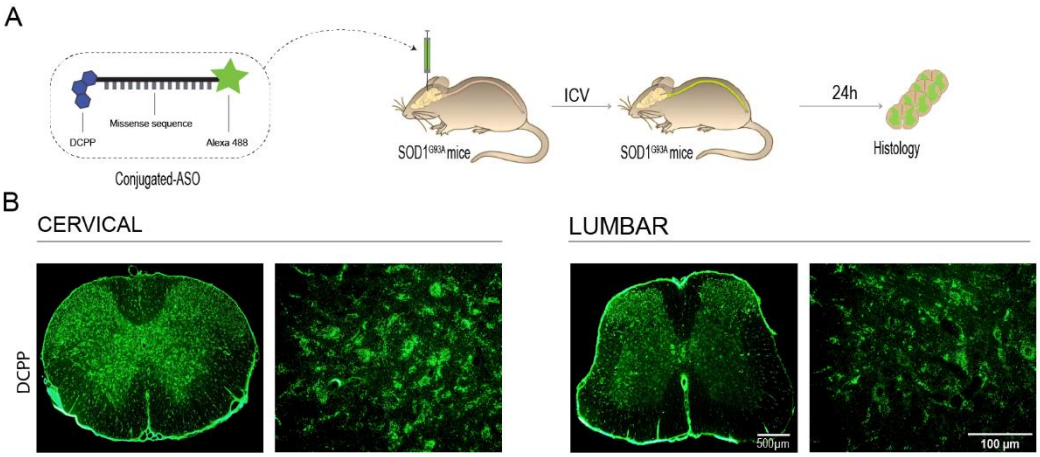

Figure 7. Cells from the spinal cord of SOD1^{G93A} mice are able to internalize the conjugated missense ASO. (A) Schematic figure of the procedure performed. **(B) R**epresentative images of cross tissue sections from the spinal cord of ALS mice at the cervical and lumbar region. Note that the conjugated ASO is able to be internalized by cells, preferably, from the gray matter (n=3).

Conjugation of ASO leads to greater efficacy in reducing *SOD1* RNA levels in ALS mice

We then assessed whether ICV delivery of a therapeutic ASO (CCGTCGCCCTTCAGCACGCA) that selectively targets the mutated human *SOD1* gene decreases SOD1 RNA levels and whether its conjugation enhances the efficacy. The SOD1 sequence was obtained from (Miller et al., 2013b), which does not show homology to other genes by BLAST search.

We firstly studied whether the DHT conjugated *SOD1* ASO (ASO 333611) was able to internalize into CNS of SOD1^{G93A} mice. Similar as reported above, the therapeutic (*SOD1*) ASO was found in the cytoplasm of neuronal and glial cells, preferably in the gray matter of the SC at 1 and 3 weeks after administration (Fig. 8A). We also assessed whether unconjugated *SOD1* ASO was uptaken by CNS cells, and observed a that this *therapeutic* ASO was also internalized by CNS even in the lack of a chemical conjugation (Fig. 8).

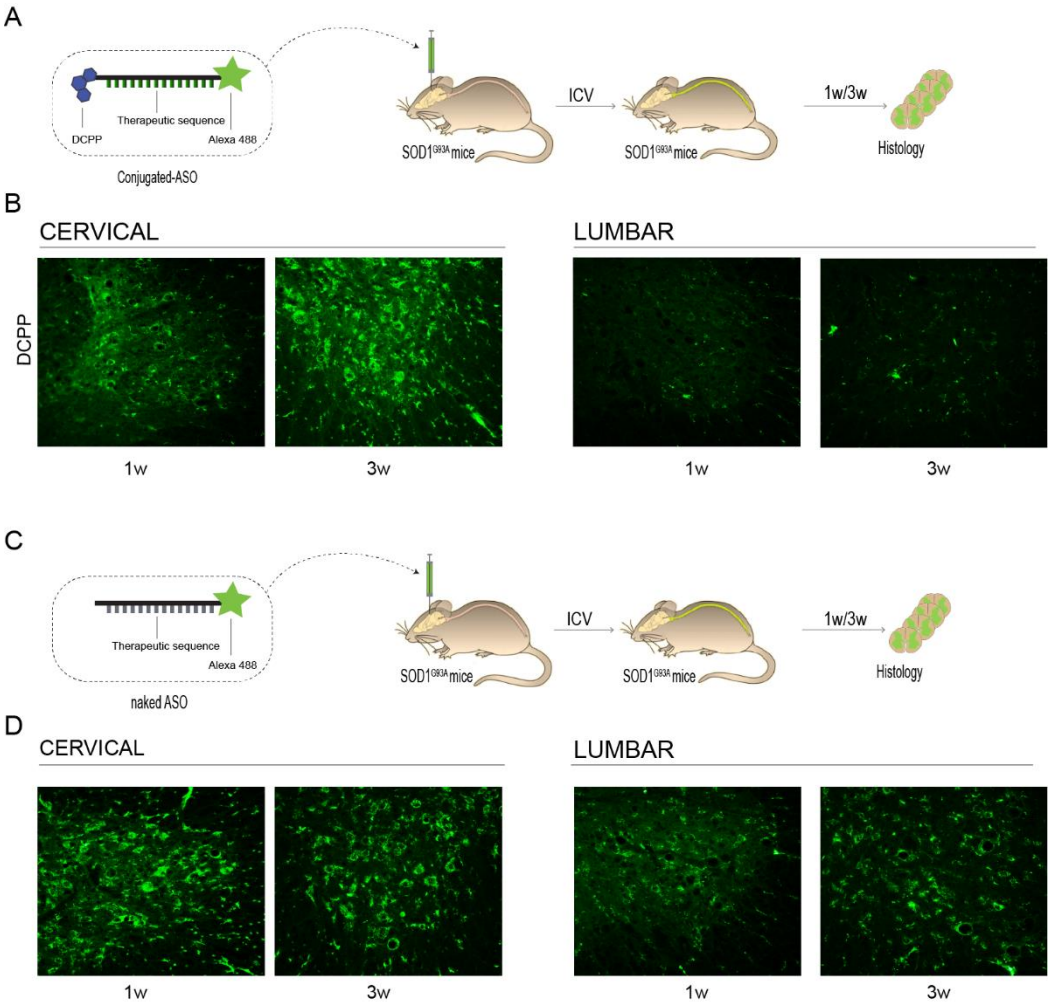

Figure 8. Distribution of the therapeutic ASO in the spinal cord of SOD1^{G93A} mice (A, D) Schematic figure of the procedure performed (**B, D**) Representative images of cross tissue sections from the spinal cord of ALS mice at the cervical and lumbar region showing the presence of the conjugated therapeutic ASO **(B)** and naked therapeutic ASO **(D)** at 1 and 3 weeks after intrathecal delivery. Note, that both, conjugated and naked ASO are internalized cell located, preferably, in the gray mater. (n=4 per time point).

In order to assess whether the presence of chemical ligand led to greater internalization of ASO in CNS cells of SOD1^{G93A} mice, we determined the levels of *SOD1* RNA at 2 weeks following ICV injection of a low dose (20nmoles) of the therapeutic ASO (unconjugated; and DCPP- and -DHT conjugated *SOD1*-ASO) (Figure 9). QPCR analysis revealed that unconjugated ASO reduced the RNA levels of *SOD1* by ~30% in the brain, as well as, in the cervical and lumbar region of the SC, demonstrating the effectivity of this siRNA sequence. DHT-conjugated ASO led to similar reduction in the transcripts of *SOD1* in these three regions of the CNS as compared to the unconjugated ASO. However, the DCPP-conjugated ASO reduced by ~60% the RNA levels of *SOD1*

in the brain and SC, doubling the efficacy of the unconjugated ASO in reducing the transcripts of this mutated gene.

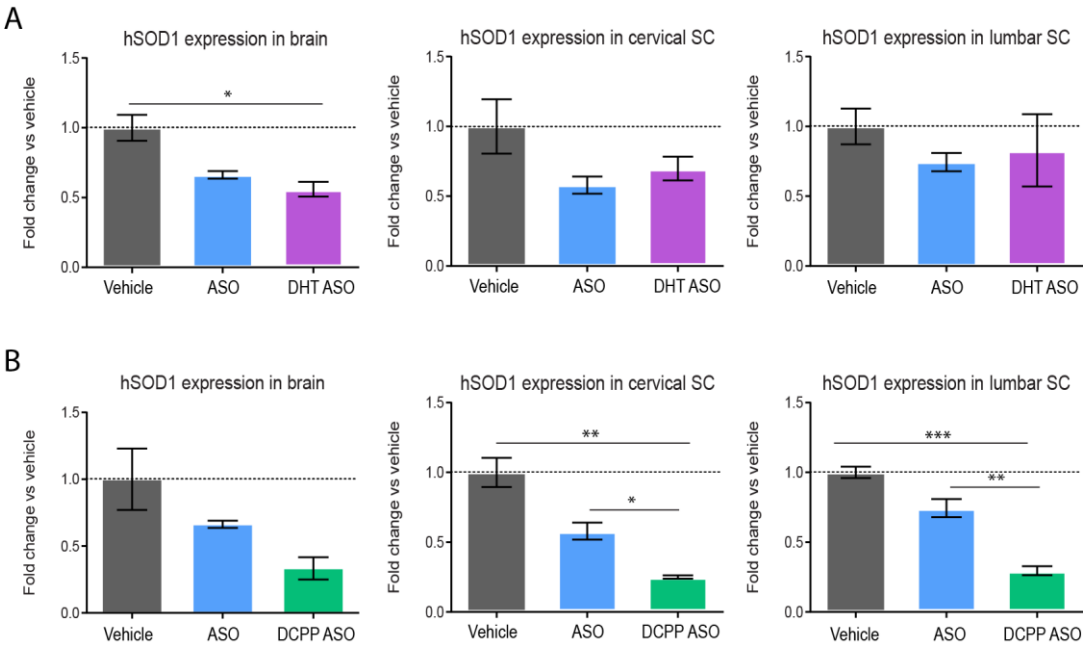

Figure 9. Therapeutic ASO conjugated with DCPP enhances h*SOD1* silencing in SOD1^{G93A} mice. (A-B) Plots showing the mRNA levels of *hSOD1* relative to vehicle in the brain, cervical and lumbar spinal cord region after ICV administration of the vehicle, naked therapeutic ASO, DHT and DCPP-conjugated ASO . N=3 for each group. One- way ANOVA, Bonferroni's post hoc test. Data is presented as mean *p<0.05, **p<0.01, *** p< 0.001 vs Vehicle. Data is presented as mean ±SEM.

Effects of ASO-Induced *SOD1* knockdown in disease progression in SOD1^{G93A} mice

To assess whether the conjugation of ASO-induced *SOD1* silencing with DCPP increased the therapeutic potential of this approach, we studied their effects in ALS disease progression. For this purpose, we ICV administered 20 nmoles of naked-, DCPP-conjugated *SOD1* ASO or saline (vehicle) in SOD1^{G93A} mice, at 8 weeks of age, and evaluated the progression of the disease. Rotarod test revealed that ASO therapy tended to delay the onset of ALS disease, as well as, to slow its progression as compared to vehicle-treated animals. This effect was more evident in females and in males (Fig. 10A, B), however, it did not reach statistical significance due to the low number of animals used. Electrophysiological analysis done based on the amplitude of the compound muscle action potential (CMAP) in the gastrocnemius (Fig 10C) and tibialis anterior muscle (Fig 10D) also revealed that the neuro-muscular integrity tended to be enhanced after the administration of the therapeutic AS. In line with the functional data, the therapeutic ASO also increase mice by 10 days the lifespan of the mice, in male and female mice, although this not reach statistical significance (Fig 10E). However, the conjugation of the therapeutic ASO with DCPP did not show any improvement in the course of ALS disease as compared to the unconjugated ASO.

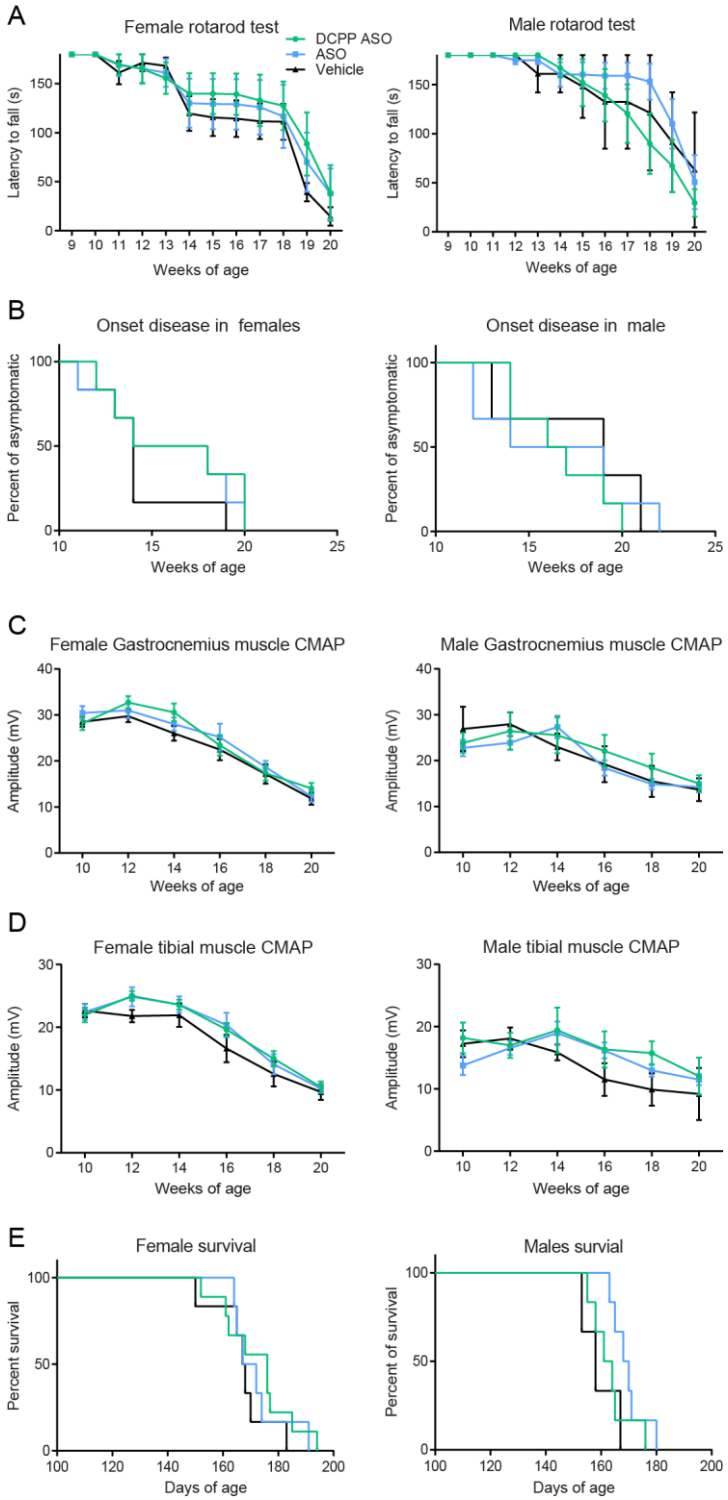

Figure 10. Effects of single administration of the therapeutic ASO conjugated with DCPP in disease progression of ALS. (A-E) (A, B) Graph showing the effect of the different therapies on functional outcomes assessed by rotarod test. **(C, D)** Electrophysiological test showing the compound muscle action potential amplitude in gastrocnemius and **(C)** tibialis anterior muscle. **(D)** of treated ALS mice. (E) Graph showing the lifespan of ALS mice after the different treatments. **A, C, D** Two-way ANOVA, Bonferroni's post hoc test. **B** and **E** Mantel-Cox test. males (n=3 in

vehicle, n=6 in ASO and n=6 in DCPP ASO), females (n=6 in vehicle, n=6 in ASO and n=9 in DCPP ASO). Data is presented as mean ±SEM.

CHAPTER II:

Contribution of the LPA-LPA_2 axis in the physiopathology of ALS

LPA levels are increased in ALS patients

Our laboratory has recently revealed that LPA contributes to the physiopathology of spinal cord injury (Santos-Nogueira et al., 2015; López-Serrano et al., 2019) However, whether this lipid mediator exerts detrimental actions in neurodegenerative disease, such as ALS, has not been addressed yet. In this chapter, we focused our attention in studying the involvement of LPA in ALS. For this purpose, we firstly performed a pilot study to know whether levels of this bioactive lipid are increased in the CSF of ALS patients. We therefore measured by mass spectrometry the concentration of LPA in CSF samples from three different ALS patients collected at the diagnosis of the disease, as well as, from two patients diagnosed with multiple sclerosis (MS) and multiple mononeuritis (MM). Levels of LPA are not increased in MS patients (Schmitz et al., 2017), and thus, it provides approximative values about the concentration of this lipid in healthy individuals.

Mass spectrometry analysis detected three LPA species in the CSF samples; 16:0, 18:0 and 18:1 LPA. Among them, 16:0 and 18:1 LPA were the most abundant species in the CSF of the MS patients, while the levels of 18:0 LPA were ~50 fold less abundant (Fig. 1A). Similar LPA levels were detected in the CSF sample from the MM individual, although 18:0 LPA was increased by 2 fold. However, these LPA species were increased in the three ALS patients (Fig. 1A). 16:0 LPA increased in ALS relative to MS, ranging from 57% to 406%. 18:1 LPA levels increased in ALS patients from 153% to 271% in comparison to MS (Fig. 1A). Strikingly, Levels of 18:0 LPA were markedly increased in the three ALS patients, being 17 to 52 fold higher than in those CSF samples from the MS patients (Fig. 1A). Importantly, we also observed a close association between the levels of these 3 LPA species with the onset and progression of disease (Fig 1B, C). Specifically, higher levels of LPA were associated with earlier disease onset and faster disease progression (Fig 1B, C). The results of this pilot study, despite the low number the patients used, suggests that LPA might be involved in ALS physiopathology.

LPA exerts its biological effects by binding to 6 G protein-coupled receptors, known as $LPA_{1\text{-}6}$. We recently demonstrated that among the different LPA receptors, only LPA_1 (Santos-Nogueira et al., 2015b) and LPA_2 (López-Serrano et al., 2019) contribute detrimentally to spinal cord injury. Therefore, we examined the RNA levels of *LPA_1* and *LPA_2* in the spinal cord (SC) tissue necropsies from ALS and control individuals. QPCR analysis revealed that *LPA_1* was constitutively expressed in the SC and its levels did not differ in ALS (Fig. 1D). The expression of *LPA_2* in the SC of control individuals was ~3 fold lower relative to LPA_1. However, levels of *LPA_2* increased ~2 fold in ALS patients

(Fig. 1E). Based on this data, we focused our work on studying the contribution of LPA-LPA_2 signalling in ALS.

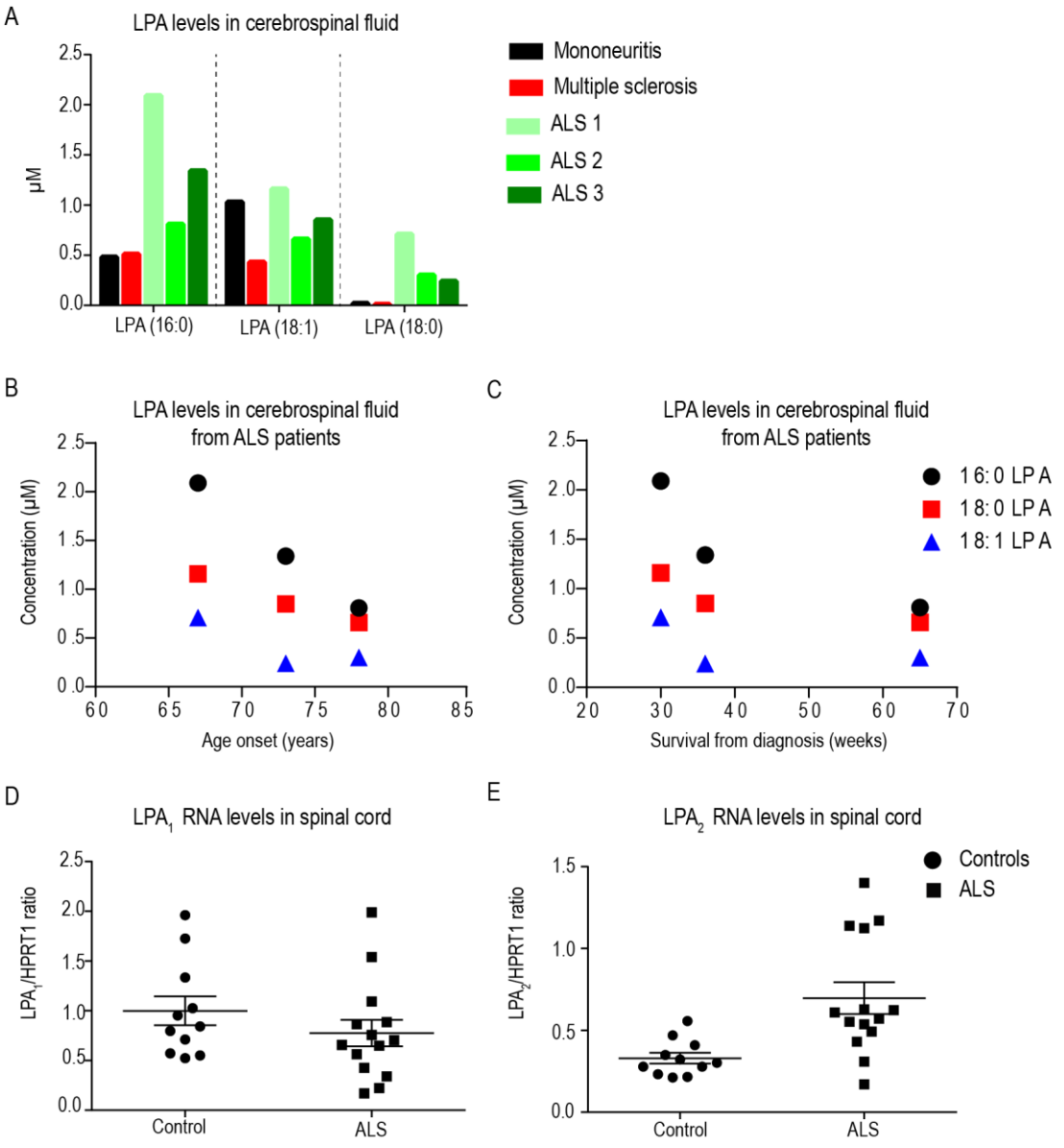

Figure 1. Characterization of LPA and the LPA receptors, LPA_1 and LPA2, in ALS patients. **A**. Graph showing the concentration of LPA species in cerebrospinal fluid of ALS patients (n=3) and two other neurodegenerative disease, mononeuritis (n=1) and multiple sclerosis (n=1). Note the increased levels of LPA species in ALS patients, preferably, of 16:0 and 18:0 LPA. (**B, C).** Plot showing the association between the levels of LPA with the onset (**B**) and progression of disease (**C**). (**D, E)** Quantification by QPCR of RNA levels of LPA_1 (**B**) and LPA_2 (**C**) in spinal cord of ALS patients (n=14) and controls (n=11). One-way ANOVA, Bonferroni's post hoc test. Errors bars indicate ±SEM.

Characterization of LPA_2 expression in $SOD1^{G93A}$ mice

We next characterized the expression of LPA_2 in the SC, sciatic nerve and muscle of $SOD1^{G93A}$ mice along disease progression. QPCR data revealed that *lpa₂* RNA levels increased progressively in the SC after disease onset, although this did not reach statistically significance as compared to SC of C57Bl/6 mice (Fig. 2A). Transcripts for LPA_2 in the sciatic nerve of $SOD1^{G93A}$ mice also increased progressively over disease progression, reaching the peak expression at the age of 16 weeks, and declined afterwards. At 16 weeks of age, the RNA levels of *lpa₂* in the sciatic nerve of $SOD1^{G93A}$ mice was increased ~2.5 fold as compared to C57Bl/6 mice (Fig. 2B). *Lpa₂* expression in the gastrocnemius muscle of $SOD1^{G93A}$ mice followed the same pattern than that observed in the sciatic nerve, but *lpa₂* transcripts were significantly increased at at 16 and 20 weeks of age as compared to C57Bl/6 mice (Fig. 2C).

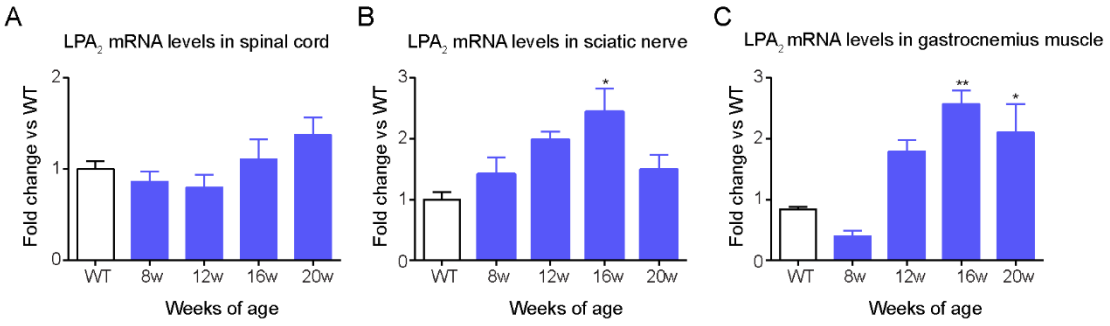

Figure 2. Dynamic changes in LPA_2 expression in $SOD1^{G93A}$ mice. (A-C) Graph showing the changes in *lpa₂* RNA levels in the spinal cord (**A**), sciatic nerve (**B**) , and gastrocnemius muscle (**C**) of $SOD1^{G93A}$ at 8, 12, 16 and 20 weeks of age mice relative wt littermate mice. **A** n=5 per group and time point. **B** and **C** n=3 per group and time point. One-way ANOVA, Bonferroni's post hoc test. *p<0.05, **p<0.01 vs WT mice. Data is presented as mean ±SEM.

LPA_2 accelerates the clinical signs of ALS but increases lifespan.

We then assessed the role of LPA_2 in the pathophysiology of ALS. For this purpose, we crossed $SOD1^{G93A}$ mice with *lpa₂* knockout mice. This double transgenic mouse ($SOD1^{G93A}$-$LPA_2^{-/-}$) will undergo ALS but it will lack LPA_2 signalling. We observed that the absence of LPA_2 significantly slowed the onset and progression of the disease in both, males and females (Fig. 3 A, D). Indeed, rotarod test revealed that genetic deletion of *lpa₂* delayed the onset of the disease in 4 and 5 weeks, in female and male mice, respectively (Fig 3 C, F). Unexpectedly, the lack of LPA_2 did not increase the lifespan of

SOD1^{G93A}, despite its absence markedly delayed the clinical signs of the disease (Fig. 3 G,I). Indeed, male and female ALS mice lacking *lpa2* died 21 and 10 days earlier, respectively (Fig 3 H, J). These data suggest that LPA-LPA$_2$ signalling has a dual role in ALS, being detrimental at pre-symptomatic/early phases of disease but protective at late stages.

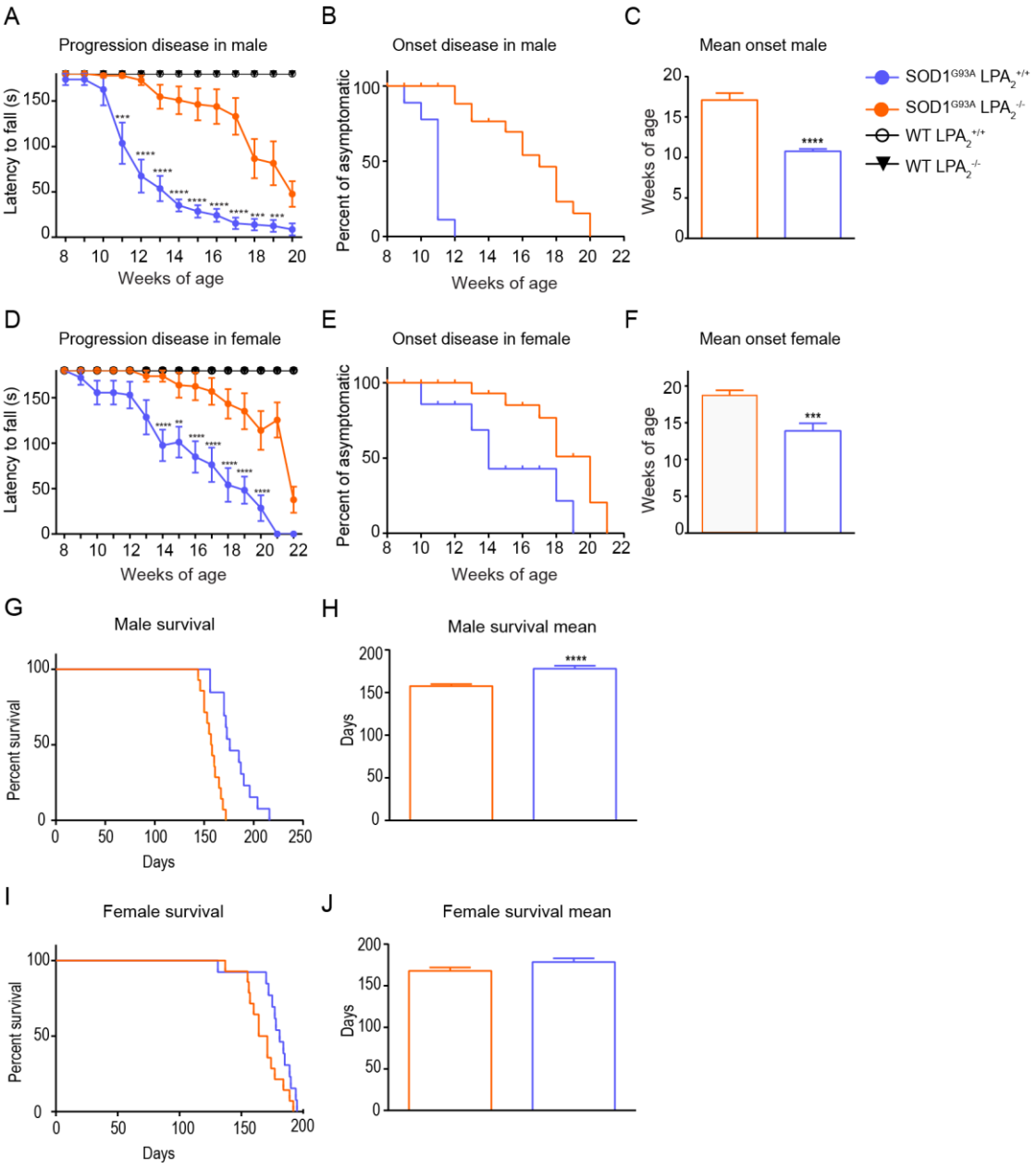

Figure 3. LPA$_2$ absence delays onset and slow progression of the disease. (A- D). Functional progression of the disease represented by the latency to fall of the rotarod test in male (**A**) and female (**D**) showing the slowness of the progression in the absence of LPA$_2$. (**B, E)** The absence of the receptor delays the onset of the disease 5 weeks in male (**C**) and 4 weeks in female (**F**). **(G-J)** Effects of the absence of LPA$_2$ in the lifespan of ALS mice. **A** and **D** Two-way ANOVA, Bonferroni's post hoc test. **B**, **E, G, I** Mantel-Cox test. **C**, **F, H, J** t-test. **A-C** Males (n=9 SOD1^{G93A}

$LPA_2^{+/+}$, n=11 $SOD1^{G93A}$ $LPA_2^{-/-}$, n= 4 WT $LPA_2^{+/+}$, n=4 WT $LPA_2^{-/-}$). **D-F** Females (n=10 $SOD1^{G93A}$ $LPA_2^{+/+}$, n=11 $SOD1^{G93A}$ $LPA_2^{-/-}$, n=4 WT $LPA_2^{+/+}$, n=4 WT $LPA_2^{-/-}$). **G-H** Males (n=14 $SOD1^{G93A}$ $LPA_2^{+/+}$, n=15 $SOD1^{G93A}$ $LPA_2^{-/-}$).**I-J** Females (n=14 $SOD1^{G93A}$ $LPA_2^{+/+}$, n=14 $SOD1^{G93A}$ $LPA_2^{-/-}$,).**p<0.01, ***p<0.001, ****p<0.0001 vs $SOD1^{G93A}$ $LPA_2^{-/-}$. Data is presented as mean ±SEM.

LPA_2 does not have any effect on motoneuron death in ALS

We then used electrophysiological and histological techniques to study the effects of LPA_2 on neuro-muscular integrity and MN survival, respectively. Compound muscle action potentials (CMAPs) of tibialis anterior and gastrocnemius muscle revealed that the absence of LPA_2 slightly increased, but significantly, the integrity of the neuro-muscular integrity at the pre-symptomatic phase of the disease (8 and 10 weeks of age) in both male and females, as well as, at early symptomatic stages (16 weeks of age) but only in female mice.(Fig. 4A-D). However, LPA_2 did not altered the neuro-muscular integrity at more advanced phases of the disease (20 weeks of age), at least the electrophysiological levels.

Since degeneration of MNs is the main feature found in both mice and ALS patients, we also quantified the number of MNs in the ventral horn of the lumbar SC regions, L4 and L5, of male ALS mice. Histological SC sections from ALS mice at 16 weeks of age, time point in which the lack of LPA_2 protected against neurological decline, revealed that the early detrimental actions of this receptor on functional outcomes were not related to MN degeneration, since no difference in MN counts were found in the lack of *lpa*$_2$. (Fig. 5 AB).

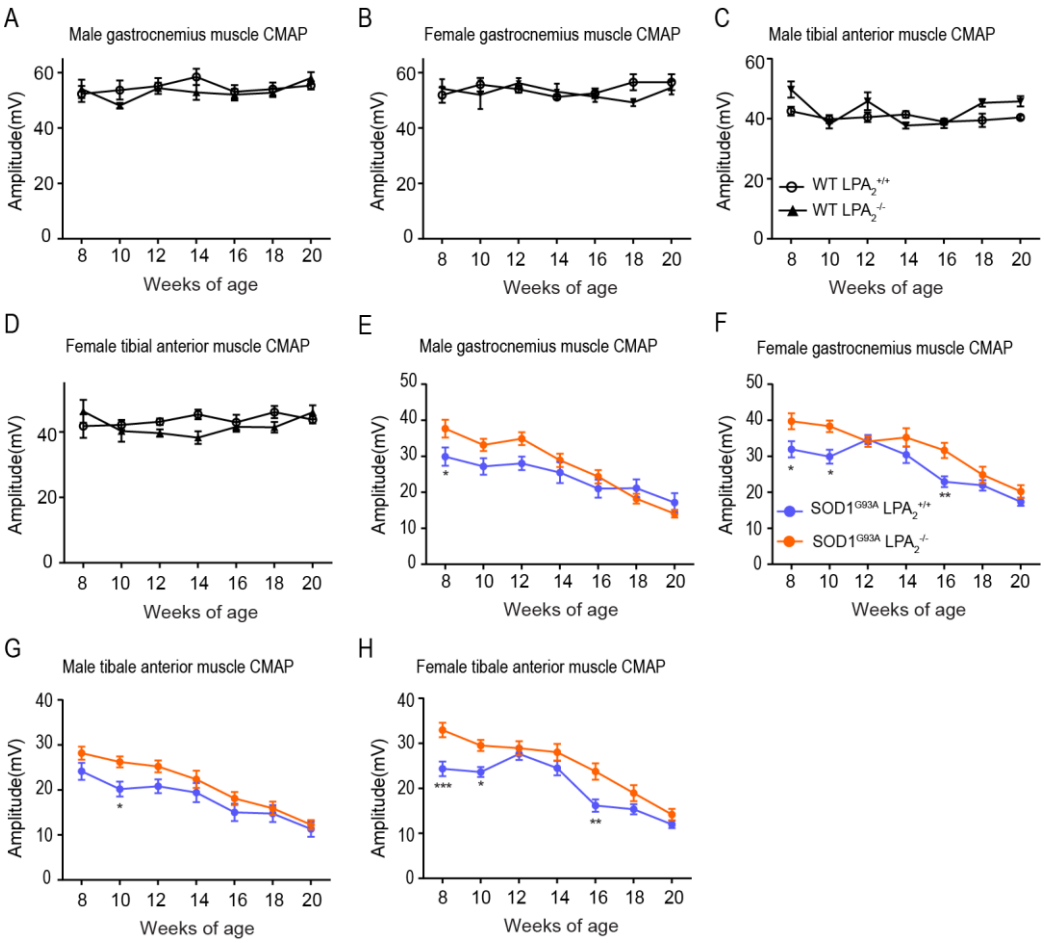

Figure 4. The lack of LPA_2 slightly preserve neuromuscular integrity in $SOD1^{G93A}$. (A-H) Plots showing the CMAP amplitude of the gastrocnemius and tibialis anterior muscle in LPA2 knockout mice and wild type littermates not carrying the $SOD1^{G93A}$ mutation **(A-D)** and in ALS mice (**E-H**) **A-H** One-way ANOVA, Bonferroni's post hoc test. **A-H** Males (n=14 $SOD1^{G93A}$ $LPA_2^{+/+}$, n=15 $SOD1^{G93A}$ $LPA_2^{-/-}$, n= 5 WT $LPA_2^{+/+}$, n=7 WT $LPA_2^{-/-}$). Females (n=14 $SOD1^{G93A}$ $LPA_2^{+/+}$, n=14 $SOD1^{G93A}$ $LPA_2^{-/-}$, n=5 WT $LPA_2^{+/+}$, n=5 WT $LPA_2^{-/-}$) *p<0.05, **p<0.01. Data is presented as mean ±SEM.

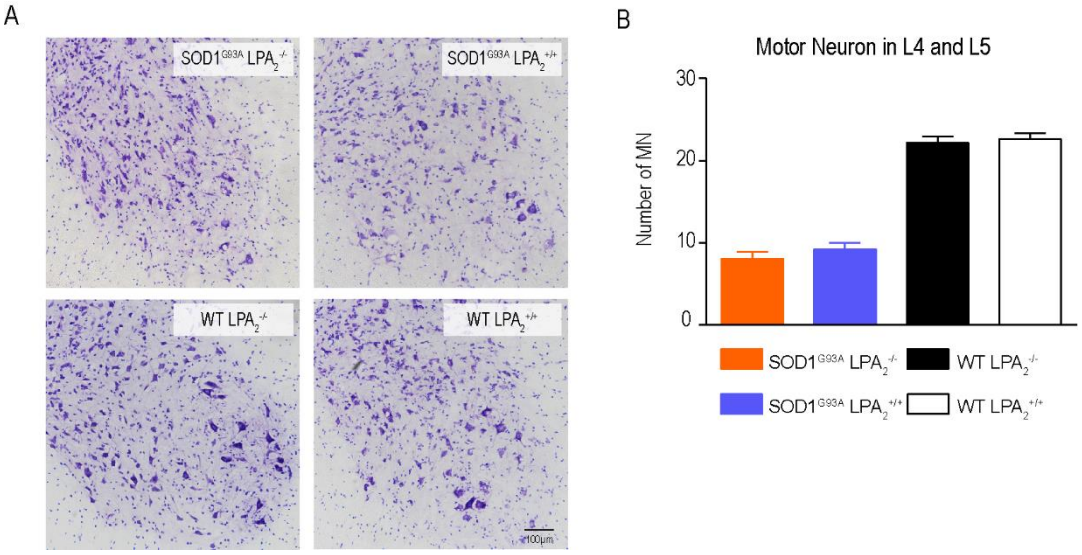

Figure 5. The absence of LPA_2 does not reduce motoneuron loss in $SOD1^{G93A}$ mice. (A) Representative micrograph of lumbar spinal cord showing motoneurons stained with cresyl violet. **(B)** Quantification of surviving motoneurons in the L4 and L5 revealing that the lack of LPA_2 does not protect against motoneuron death non neuroprotector effect in the lack of LPA_2 (n=6 $SOD1^{G93A}$ $LPA_2^{+/+}$, n=9 $SOD1^{G93A}$ $LPA_2^{-/-}$, n=7 WT $LPA_2^{+/+}$, n=8 WT $LPA_2^{-/-}$). One-way ANOVA, Bonferroni's post hoc test. Data is presented as mean ±SEM.

LPA_2 does not contribute to microgliosis and astrogliosis in ALS

We recently reported that microglial cells become cytotoxic upon LPA_2 signaling (López-Serrano et al., 2019). We therefore evaluated whether LPA_2 may contribute microgliosis or astrogliosis in the lumbar SC of $SOD1^{G93A}$ mice. Histological tissue sections of SC harvested at 16 weeks of age revealed that immunoreactivity for Iba1, a marker for microglial cells, tended to be increased in the ventral horn of ALS mice lacking LPA_2, although it did not reach statistical significance (Fig 6. A, B). Similar to microgliosis, immunoreactivity against GFAP, a marker for astrocytes, in the ventral horn of *lpa2* knockout mice showed that this receptor did not contribute to astrogliosis. (Fig 6 C, D). These results indicate that LPA_2 does not alter gliosis in ALS, at least, at early symptomatic stages of the disease.

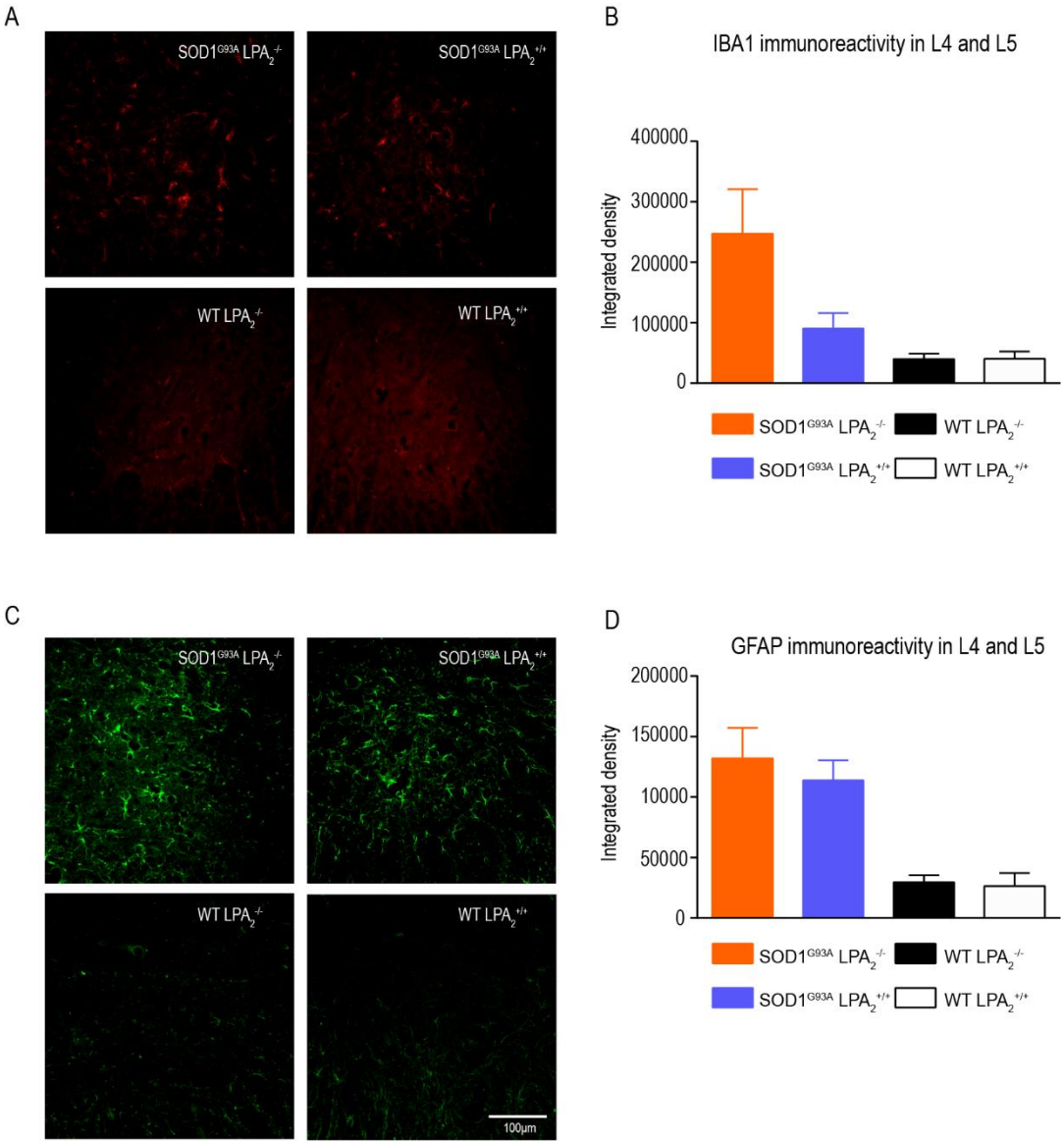

Figure 6. The lack of LPA_2 does not reduce astrogliosis and microgliosis in the lumbar spinal cord of $SOD1^{G93A}$. (A) Representative images of the lumbar spinal cord stained against IBA1. (**B)** Plot showing the quantification of the IBA1 immunoreactivity in the L4 and L5 spinal cord segments (n=3 $SOD1^{G93A}$ $LPA_2^{+/+}$, n=4 $SOD1^{G93A}$ $LPA_2^{-/-}$, n=3 WT $LPA_2^{+/+}$, n=3 WT $LPA_2^{-/-}$). (**C)** Representative images of the lumbar spinal cord showing stained against GFAP. (**D**) Graph showing quantification of GFAP immunoreactivity in the L4 and L5 segments (n=3 $SOD1^{G93A}$ $LPA_2^{+/+}$, n=4 $SOD1^{G93A}$ $LPA_2^{-/-}$, n=4 WT $LPA_2^{+/+}$, n=4 WT $LPA_2^{-/-}$). One-way ANOVA, Bonferroni's post hoc test. Data is presented as mean ±SEM.

LPA_2 absence does not enhance the preservation of myelinated axons

LPA contributes to demyelination in the spinal cord by signalling via LPA_1 (Santos-Nogueira et al., 2015b) and LPA_2 (López-Serrano et al., 2019). Since our QPCR data indicated that the transcripts of lpa_2 were increased in the sciatic nerve of ALS mice, we assessed whether the detrimental actions of LPA-LPA_2 signalling at early stages of ALS disease was due to demyelination and/or denegeration of motor axons. For this purpose, we harvested that ventral root of the L4 SC segment and quantified the number of spared myelinated axons with intact myelin sheath, and those that showed signs of wallerian degeneration. These results revealed that the number of spared motor axons tended to higher in the lack of *lpa2*, although it did not reach statistically significance (Fig. 7A, B). In this line, quantification of motor axons with signs of Wallerian degeneration did not show any difference between both experimental groups (Fig 7. A, B). The results suggest that the detrimental effects of LPA_2 in the early stages of ALS are unlikely to be mediated by cytotoxic effects of this receptor in the peripheral nerve.

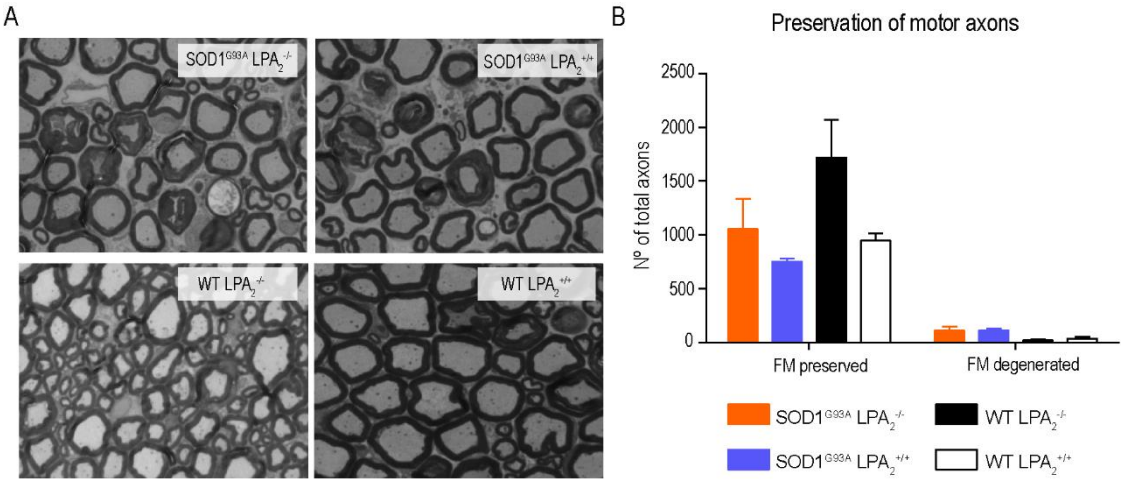

Figure 7. LPA_2 deletion does not preserve motor axons in $SOD1^{G93A}$ mice. (A) Representative cross-section images of the ventral root stained for toluidine blue. (**B)** Quantification of the total number of preserved and degenerated axons at 16 weeks of age (n=3 $SOD1^{G93A}$ $LPA_2^{-/-}$, n=5 $SOD1^{G93A}$ $LPA_2^{+/+}$, n=4 WT $LPA_2^{-/-}$, n=3 WT $LPA_2^{+/+}$). Two-way ANOVA, Bonferroni's post hoc test. Data is presented as mean ±SEM.

The absence of LPA_2 prevents muscle atrophy in $SOD1^{G93A}$ mice

Since LPA_2 transcripts were increased in the gastrocnemius muscle of $SOD1^{G93A}$ mice, we then assessed whether the early harmful actions of LPA_2 signalling in this ALS mouse was due to muscle atrophy. For this purpose, we harvested gastrocnemius muscle of the male mice from the different experimental groups at 16 weeks of age and performed histological analysis. Muscle cross tissue sections stained for haematoxylin and eosin revealed that the mean fiber thickness in $SOD1^{G93A}$ mice was significantly increased in the lack of LPA_2 (Fig 8A, B). This effect was specific for ALS mice, since the gene deletion of *lpa2* did not affect muscle fiber thickness in C57bl/6 mice (Fig 8). Further analysis based on area fiber distribution revealed that $SOD1^{G93A}$ $LPA_2^{+/+}$ presented significant higher percentage of small fibers relative to $SOD1^{G93A}$ $LPA_2^{-/-}$ mice. Contrarywise, genetic deletion of *lpa2* in $SOD1^{G93A}$ mice showed significant greater counts of larger muscle fibers (Fig. 8C). These data reveal that LPA_2 accelerates muscle atrophy in $SOD1^{G93A}$ mice.

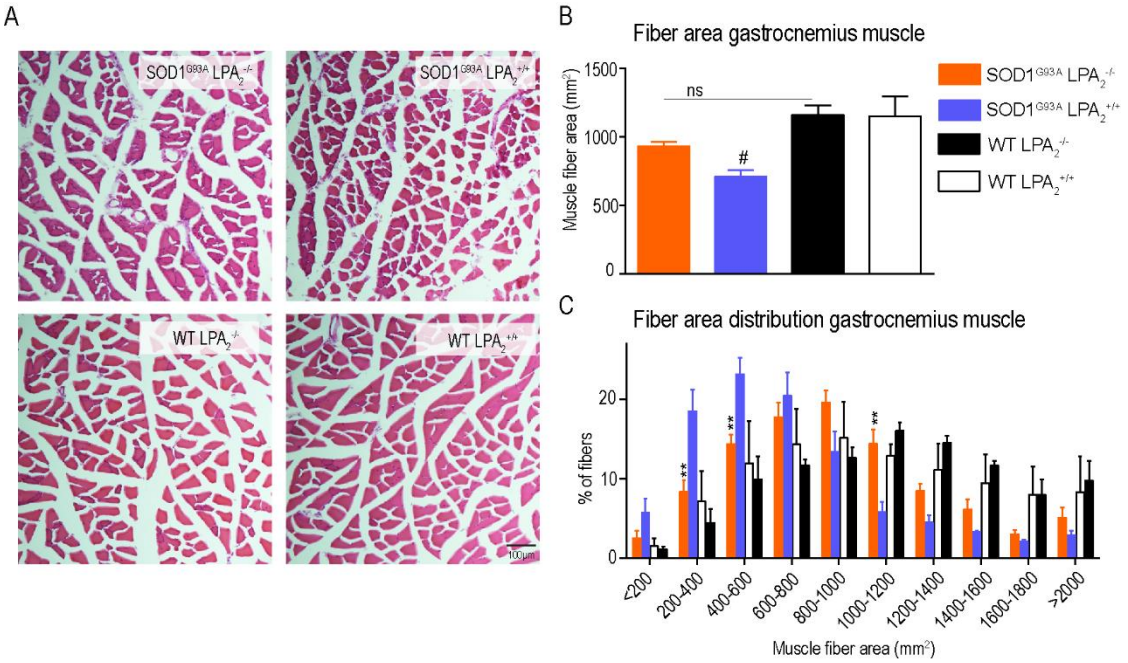

Figure 8. LPA_2 gene deletion prevents muscle atrophy in $SOD1^{G93A}$ mice. (A) Representative images of gastrocnemius muscle stained for haematoxylin and eosin. (**B)** Quantification of the muscle cross-section area at 16 weeks of age. (**C)** Plot showing the distribution of muscle fiber width. (n=4 $SOD1^{G93A}$ $LPA_2^{-/-}$, n=3 $SOD1^{G93A}$ $LPA_2^{+/+}$, n=4 WT $LPA_2^{-/-}$, n=3 WT $LPA_2^{+/+}$). One-way ANOVA, Bonferroni's post hoc test. $^{\#}p<0.05$ vs WT $LPA_2^{+/+}$ in B ; Two -way ANOVA, Bonferroni's post hoc test in C. $^{**}p<0.01$ vs $SOD1^{G93A}$ $LPA_2^{-/-}$. Data is presented as mean ±SEM.

Collateral sprouting of motor axons is one of the potential mechanisms that may explain the protection against muscle atrophy observed in the muscles of $SOD1^{G93A}$-$LPA_2^{-/-}$ mice in the lack of greater MN survival. For this reason, we evaluated whether neuromuscular junction (NMJ) integrity of the gastrocnemius muscle of ALS mice at 16 weeks of age. Histological section of revealed that the number of innervated endplates in the gastrocnemius muscle was not affected in the lack of *lpa*$_2$ (Fig 9E). To confirm these findings, we also assessed this phenomenon electrophysiologicaly by means of the estimation of the motor unit number (MUNE). In line with histological data, we found that the absence of *lpa*$_2$ did not increase the MUNEs (Fig. 10A), the mean amplitude of single motor unit potential (SMUA) (Fig. 10B) and the frequency distribution of motor unit potential amplitude (Fig 10C). These data suggest that collateral sprouting is not the mechanisms that explains harmful effects of LPA_2 on muscle atrophy.

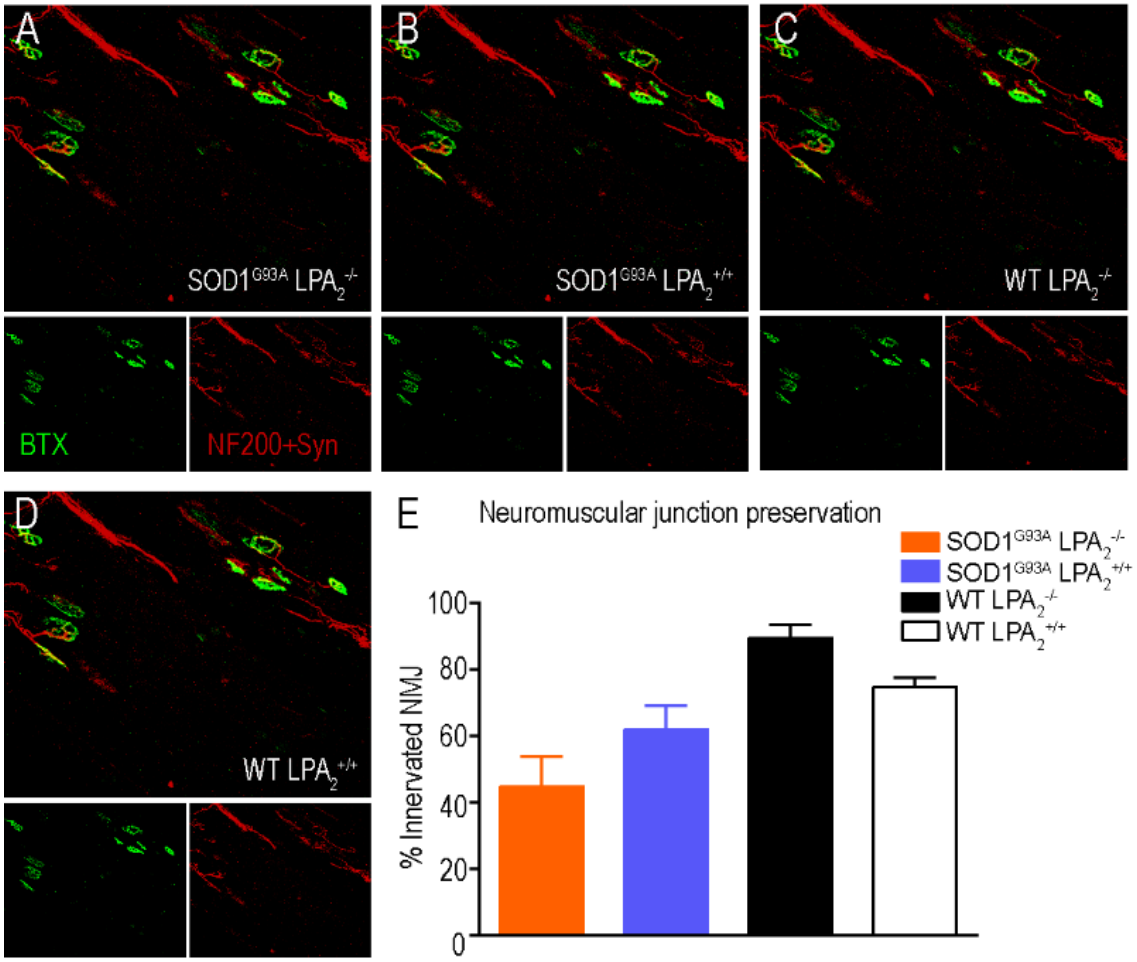

Figure 9. The absence of LPA_2 does not increase neuromuscular junction preservation. (A-D). Representative confocal images of neuromuscular junction (NMJ) of gastrocnemius muscle at 16 weeks of age. Immunolabeling against α-bungarotoxin (nicotine receptor), neurofilament 200 + synaptophysin (synapse) was done to show the innervated and dennervated motor NMJ. (E) Plot showing the percentage of innervated NMJ (overlap of signals) in the different groups (n=4 $SOD1^{G93A}$ $LPA_2^{-/-}$, n=4 $SOD1^{G93A}$ $LPA_2^{+/+}$, n=4 WT $LPA_2^{-/-}$, n=3 WT $LPA_2^{+/+}$). One-way ANOVA, Bonferroni's post hoc test. Data is presented as mean ±SEM.

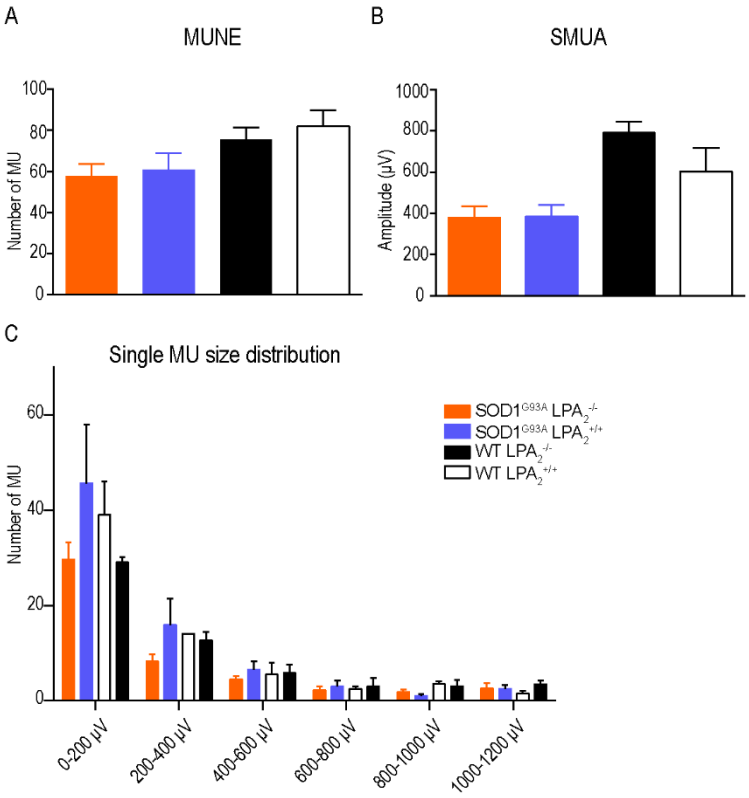

Figure 10. The absence of LPA_2 does not enhance collateral sprouting. (A-C) Electrophysiological estimation of motor unit number (**A**), mean amplitude of single motor unit potential (**B**), and single size of motor units (**C**) of the gastrocnemius muscle at 16 weeks of age. Note that the absence of LPA_2 does not alter any of these parameter (n=5 $SOD1^{G93A}$ $LPA_2^{-/-}$, n=8 $SOD1^{G93A}$ $LPA_2^{+/+}$, n=5 WT $LPA_2^{-/-}$, n=3 WT $LPA_2^{+/+}$). **A-B**. One- way ANOVA and **C** Two-way ANOVA, Bonferroni's post hoc test. Data is presented as mean ±SEM.

A previous work revealed that muscle is a primary target of SOD1^{G93A} and that selective expression of SOD1^{G93A} in skeletal muscle cells induces atrophy and functional impairments (Dobrowolny et al., 2008). Thus, we then studied whether the lack of LPA_2 signalling slowed muscle atrophy or, by contrast, protected against muscle toxicity caused by SOD1^{G93A}. For this purpose, we induced muscle denervation in *lpa*$_2$ knockout and WT littermate mice by doing sciatic nerve transection and its subsequent ligation in order to impede axon regeneration and reinnervation. Histological cross sections of gastrocnemius muscles harvested at 21 after lesion revealed that that the lack of LPA_2 did not alter muscle atrophy caused by the denervation of the nerve (Fig. 11A-C). These data therefore suggest that the lack of LPA_2 confers protection against toxicity mediated by the mutant SOD1.

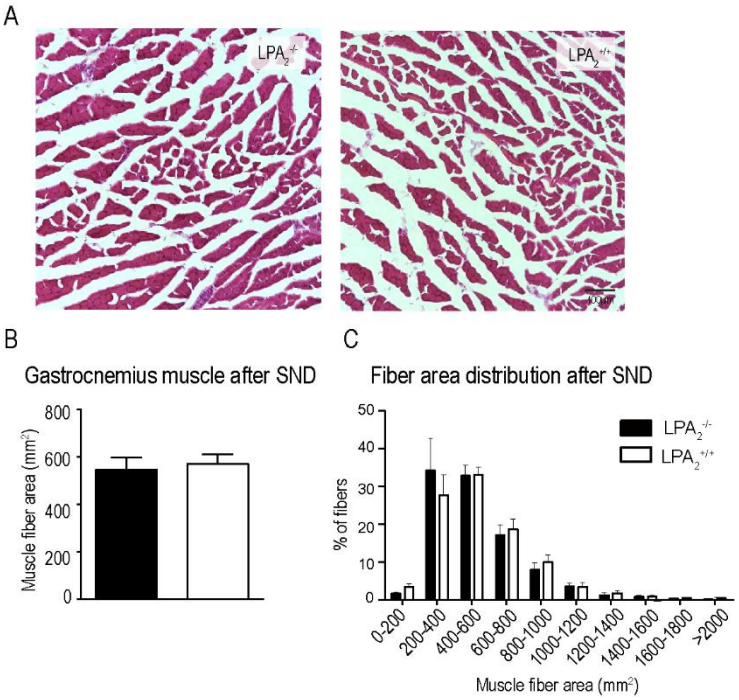

Figure 11. LPA_2 gene deletion in does not prevent muscle atrophy after sciatic nerve injury. **(A)** Representative images of gastrocnemius muscle cross tissue section at 21 days after sciatic nerve transection. (**B, C)** Plot showing the quantification of the muscle cross-section area **(B)** and the distribution of muscle fiber width **(C)**. $LPA_2^{-/-}$ mice (n=4) $LPA_2^{+/+}$ mice (n=6). T-student in **B** and one-way ANOVA with Bonferroni's post hoc test in C. Data is presented as mean ±SEM.

DISCUSSION

Unlike Charcot in 1869, our knowledge of the CNS at the molecular, genetic and functional level has increased exponentially over the last decades, as well as, our understanding on molecules, genes and processes involved in the pathophysiology of ALS (Mancuso and Navarro, 2015). Nevertheless, we do not know yet the exact mechanisms that lead to MN death in ALS, hindering the development of new therapeutic treatments.

Medicine has been able to increase the quality of life and the survival of ALS individuals in a few months by (i) handling these patients in multidisciplinary units (Mathis et al., 2017; Rodríguez de Rivera et al., 2011); (ii) treating the symptoms with pharmacological and non-pharmacological interventions; (iii) and by the administration Riluzole, the only approved drug for ALS in Europe (Bensimon et al., 1994). The cure of ALS is unlikely to occur in a mid-term scenario, and thus, further research to understand the exact mechanisms underlaying ALS is needed to develop novel and more potent therapies. The scientific community is aware that in the last 20 years, after Riluzole was approved, over 60 molecules have been investigated as potential treatments for ALS. However, the vast majority failed to demonstrate clinical efficacy (Petrov et al., 2017). This lack of success could be due to the fact that most of these treatments targeted only one of the multiple pathologic mechanisms involved in ALS. A clear example is Edaravone, one of the most novel drugs approved by the FDA to treat ALS in USA based on the positive results observed in a small cohort of Japanese patients. Edaravone (Radicava®) is an anti-oxidative compound that aims at mitigating oxidative stress. However, the European of Medicine Agency's (EMA) did approved the use of this compound for ALS in the European Union.

For many years, the main target for the treatment of ALS has been the MN since this is main character involved in the pathophysiology of this disease. However, we know now that glial cells also play a deleterious role in this neurodegenerative conditions. Consequently, in the present thesis, we proposed to evaluate the efficacy of two independent mechanisms involved in ALS, that affect neuronal and non-neuronal cells, and that they should ideally be administrated in combination. In the first chapter, we tested a new approach to increase the efficacy of gene silencing of mutant *SOD1 (SOD1G93)*. In the second chapter, we evaluated the potential of targeting LPA_2 receptor as a candidate to modulate ALS disease progression.

The first causative mutation for ALS was described in the gene that encodes for the protein SOD1 (Rosen et al., 1993b). This finding allowed the development of ALS animal models with a similar phenotype to human ALS patients (Gurney et al., 1994). Since then, the involvement of several mutant forms of SOD1 in the physiopathology of ALS has been very extensively investigated. As the main function of this enzyme is to metabolize superoxide radicals to molecular oxygen and hydrogen peroxide (Fridovich, 1986), the first pathologic mechanism described in this ALS mouse was its susceptibility against oxygen toxicity as a consequence of the loss of dismutase activity (Rosen et al., 1993a). However, later studies using this ALS mouse questioned the loss of dismutase activity as the main pathological mechanisms underlying MN degeneration since *sod*1 null mice does not show any sign of ALS (Reaume et al., 1996). In addition, despite the evidence of loss in dismutase activity also occurs in ALS patients (Robberecht et al., 1994), there is no correlation between SOD1 activity and aggressiveness of clinical phenotype (Ratovitski et al., 1999).

More than 180 mutations of the *SOD1* gene has been described so far, some of them affecting the non-catalytic part of the metalloenzyme, and the vast majority are missense mutations that does not result in a loss of function of the enzyme (Hayward et al., 2002b). This put in front the possible gain of function of the mutant SOD1 as main disease mechanism. However, this was also refuted since both elimination and elevation of wild-type SOD1 did not show any effect in mice developing ALS disease ($SOD1^{G85R}$ mouse) (Bruijn et al., 1998).

SOD1 is an homodimer, soluble, highly stable and protease resistant enzyme in its native state (Fridovich, 1986). However, maturation of SOD1 to a functional enzyme is a complex and multistep process, and any failure during protein maturation may predispose SOD1 to misfold and /or polymerize (Gill et al., 2019). It has been postulated that the toxic function of this protein comes from the increase instability of the SOD1 polypeptide, due to mutation or oxidative environment, promoting the oligomerization with itself or with other proteins and the consequent formation of aggregates (Shaw and Valentine, 2007). Several mechanisms have been related with protein misfolding and/or toxic aggregates, including the disruption of axonal transport (Tateno et al., 2009), the aberrant binding to apoptosis regulators (Pasinelli et al., 2004), inhibition of the proteasome (Cheroni et al., 2005), perturbations in mitochondrial function and Ca^{+2} homeostasis (Hervias et al., 2006), and glutamate excitotoxicity.

SOD1 aggregates have been observed in the post-mortem CNS of SOD1 fALS. Surprisingly the presence of misfolded wildtype SOD1 has been also described in the CNS of ALS patients that do not carry SOD1 mutations (Rotunno and Bosco, 2013). These findings, together with the contiguously spread of the symptoms to adjacent regions from the site of onset (Ravits and La Spada, 2009), has led to the hypothesis of ALS as a possible prion-like disease, and SOD1, as the self-propagating and transmissible prion (Münch et al., 2011). In this line, mutant SOD1 can impose its abnormal confirmation on a WT SOD1 natively folded, even in the absence of the original misfolded seed (Grad et al., 2011). Furthermore, it has been demonstrated the serially transmission of SOD1 aggregates in mice, even within different SOD1 mice strains (Ayers et al., 2014).

Two mechanisms are involved in the transmission of misfolded SOD1 between cells based on MN like cells studies (Grad et al., 2014a). The first one takes place in the early stages of disease. For unknown mechanisms, the misfolded SOD1 accumulates in the ER-Golgi system. This is then incorporated in the outer surface of the vesicles, leaves the cell via exosome release and the exosome is taken up by neighbouring cells. The second mechanisms occurs at the late stages of disease, when neural cells are injured and dying. This causes the release in the extracellular milieu of naked aggregates of misfolded SOD1 that can be taken up by neighbouring cells via micropinocytosis (Grad et al., 2014b).

In healthy cells, misfolded SOD1, along with other proteins, are immediately targeted for degradation through the ubiquitin proteasome pathway. However, in ALS, despite misfolded SOD1 is marked by the ubiquitination complex this will never end up in the proteasome, and will oligomerize and conform aggregates. However, it is still unclear the mechanism that misfolded species use to avoid the proteasome (Tashiro et al., 2012).

As a constitutive enzyme, SOD1 is expressed throughout all the life of individuals, although the disease manifests in mid-adult life when this enzyme is mutated. Since motor deficits and SOD1 aggregates are age-dependent processes in ALS mice and patients, (Wang et al., 2009), this suggest that ALS cells may present aberrant protein quality control mechanisms and lead to slow, but progressive, accumulation of misfolded SOD1 protein and aggregates along time, and consequently, exert toxicity at long term (Sibilla and Bertolotti, 2017).

Therefore, considering the toxic contribution of SOD1 in ALS through several mechanisms, together with the fact that aggregation of SOD1 is not only present in fALS individuals that carry mutations in this gene, but also in some sALS patients, a potential

approach to treat this neurodegenerative disease is to reduce the levels of SOD1 species.

Initial attempts to reduce the accumulation of SOD1 species were based on immunological approaches. Both, passive (Urushitani et al., 2007) and active (Liu et al., 2012) immunization against aminoacidic residues differentially exposed in various folded states of SOD1 resulted in beneficial effects in transgenic ALS animal models (Liu et al., 2012; Urushitani et al., 2007). Despite immunotherapy has markedly improved over the last years and now is able to selectively target the misfolded SOD1 (Patel et al., 2014), these strategies have some disadvantages. First, the antibodies do not cross the BBB, and thus, they must be administrated directly into the CNS. Second, passive immunization implies chronic administration of the antibody, or alternatively, the chronic AAV-mediated delivery of a recombinant single-chain antibody against misfolded SOD1 (Patel et al., 2014). Third, the principal target of immunotherapy is the extracellular naked misfolded SOD1, since antibodies do not cross the cell membrane. Therefore the use of antibodies will only target the extracellular misfolded SOD1 and only minimize the propagation of these protein to cells (Grad et al., 2014b). However, this therapy is incapable to stop the toxic signalling cascade that triggers the misfolded SOD1 within the cells and the lead to cell death. Despite these limitations, this approach has been able to increase the survival in treated mice models (Liu et al., 2012; Urushitani et al., 2007).

Immunotherapy against misfolded proteins has been also used to treat other neurodegenerative diseases, such Alzheimer diseases (AD). However, clinical trials using immunotherapy to treat AD have failed to show efficacy and have resulted in various adverse effects (Salloway et al., 2009). Nowadays, in an attempt to overcome the difficulties encountered to date and reduce potential adverse effects of the immunotherapy, new experimental approaches are currently being investigated, such as, the use of single chain fragment antibodies or intrabodies (Valera and Masliah, 2013). Nevertheless, these approaches are currently in development and must be deeply investigated before entering into clinical trials.

An alternative strategy to reduce SOD1 toxicity was suggested by Bertolotti based on decreasing the rate of protein synthesis to enhance the ability of chaperons to fold SOD1 correctly. It is known that the folding capacity of cells depends on the availability of chaperones, and this is inversely correlated with rates of protein synthesis (Sibilla and Bertolotti, 2017). This therapy demonstrated that the inhibition of a phosphatase regulatory subunit protects mice from ALS caused by the mutant SOD1 form, $SOD1^{G85R}$

(Wang et al., 2014). However, this approach implies the unspecific slow down for the production of all the proteins expressed under stress conditions, independently or not of the targeted protein (mutant SOD1).

Going upstream, an approach that promote RNA degradation, present an effective perspective to reduce the toxic protein even before it is translated. The silencing strategies mimic endogenous RNA interference mechanisms to specifically modify gene expression. It has been developed synthetic molecules that promote gene silencing by interacting with the different RNA species. Depending on the structure (double or single chain), nature (DNA or RNA) and chemical characteristics, each molecule will incorporate in the system to target RNA and interrupt the toxic protein formation (Crooke et al., 2018; Davidson and McCray, 2011). In the case of RNA-targeted therapeutics for ALS, the studies of silencing SOD1 include the use of siRNA, shRNA, miRNA and ASO (van Zundert and Brown, 2017b). Among these options, we used ASO to target the mutant SOD1 for the following reasons. First, the use of siRNA unlike others, requires their processing in the nucleus for the enzyme Drosha/DGCR8 (Davidson and McCray, 2011). In order to reach the nucleus, viral vectors are commonly used, which may lead to prejudicial immune responses and oncogenesis, hindering the translation to humans (Marshall, 1999; Schnell et al., 2001). The most recent viral vectors administrated, the AAV, do not show pathogenic effects, although they have small packaging capacity (Thomas et al., 2003) . Second, siRNA and shRNA match to the target RNA with only a seed of 8 nucleotides in the 3' untranslated region, increasing the off target silencing of undesired mRNA and, in consequence, the possibility of producing different side effects (Nunes et al., 2013; Scaggiante et al., 2011). Contrarywise, ASO recruits RNAse H that acts mainly in the cytoplasm. Their antisense sequence have a perfect match to the target RNA reducing the unspecific gene silencing. Moreover, ASO structure can be easily chemically modified to avoid their degradation, the immune system response and enhance their functionality (Crooke et al., 2018). The last but not the least, the ASO technology has been approved for the FDA and until 2017, six treatments has been commercialized for different diseases, including hypercholesterolemia, age-related macular degeneration and spinal muscular atrophy, which show the most promising results (Stein and Castanotto, 2017). Besides, the ASO therapy has been tested in ALS patients for safety studies (Miller et al., 2013a), there is currently a phase 3 clinical trial ongoing.

One of the main limitation of ASO therapy is the high amounts of the molecule that needs to be administered. Over the last years, chemical modifications of the ASO has been developed to reduce its therapeutic dose. Among them, the conjugation of the naked

transgene with a driver is one of the most effective ones (Jayant et al., 2016). The technology designed by the company nLife Therapeutics is based in this last option. In particular, it consisted in the conjugation of the ASO with different ligands that have high affinity for different serotonin and/ or dopamine receptors, which are expressed in neuronal and glial cells, and thus, they are likely to enhance their internalization.

Since MNs are the main cells that die in ALS (Mancuso and Navarro, 2015), we tested the internalization of missense ASO conjugated with different ligands (DCPP; DHT, CLZ-Alkyl) and tagged with Alexa 488, in NSC34*, a* MN-like cell line. These experiments revealed that the three ligands allowed the internalization of the ASO in NSC34. These results led us to study the internalization of these ASO in mice. Since the chemical modifications of the ASO are focused on enhancing their cell uptake but not to cross the BBB, we administrated the compounds by IT injection (Evers et al., 2015; Dowdy, 2017). One day after administration, we observed the presence of the ASO in the cytoplasm of most neurons, including MN, but also by microglia and astrocytes, but not in oligodendrocytes. However, the biodistribution of these molecules were not homogeneous along the SC, since they become concentrated in the lumbar spinal cord and their presence in the cervical region was scarce. Although IT administration is the most clinical relevant delivery route for drugs in the CNS (Miller et al., 2013a), we tested whether the intraventricular injection of the compounds enhanced their dissemination along the CNS. These experiments revealed that this delivery route allows the distribution of these ASO along the whole spinal cord, since they were found at cervical and lumbar regions. Moreover, we found the presence of the molecules in the cytoplasm of neurons and glial cells for at least 1 week, indicating that the ASO were not degraded for the lysosome for the first 7 days (Crooke et al., 2017).

Once verified internalization and stability in WT mice cells, we evaluated whether these conjugated-ASO were able to be internalized in the CNS cells of in our mouse ALS, the $SOD1^{G93A}$ mouse, achieving a similar pattern of distribution and durability. Importantly, the therapeutic ASO (ASO 333611) was also internalized by CNS cells of ALS mice. However, we also observed the internalization of the therapeutic ASO in the absence of any ligand.

Internalization of the ASO does not necessarily mean it is functionally reducing the transcripts of mSOD1, since ASO could be staked in the endosomal pathways. Furthermore, other uptake processes have been related to the naked ASO. For instance, Miller and colleges reported for the first time the involvement of Stabilin receptors in the binding and functional internalization of phosphorothiate ASO. However, the analysis of

the internalization in knock out animals for these same receptors also reported a slide entrance in the cells (Miller et al., 2016).

To evaluate the ability of the ligands to direct the therapeutic ASO towards a productive route, we analysed their ability to reduced hSOD1 expression after the treatment. Previous reports have shown that our therapeutic ASO needs to be administrated at a dose of 200-300 µg (40-60 nmoles) in order to be effective. We therefore evaluate whether the conjugation of the therapeutic ASO with a ligand was able to enhance the silence hSOD1 expression at approximately half of the dose (20 nmoles). Our results showed that the naked therapeutic ASO (ASO 333611) was able to reduce the levels of SOD1 by 25%. This reduction is in line with previous data using the same low dose (McCampbell et al., 2018). The same reduction was observed when the therapeutic ASO was conjugated with the ligand DHT. Interestingly, the conjugation of the therapeutic ASO with DCPP reduced the levels of SOD1 by 60%. This reduction is comparable to that observed with the naked therapeutic ASO at a dose of 600µg (120 nmoles; 6 fold higher the dose), highlighting the effectivity of this ligand to boost the functional internalization of the ASO.

Despite we demonstrated the effectivity of the DCPP-conjugated ASO in reducing hSOD1 transcript, we observed that single intracerebroventricular administration of this low DCPP-conjugated ASO only tended to delay, although not significantly, the course of the disease. Previous studies have revealed that this naked therapeutic ASO (ASO 333611) slows the progression of ALS disease in mice and rats and extends lifespan of the animals (Smith et al., 2006; Miller et al., 2008; McCampbell et al., 2018). However, in contrast to our study, the therapeutic naked ASO was administered for several times. This could explain, in part, the poor efficacy on disease progression of our approach, since the ASO was administered only once. I strongly believe that the repeated administration of low doses of DCPP-conjugated ASO would have led better therapeutic effects, at least to similar outcomes achieved by repetitive administration of high doses of naked ASO (Smith et al., 2006; Miller et al., 2008). However, these experiments could not be done since nLife Therapeutic entered into an arrangement with creditors in 2018, which impeded the progression of this project

It has to be highlighted that although there was tremendous enthusiasm in the scientific community of the results obtained from for the early SOD1 ASO (ASO 333611), the effects in the animal models were modest. This has led the development of more effective ASO designs for CNS disease. In this line, a recent work has shown that ASO containing phosphorothioate backbone modifications, 2′-O-methoxyethylribose or (S)-

2′,4′- constrained 2′-O-ethyl groups in the 5′ and 3′ wings are much more potent ASO, and its delivery in the CNS at 50 and 94 days of age resulted in striking beneficial effects on disease progression in $SOD1^{G93A}$ mice and rats, increasing the lifespan of both, mice and rats, in about 200 days (McCampbell et al., 2018).

The promising results of McCampbell and colleges support the ASO technology as a good approach for the treatment of fALS. Conjugation of these novel ASO with ligands such as DCPP, or others, could even enhance their therapeutic actions and reduce the amount needed. This may minimize the potential side effects of this technology, and importantly, to reduce the cost of the treatments in the clinical setup.

CHAPTER 2

Inflammation is the cellular and molecular response of the immune system against pathogens and injuries to protect the body from infections and promote healing and return to homeostasis. However, inflammatory response can also cause bystander effects lead to cell damage and tissue degeneration. Therefore, it is extremely important to control inflammation in space and time (Alberts B, Johnson A, Lewis J, 2002; David et al., 2012).

Ideally, inflammation is self-limiting response that follows a strict pattern of recruitment and clearance of cells from the tissue. However, if the inflammatory response is driven against an auto-antigen rather than pathogens, or if resolution does not occur properly, it may become chronic an cause damage (David et al., 2012). It must take into account that the damaging effects of inflammation are more pronounced in the CNS than in other tissues due to the limited capacity of the CNS for axon regeneration and replenishment of damaged neurons (Perretti et al., 2015).

Since the inflammatory response is crucial for tissue repair, it is important not to prevent inflammation in pathological conditions. It is better to learn how to modulate this physiological response to minimize its harmful effects. Therefore, understanding the mechanisms that mediate harmful effects of inflammation is required to design novel and more potent therapeutic approaches (David et al., 2012; Fullerton and Gilroy, 2016).

Nowadays, it is clear that inflammation is a hallmark of neurodegenerative diseases, typified by reactive morphology of astrocytes and microglia, accompanied by release of inflammatory mediators in the parenchyma (Ransohoff, 2016). This cellular and molecular reaction has been shown in ALS, in both patients and animal models (Philips and Robberecht, 2011), as wells as, in most neurological conditions such as Alzheimer,

Parkinson and frontotemporal lobe dementia among others (Newcombe et al., 2018; De Virgilio et al., 2016; Bright et al., 2019). Researchers attribute this inflammatory reaction as a consequence of neurodegeneration, understanding glial activation as a secondary phenomenon following neuronal death (Kreutzberg, 1996).

The important contribution of inflammation to ALS was demonstrated by Boillée and collaborators in 2006, when they demonstrated that genetic deletion of mutant SOD1 in microglia increases the lifespan of ALS mice, despite the mutant protein was expressed in MN and all the other cells but not microglia (Boillée et al., 2006b). This work also revealed that inflammatory response initiates in presymptomatic stages of the ALS, even before MN death. These results put in front the non- cellular autonomous theory, giving weigh the involvement of astrocyte and microglia in the pathophysiology of ALS.

Microglia display active proliferation and phenotypic changes in ALS subjects and animal models (Solomon et al., 2006; Corcia et al., 2012; Martínez-Muriana et al., 2016; Kovacs et al., 2019). Indeed, several studies have highlighted the detrimental role of microglia to ALS pathology at least *in vitro* (Xiao et al., 2007; Liao et al., 2012; Frakes et al., 2014). Our group demonstrated beneficial effects on ALS disease after reducing microglia proliferation through pharmacological blockage of the receptor known as CSF-1R (Martínez-Muriana et al., 2016). The detrimental actions of microglial cell in ALS are mediated, in part, via NFκB activation (Frakes et al., 2014). Consequently, all these findings suggest that microglia could be a therapeutic target for the treatment of ALS.

Several approaches have been proposed to modulate inflammation in ALS leading to divergent results (Fullerton and Gilroy, 2016). For instance, Celecoxib, an approved inhibitor for the COX-2 enzyme and glatiramer acetate, a drug used for the MS, have demonstrated beneficial actions in animal models of ALS, to be safe for humans, but clinical trials in ALS individual have failed to show efficacy. Another example is minocycline, an antibiotic molecule with anti-apoptotic and anti-inflammatory features, which led to positive effects in mice models of ALS mice but resulted in detrimental action in clinical trials (Cudkowicz et al., 2006; Meininger et al., 2009; Gordon, et al 2007; Petrov et al., 2017b).

Studies over the last years have demonstrated that lipids play a crucial role in the inflammatory response. Among them, lipids such as of lysophospholids (LPLs), have demonstrated to modulate detrimental action of inflammation, including in the CNS (David et al., 2012). LPA is a LPLs that acts as extracellular and intracellular signalling molecule and controls a wide variety of physiological responses. The effects of LPA are mediated by 6 G protein-coupled receptors known as LPA_1-LPA_6 (Choi and Chun, 2013).

Little is known about the role of LPA in CNS, but earlier studies demonstrated that this biolipid was able to activate astrocytes in cell culture conditions (Choi et al., 2010) and *in vivo* (Sorensen et al., 2003). Our laboratory has been working on the role of LPA after CNS over the last years. Our findings reveal that a local increase in LPA levels in the spinal cord parenchyma causes microgliosis and this leads to demyelination if LPA levels raises in the white matter (Santos-Nogueira et al., 2015a). In the search for the mechanisms underlying the detrimental actions of LPA, we uncovered that activation of microglial LPA_1 is involved in the harmful effects of this biolipid after spinal cord injury (Santos-Nogueira et al., 2015a). More recently, we have also demonstrated that microglial LPA_2 leads to similar detrimental effects on demyelination than LPA_1. The deleterious actions of microglial LPA_2 are mediated by the release of purines and the subsequent activation of P2X7 in oligodendrocytes, which trigger their death (López-Serrano et al., 2019). Furthermore, we also observed that, a part from myelin loss, LPA_2 contributes to MN after spinal cord injury (unpublished data).

Since LPA levels increase in the CNS parenchyma after spinal cord and brain injury (Santos-Nogueira et al., 2015;Crack et al., 2014), but not in multiple sclerosis (Schmitz et al., 2017), we performed a pilot study to address whether LPA levels are augmented in the CNS of ALS patients. Mass spectrometry analysis of CSF samples obtained from 3 ALS patients and two other neurodegenerative diseases, mononeuritis and multiple sclerosis, at the diagnosis of disease revealed the presence of 3 LPA species (16:0, 18:0 and 18:1 LPA). These results showed marked increased in the concentration of LPA 16:0 and LPA 18:0 in ALS patients relative to the other two neurodegenerative conditions, being LPA 18:0 levels between 17 and 52 fold higher. Furthermore, when comparing the total concentration of LPA from our ALS samples (range from 2 to 4 μM) to previous studies analysing LPA levels in healthy individuals (a mean value of 0.131 μM) , as well as, in other CNS pathologies, such as, brain injury (mean values 0.4μM) (Gotoh et al., 2019; Crack et al., 2014), we observed that LPA levels are much higher in the ALS samples. Interestingly, we also found correlation of LPA levels in the CSF with the clinical onset and progression of ALS. Indeed, higher levels of LPA were associated to earlier disease onset and faster disease progression. Although these results are very preliminary due to the low number of samples analysed, they suggest that LPA could be involved in ALS disease.

We recently show that LPA_1 and LPA_2 were expressed constitutively in the spinal cord of mice (Santos-Nogueira et al., 2015a). In the present thesis, we found that both LPA receptors were also expressed constitutively in the human spinal cord. We also showed that LPA_1 transcripts were not increased in the spinal cord of ALS patients. Similarly,

the expression of LPA_2 did not increased significantly in the spinal cord, although it showed a trend to be increased. Considering the recent reports demonstrating the deleterious actions of microglia in ALS, the detrimental effects of LPA in the CNS, and the involvement of LPA-LPA_2 axis in the MN death after spinal cord injury; we addressed whether LPA could be involved in ALS pathophysiology by signalling via LPA_2.

Previous work demonstrated that the expression of LPA_2 transcripts are expressed at high levels in the testis and leukocytes in the mouse. However the expression of this receptor in other tissue is much lower, such as in CNS (Choi and Chun, 2013). Similar to ALS patients, the expression of LPA_2 in the spinal cord of $SOD1^{G93A}$ mice tended to increase over disease progression but not significantly. RNAseq analysis done in isolated neural cells from the CNS showed that LPA_2 expression in neurons, oligodendrocytes, microglia and peripheral macrophages (Zhang et al., 2014). We have also shown that LPA_2 is expressed in microglia sorted from the spinal cord (López-Serrano et al., 2019). Contrary to the SC, we found significant up regulation of this LPA receptor in the sciatic nerve and the gastrocnemius muscle of ALS mice from 16 weeks of age.

To assess whether LPA-LPA_2 axis contribute to ALS, we crossed mice lacking LPA_2 with the $SOD1^{G93A}$ mice. This double transgenic mouse revealed for the first time that the absence of LPA_2 delays the onset of ALS in males and females, and slows disease progression. Strikingly, despite the marked beneficial effects of the lack of LPA_2 on disease onset and progression this not resulted in increased survival.

To elucidate the potential pathological role of the LPA-LPA_2 axis on ALS disease we assessed its effects at different levels in which motor function is involved. Firstly, we focused out attention in the spinal cord, where lower MN are located. Traditionally, therapeutic approaches for ALS aim at enhancing the survival of lower MN (Mancuso et al., 2014; Martínez-Muriana et al., 2016; McCampbell et al., 2018). Despite we previously showed that activation of microglial LPA_2 exert toxic effect after spinal cord injury (López-Serrano et al., 2019), we observed that the number of MN did not differ in ALS mice lacking LPA_2, suggesting that the harmful effect of LPA_2 was independent on MN cell death. Indeed, the lack of this LPA receptor did not result in any significant change in astrogliosis and microgliosis in the lumbar SC of ALS mice. These data suggested that the deleterious effects of LPA_2 in ALS were unlikely to be mediated in the spinal cord

In ALS, axonopathy precedes and underlies skeletal muscle weakness and progressive paralysis. Indeed, peripheral axons degenerate before the death of cell bodies in the CNS, according to evidence in ALS patients and murine models (Fischer and Glass,

2007; Moloney et al., 2014; Trias et al., 2019). Unlike peripheral nerve injury, axonal growth of degenerated axons is limited in ALS, leading to chronic and progressive axon degeneration, recruitment of immune cells and promotion of inflammation (Trias et al., 2019). In this line, treatment with an CSF1R antagonist attenuated the influx of macrophages into the nerves of ALS mice, that together with its effects on minimizing microgliosis, extended mice survival (Martínez-Muriana et al., 2016). Little is known about the specific functions of LPA_2 in the sciatic nerve, but similar to LPA_1, this receptor is found on oligodendrocytes and Schwann cells and its expression appears shortly before maturation/myelination (Weiner et al., 2001; García-Díaz et al., 2015). Indeed, activation of LPA_2 in myelinating cells seems to play a key role in myelin formation (Weiner et al., 2001; García-Díaz et al., 2015). Since previous works from our laboratory revealed that LPA_2, as well as, LPA_1 activation led to demyelination after spinal cord injury (Santos-Nogueira et al., 2015; López-Serrano et al., 2019), and LPA_2 is up-regulated in the nerve of ALS mice, we wondered whether functional improvement of ALS mice lacking LPA_2 was due to harmful effects of this LPA receptor on demyelination of motor axons and/or their degeneration. However, histological analysis of motor roots harvesting from ALS mice at the age of 16 weeks revealed that the absence of LPA_2 did not alter the preservation of motor axons or myelin. These results suggested that the detrimental actions of LPA-LPA_2 axis in ALS are unlikely to be mediated in the peripheral nerve.

Skeletal muscle atrophy in ALS has been interpreted as a consequence to axon degeneration. Nevertheless, it has been postulated that skeletal myocytes could play an active role in muscle atrophy and contribute to the pathological process, independent from MN loss This is clear from experiments using mice that show selective expression of $SOD1^{G93A}$ in muscle cells, which revealed that skeletal muscle is a primary target of $SOD1^{G93A}$ -mediated toxicity and causes progressive muscle atrophy (Dobrowolny et al., 2008). Thereby numerous studies have attempted to palliate muscle pathology in order to counterbalance the effects of MN degeneration (Derave et al., 2003; Gifondorwa et al., 2007; Yoo and Ko, 2012; Halon et al., 2014;Loeffler et al., 2016). In this line, we observed that histological analysis of the gastrocnemius muscle of ALS mice that muscle atrophy was evident at 16 weeks of age and that the lack of LPA_2 significantly protect against this phenomena.

Axonal sprouting is a natural mechanism that has been described in ALS disease, in which surviving MN expand reinnervate dennervated end-plates within the same muscle, enabling to compensate for the loss of functional motor units and prevent muscle atrophy (Siu and Gordon, 2003). However, electrophysiological and histological analysis

revealed that the lack LPA_2 did not enhance collateral sprouting in ALS. We also discard that this LPA receptor is key component to allow muscle atrophy since we did not observe any alteration in muscle atrophy caused by sciatic nerve injury in LPA_2 null mice.

As reported above, mutant SOD1 cause direct toxic effect of skeletal muscle cell and leads to muscle atrophy (Dobrowolny et al., 2008). A recent study revealed that administration of LPA after muscle injury worsens atrophy (Davies et al., 2017). The same work demonstrated that these effects were likely due to the actions of LPA on inflammation, since administration of LPA to damaged muscles increased the expression of pro-inflammatory cytokines, such as TNFα, and increased invasion of immune cells. In this line, a recent study has been reported that there is recruitment of different immune cells populations, such as mast cells and neutrophils (Trias et al., 2018), in the skeletal muscles of ALS animals, and that administration of a tyrosine kinase inhibitor (masitinib), reduces the recruitment of immune cells in muscles and nerves and exerts therapeutic effects in ALS rats. Taking in account that mutant SOD1 causes muscle toxicity, LPA increases muscle degeneration after injury, and that LPA_2 is involved in immune cell activation, as we previously showed in microglial cells after spinal cord injury (López-Serrano et al., 2019), I do not discard that the LPA-LPA_2 axis could be involved in boosting inflammation in the skeletal muscles of ALS mice, and consequently, led to greater muscle atrophy. Due to time constrains I was unable to assess the contribution of the LPA-LPA_2 signalling in muscle inflammation, but these experiments will be studied in the laboratory in the following months.

GENERAL DISCUSSION

Over the years, several mechanisms involved in ALS pathology have been described. However, the exact mechanisms that promote MN death in ALS are not fully known. Over the last two decades, most of the clinical approaches in ALS patients have been focused exclusively in targeting one of the multiple molecular mechanisms that are likely to be involved in ALS disease. Unfortunately, these clinical trials have failed to show efficacy (Petrov et al., 2017). Therefore, ALS is likely to require a combined therapy in order to lead to marked clinical efficacy. For this reason, in the present thesis we addressed two experimental approaches that target two different events that are involved in ALS and that could be combined: (i) protein aggregation of mutant SOD1 by means of gene therapy, and (ii) the modulation of LPA-LPA_2 axis to contain inflammation.

When working in ALS, one have to have into account that there are more than 100 mutations described in this disease, multiple molecular mechanisms altered and the huge differences in the clinical manifestation of the patient, among other characteristics. This makes ALS a highly heterogeneous disease. I agree with other colleagues that propose ALS as group of different pathologies with similar manifestations rather than a unique disease. This is an important and could determine disease prognosis, response to therapy and design of therapeutic approaches. Accordingly, more research is necessary to disaggregate patients to increase the accuracy of future clinical trials (Beghi et al., 2011; Al-Chalabi et al., 2016)

In the first chapter of the present thesis, we proposed to silence mutant SOD1 by means of ASO, in order to reduce the expression and aggregation of the mutant protein. However, this therapy cannot completely prevent the formation of the mutant SOD1. Importantly, increasing the dose of ASO to further minimize the expression of mutant SOD1 can lead to adverse effects and is not recommended. Some therapies has attempted to increase the efficacy of the ASO therapy by using viral vectors. However, this can lead to activation of the immune response in a pathology in which inflammation contributes detrimentally to the course of the disease. We therefore proposed to use of ligand conjugated-ASO to facilitate their internalization into cells. Despite we demonstrated that this approach leads to substantial reduction in SOD1 levels when using low amounts of the drug, we did not observe any significant effect on disease progression. Other reports have demonstrated positive results using the ASO therapy against mutant SOD1. However, the sequence we used has led to only limited therapeutic effects when administered at multiple doses (Smith et al., 2006; Miller et al., 2008) . More recently, the ASO therapy for ALS have been markedly improved by given multiple doses of novel ASO sequences containing phosphorothioate backbone modifications, 2′-O-methoxyethylribose or (S)-2′,4′- constrained 2′-O-ethyl groups in the 5′ and 3′ wings (McCampbell et al., 2018). Nevertheless, we could not study the efficacy of multiple administrations of the conjugated ASO in ALS mice due to economic problems of nLife therapeutics, which was responsible of manufacturing the ASO.

Misfolding proteins can also act as damage-associated molecular patterns (DAMPs) and cause direct activation of inflammasome, capable in turn, to upregulate inflammation. In ALS, the increased levels of cytokines has been attributed, in part, to activation of the immunological complex known as the nucleotide-binding domain-like receptor protein 3 (NLRP3) inflammasome (Michaelson et al., 2017). Moreover, inflammasome activation and upregulation of NLRP3 has been also observed in ALS patients (Deora et al., 2019).

Previous studies of the lab focused on spinal cord injury, Lopez-Serrano demonstrated that LPA_2 activation in microglia drove this cells towards a cytotoxic profile and to release purines that caused demyelination by triggering oligodendrocyte cell death via P_2X_7 receptor activation (López-Serrano et al., 2019). In this line, LPA an their signalling through LPA_5 has been also related with the induction of pro-inflammatory microglia phenotype (Plastira et al., 2017). However, unpublished studies from our laboratory have not shown any effect of LPA_5 in spinal cord injury or in a mouse model of multiple sclerosis (EAE). Taking into account that NFκB has been suggested as a potential mechanisms that trigger microglia neurotoxicity (Frakes et al., 2014), and that LPA_2 activation is a one of main triggers of NFκB activation (Chuang et al., 2014), we hypothesized that LPA through LPA_2 in microglia promote the neurotoxicity in ALS. The genetic ablation of LPA_2 in a mouse model of ALS protected against disease onset and progression. However, these effects were independent on MN death, damage of motor axons or their myelin sheaths, and collateral sprouting. Indeed, we uncover that the detrimental actions of LPA_2 in ALS were mediated in the muscle, which were likely related with the immune response.

This may indicate that the development of potent LPA_2 antagonist may be effective for ameliorating the clinical signs of ALS. We would like to emphasize that even if LPA_2 is blocked, other elements contribute to the physiopathology of the disease, such as the misfolding of SOD1 in cases of fALS. Therefore, we support the combination of the ASO therapy against mutant SOD1 or other alter genes associated to ALS, with LPA_2 antagonist as novel approaches to be tested in fALS.

CONCLUSIONS

Chapter I: Administration of conjugated ASO against *SOD1* to ameliorate the clinical signs of ALS in SOD1^{G93A} mice.

- Motoneuron like cells internalize the three different conjugated- missense ASO.
- Neurons, microglia and astrocytes, but not oligodendrocytes, uptake the conjugated-missense ASO *in vivo*.
- Conjugated and naked therapeutic ASO are internalized by neurons and glial cells *in vivo* and remains within the cytoplasm for at least 3 weeks.
- Conjugation of the therapeutic ASO with DCPP shows greater efficacy in silencing the transcripts of *SOD1* in the spinal cord of SOD1^{G93A} mice
- Single administration of the therapeutic ASO conjugated with DCPP does not ameliorates the clinical signs of ALS disease.

Chapter II: Contribution of the LPA-LPA$_2$ axis in the physiopathology of ALS

- Levels of the LPA species 16:0, 18:0 and 18:1 are increased in the cerebrospinal fluid of ALS patients and LPA levels are associated with disease onset and progression.
- LPA$_1$ and LPA$_2$ are constitutively expressed in the human spinal cord and their expression is not upregulated in ALS patients
- LPA$_2$ expression is not upregulated in the spinal cord of SOD1^{G93A} mice but its transcripts are increased in the sciatic nerve and gastrocnemius muscle.
- LPA$_2$ accelerates the onset and the progression of disease in SOD1^{G93A} mice.
- LPA$_2$ increase lifespan of SOD1^{G93A} mice.
- LPA$_2$ does not promote motoneuron death is the spinal of ALS mice
- LPA$_2$ does not contribute to microgliosis and astrogliosis in SOD1^{G93A} mice.
- Gene deletion of LPA$_2$ does not enhance the preservation of motor axons.
- The absence of LPA$_2$ prevents muscle atrophy in SOD1^{G93A} mice.

REFERENCES

Abe, K., Aoki, M., Tsuji, S., Itoyama, Y., Sobue, G., Togo, M., Hamada, C., Tanaka, M., Akimoto, M., Nakamura, K., et al. (2017). Safety and efficacy of edaravone in well defined patients with amyotrophic lateral sclerosis: a randomised, double-blind, placebo-controlled trial. Lancet Neurol. *16*, 505–512.

Ahmed, R.M., Newcombe, R.E.A., Piper, A.J., Lewis, S.J., Yee, B.J., Kiernan, M.C., and Grunstein, R.R. (2015). Sleep disorders and respiratory function in amyotrophic lateral sclerosis. Sleep Med. Rev.

Ajami, B., Bennett, J.L., Krieger, C., Tetzlaff, W., and Rossi, F.M. V (2007). Local self-renewal can sustain CNS microglia maintenance and function throughout adult life. Nat. Neurosci. *10*, 1538–1543.

Al-Chalabi, A., Hardiman, O., Kiernan, M.C., Chiò, A., Rix-Brooks, B., and van den Berg, L.H. (2016). Amyotrophic lateral sclerosis: moving towards a new classification system. Lancet Neurol. *15*, 1182–1194.

Alarcón-Arís, D., Recasens, A., Galofré, M., Carballo-Carbajal, I., Zacchi, N., Ruiz-Bronchal, E., Pavia-Collado, R., Chica, R., Ferrés-Coy, A., Santos, M., et al. (2018). Selective α-Synuclein Knockdown in Monoamine Neurons by Intranasal Oligonucleotide Delivery: Potential Therapy for Parkinson's Disease. Mol. Ther. *26*, 550–567.

Albers, H.M.H.G., Dong, A., van Meeteren, L.A., Egan, D.A., Sunkara, M., van Tilburg, E.W., Schuurman, K., van Tellingen, O., Morris, A.J., Smyth, S.S., et al. (2010). Boronic acid-based inhibitor of autotaxin reveals rapid turnover of LPA in the circulation. Proc. Natl. Acad. Sci. U. S. A. *107*, 7257–7262.

Alberts B, Johnson A, Lewis J, et a (2002). Molecular biology of the cell.

Alexianu, M.E., Ho, B.-K., Mohamed, A.H., La Bella, V., Smith, R.G., and Appel, S.H. (1994). The role of calcium-binding proteins in selective motoneuron vulnerability in amyotrophic lateral sclerosis. Ann. Neurol. *36*, 846–858.

Andersen, P.M. (2006). Amyotrophic lateral sclerosis associated with mutations in the CuZn superoxide dismutase gene. Curr. Neurol. Neurosci. Rep. *6*, 37–46.

Aoki, J., Inoue, A., and Okudaira, S. (2008). Two pathways for lysophosphatidic acid production. Biochim. Biophys. Acta - Mol. Cell Biol. Lipids *1781*, 513–518.

Arnold, W.D., Sheth, K.A., Wier, C.G., Kissel, J.T., Burghes, A.H., and Kolb, S.J. (2015). Electrophysiological motor unit number estimation (MUNE) measuring compound muscle action potential (CMAP) in mouse hindlimb muscles. J. Vis. Exp. *2015*, 1–8.

Atkin, J.D., Farg, M.A., Walker, A.K., McLean, C., Tomas, D., and Horne, M.K. (2008). Endoplasmic reticulum stress and induction of the unfolded protein response in human sporadic amyotrophic lateral sclerosis. Neurobiol. Dis. *30*, 400–407.

Ayers, J.I., Fromholt, S., Koch, M., DeBosier, A., McMahon, B., Xu, G., and Borchelt, D.R. (2014). Experimental transmissibility of mutant SOD1 motor neuron disease. Acta Neuropathol. *128*, 791–803.

Bandoh, K., Aoki, J., Hosono, H., Kobayashi, S., Kobayashi, T., Murakami-Murofushi, K., Tsujimoto, M., Arai, H., and Inoue, K. (1999). Molecular Cloning

and Characterization of a Novel Human G-protein-coupled Receptor, EDG7, for Lysophosphatidic Acid. J. Biol. Chem. *274*, 27776–27785.

Banerjee, V., Shani, T., Katzman, B., Vyazmensky, M., Papo, N., Israelson, A., and Engel, S. (2016). Superoxide Dismutase 1 (SOD1)-Derived Peptide Inhibits Amyloid Aggregation of Familial Amyotrophic Lateral Sclerosis SOD1 Mutants. ACS Chem. Neurosci. *7*, 1595–1606.

Banfi, P., Ticozzi, N., Lax, A., and Guidugli, G.A. (2015). A Review of Options for Treating Sialorrhea in Amyotrophic Lateral Sclerosis. 1–9.

Barbara, J.G., and Clarac, F. (2011). Historical concepts on the relations between nerves and muscles. Brain Res. *1409*, 3–22.

Barson, A.J. (1970). The vertebral level of termination of the spinal cord during normal and abnormal development. J. Anat. *106*, 489–497.

Barton, S.K., Gregory, J.M., Chandran, S., and Turner, B.J. (2019). Could an Impairment in Local Translation of mRNAs in Glia be Contributing to Pathogenesis in ALS? Front. Mol. Neurosci. *12*, 124.

Becker, L.A., Huang, B., Bieri, G., Ma, R., Knowles, D.A., Jafar-Nejad, P., Messing, J., Kim, H.J., Soriano, A., Auburger, G., et al. (2017). Therapeutic reduction of ataxin-2 extends lifespan and reduces pathology in TDP-43 mice. Nature *544*, 367–371.

Beers, D.R., Henkel, J.S., Xiao, Q., Zhao, W., Wang, J., Yen, A.A., Siklos, L., McKercher, S.R., and Appel, S.H. (2006). Wild-type microglia extend survival in PU.1 knockout mice with familial amyotrophic lateral sclerosis. Proc. Natl. Acad. Sci. *103*, 16021–16026.

Beers, D.R., Henkel, J.S., Zhao, W., Wang, J., and Appel, S.H. (2008). CD4+ T cells support glial neuroprotection, slow disease progression, and modify glial morphology in an animal model of inherited ALS. Proc. Natl. Acad. Sci. U. S. A. *105*, 15558–15563.

Beers, D.R., Zhao, W., Wang, J., Zhang, X., Wen, S., Neal, D., Thonhoff, J.R., Alsuliman, A.S., Shpall, E.J., Rezvani, K., et al. (2017). ALS patients' regulatory T lymphocytes are dysfunctional, and correlate with disease progression rate and severity. JCI Insight *2*, e89530.

Beghi, E., Chiò, A., Couratier, P., Esteban, J., Hardiman, O., Logroscino, G., Millul, A., Mitchell, D., Preux, P.M., Pupillo, E., et al. (2011). The epidemiology and treatment of ALS: Focus on the heterogeneity of the disease and critical appraisal of therapeutic trials. Amyotroph. Lateral Scler. *12*, 1–10.

Bennett, C.F., and Swayze, E.E. (2010). RNA Targeting Therapeutics: Molecular Mechanisms of Antisense Oligonucleotides as a Therapeutic Platform. Annu. Rev. Pharmacol. Toxicol. *50*, 259–293.

Bensimon, G., Lacomblez, L., and Meininger, V. (1994). A Controlled Trial of Riluzole in Amyotrophic Lateral Sclerosis. N. Engl. J. Med. *330*, 585–591.

Bilsland, L.G., Sahai, E., Kelly, G., Golding, M., Greensmith, L., and Schiavo, G. (2010). Deficits in axonal transport precede ALS symptoms in vivo. Proc. Natl. Acad. Sci. U. S. A. *107*, 20523–20528.

Boillée, S., Vande Velde, C., and Cleveland, D.W.W. (2006a). ALS: A Disease of Motor Neurons and Their Nonneuronal Neighbors. Neuron *52*, 39–59.

Boillée, S., Yamanaka, K., Lobsiger, C.S., Copeland, N.G., Jenkins, N.A., Kassiotis, G., Kollias, G., and Cleveland, D.W. (2006b). Onset and Progression in Inherited ALS Determined by Motor Neurons and Microglia. Science (80-.). *312*, 1389–1392.

Bostock, H., Sharief, M.K., Reid, G., and Murray, N.M.F. (1995). Axonal ion channel dysfunction in amyotrophic lateral sclerosis. Brain *118*, 217–225.

Bourke, S.C., Tomlinson, M., Williams, T.L., Bullock, R.E., Shaw, P.J., and Gibson, G.J. (2006). Effects of non-invasive ventilation on survival and quality of life in patients with amyotrophic lateral sclerosis: a randomised controlled trial. Lancet Neurol. *5*, 140–147.

Bowerman, M., Vincent, T., Scamps, F., Perrin, F.E., Camu, W., and Raoul, C. (2013). Neuroimmunity dynamics and the development of therapeutic strategies for amyotrophic lateral sclerosis. Front. Cell. Neurosci. *7*, 214.

Bozzo, F., Mirra, A., and Carrì, M.T. (2017). Oxidative stress and mitochondrial damage in the pathogenesis of ALS: New perspectives. Neurosci. Lett. *636*, 3–8.

Brettschneider, J., Van Deerlin, V.M., Robinson, J.L., Kwong, L., Lee, E.B., Ali, Y.O., Safren, N., Monteiro, M.J., Toledo, J.B., Elman, L., et al. (2012). Pattern of ubiquilin pathology in ALS and FTLD indicates presence of C9ORF72 hexanucleotide expansion. Acta Neuropathol. *123*, 825–839.

Breuer, A.C., Lynn, M.P., Atkinson, M.B., Chou, S.M., Wilbourn, A.J., Marks, K.E., Culver, J.E., and Fleegler, E.J. (1987). Fast axonal transport in amyotrophic lateral sclerosis: An intra-axonal organelle traffic analysis. Neurology *37*, 738–738.

Bright, F., Werry, E.L., Dobson-Stone, C., Piguet, O., Ittner, L.M., Halliday, G.M., Hodges, J.R., Kiernan, M.C., Loy, C.T., Kassiou, M., et al. (2019). Neuroinflammation in frontotemporal dementia. Nat. Rev. Neurol. *15*, 540–555.

Bristol, L.A., and Rothstein, J.D. (1996). Glutamate transporter gene expression in amyotrophic lateral sclerosis motor cortex. Ann. Neurol. *39*, 676–679.

Bruijn, L.I., Houseweart, M.K., Kato, S., Anderson, K.L., Anderson, S.D., Ohama, E., Reaume, A.G., Scott, R.W., and Cleveland, D.W. (1998). Aggregation and motor neuron toxicity of an ALS-linked SOD1 mutant independent from wild-type SOD1. Science (80-.). *281*, 1851–1854.

Bruijn, L.I., Miller, T.M., and Cleveland, D.W. (2004). Unraveling the mechanisms involved in motor neuron degeneration in ALS. Annu. Rev. Neurosci. *27*, 723–749.

C., P., M.-F., S., P., V., and J.S., S.-B. (2001). Lysophosphatidic acid synthesis and release. Prostaglandins Other Lipid Mediat. *64*, 1–10.

Campanari, M.-L., García-Ayllón, M.-S., Ciura, S., Sáez-Valero, J., and Kabashi, E. (2016). Neuromuscular Junction Impairment in Amyotrophic Lateral Sclerosis: Reassessing the Role of Acetylcholinesterase. Front. Mol. Neurosci. *9*, 160.

Carlson, N.R. (2013). Foundations of Behavioral Neuroscience.

Carrì, M.T., D'Ambrosi, N., and Cozzolino, M. (2017). Pathways to mitochondrial dysfunction in ALS pathogenesis. Biochem. Biophys. Res. Commun. *483*, 1187–1193.

Carvalho, M. De, and Swash, M. (2009). Awaji diagnostic algorithm increases sensitivity of El Escorial criteria for ALS diagnosis. Amyotroph. Lateral Scler. *10*, 53–57.

Cashman, N.R., Durham, H.D., Blusztajn, J.K., Oda, K., Tabira, T., Shaw, I.T., Dahrouge, S., and Antel, J.P. (1992a). Neuroblastoma × spinal cord (NSC) hybrid cell lines resemble developing motor neurons. Dev. Dyn. *194*, 209–221.

Cashman, N.R., Durham, H.D., Blusztajn, J.K., Oda, K., Tabira, T., Shaw, I.T., Dahrouge, S., and Antel, J.P. (1992b). Neuroblastoma × spinal cord (NSC) hybrid cell lines resemble developing motor neurons. Dev. Dyn. *194*, 209–221.

Catala, M., and Kubis, N. (2013). Gross anatomy and development of the peripheral nervous system. Handb. Clin. Neurol. *115*, 29–41.

Cell, T., and Marrow, B. KRAUSE ' S ESSENTIAL HUMAN HISTOLOGY FOR MEDICAL STUDENTS Third Edition William J . Krause , Ph . D . Professor of Anatomy Department of Pathology and Anatomical Sciences University of Missouri School of Medicine Columbia , Missouri Table of Contents. 1–315.

Chang, Q., and Martin, L.J. (2011). Glycine receptor channels in spinal motoneurons are abnormal in a transgenic mouse model of amyotrophic lateral sclerosis. J. Neurosci. *31*, 2815–2827.

Chang, Y., Kong, Q., Shan, X., Tian, G., Ilieva, H., Cleveland, D.W., Rothstein, J.D., Borchelt, D.R., Wong, P.C., and Lin, C.L.G. (2008). Messenger RNA oxidation occurs early in disease pathogenesis and promotes motor neuron degeneration in ALS. PLoS One *3*.

Cheroni, C., Peviani, M., Cascio, P., DeBiasi, S., Monti, C., and Bendotti, C. (2005). Accumulation of human SOD1 and ubiquitinated deposits in the spinal cord of SOD1G93A mice during motor neuron disease progression correlates with a decrease of proteasome. Neurobiol. Dis. *18*, 509–522.

Chiò, A., Logroscino, G., Hardiman, O., Swingler, R., Mitchell, D., Beghi, E., Traynor, B.G., and Eurals Consortium (2009). Prognostic factors in ALS: A critical review. Amyotroph. Lateral Scler. *10*, 310–323.

Chiò, A., Battistini, S., Calvo, A., Caponnetto, C., Conforti, F.L., Corbo, M., Giannini, F., Mandrioli, J., Mora, G., Sabatelli, M., et al. (2014). Genetic counselling in ALS: facts, uncertainties and clinical suggestions. J. Neurol. Neurosurg. Psychiatry *85*, 478–485.

Chiò, A., Mora, G., and Lauria, G. (2017). Pain in amyotrophic lateral sclerosis. Lancet Neurol. *16*, 144–157.

Chiu, S., and Bharat, A. (2016). Role of monocytes and macrophages in regulating immune response following lung transplantation. Curr. Opin. Organ Transplant. *21*, 239–245.

Chiu, I.M., Chen, A., Zheng, Y., Kosaras, B., Tsiftsoglou, S.A., Vartanian, T.K., Brown, R.H., and Carroll, M.C. (2008). T lymphocytes potentiate endogenous neuroprotective inflammation in a mouse model of ALS. Proc. Natl. Acad. Sci. U. S. A. *105*, 17913–17918.

Chiu, I.M., Phatnani, H., Kuligowski, M., Tapia, J.C., Carrasco, M.A., Zhang, M., Maniatis, T., and Carrolla, M.C. (2009). Activation of innate and humoral immunity in the peripheral nervous system of ALS transgenic mice. Proc. Natl. Acad. Sci. U. S. A. *106*, 20960–20965.

Choi, J.W., and Chun, J. (2013). Lysophospholipids and their receptors in the central nervous system. Biochim. Biophys. Acta - Mol. Cell Biol. Lipids *1831*, 20–32.

Choi, J.W., Herr, D.R., Noguchi, K., Yung, Y.C., Lee, C.-W., Mutoh, T., Lin, M.-E., Teo, S.T., Park, K.E., Mosley, A.N., et al. (2010). LPA Receptors: Subtypes and Biological Actions. Annu. Rev. Pharmacol. Toxicol. *50*, 157–186.

Chuang, Y.W., Chang, W.M., Chen, K.H., Hong, C.Z., Chang, P.J., and Hsu, H.C. (2014). Lysophosphatidic acid enhanced the angiogenic capability of human chondrocytes by regulating Gi/NF-kB-dependent angiogenic factor expression. PLoS One *9*.

Chun, J., Hla, T., Spiegel, S., and Moolenaar, W. (2013). Lysophospholipid receptors.

Contos, J.J., Fukushima, N., Weiner, J.A., Kaushal, D., and Chun, J. (2000). Requirement for the lpA1 lysophosphatidic acid receptor gene in normal suckling behavior. Proc. Natl. Acad. Sci. U. S. A. *97*, 13384–13389.

Cooper-Knock, J., Hewitt, C., Highley, J.R., Brockington, A., Milano, A., Man, S., Martindale, J., Hartley, J., Walsh, T., Gelsthorpe, C., et al. (2012). Clinico-pathological features in amyotrophic lateral sclerosis with expansions in C9ORF72. Brain *135*, 751–764.

Corti, S., Donadoni, C., Ronchi, D., Bordoni, A., Fortunato, F., Santoro, D., Del Bo, R., Lucchini, V., Crugnola, V., Papadimitriou, D., et al. (2009). Amyotrophic lateral sclerosis linked to a novel SOD1 mutation with muscle mitochondrial dysfunction. J. Neurol. Sci. *276*, 170–174.

Crack, P.J., Zhang, M., Morganti-Kossmann, M.C., Morris, A.J., Wojciak, J.M., Fleming, J.K., Karve, I., Wright, D., Sashindranath, M., Goldshmit, Y., et al. (2014). Anti-lysophosphatidic acid antibodies improve traumatic brain injury outcomes. J. Neuroinflammation *11*, 37.

Crooke, S.T., Wang, S., Vickers, T.A., Shen, W., and Liang, X.H. (2017). Cellular uptake and trafficking of antisense oligonucleotides. Nat. Biotechnol. *35*, 230–237.

Crooke, S.T., Witztum, J.L., Bennett, C.F., and Baker, B.F. (2018). RNA-Targeted Therapeutics. Cell Metab. *27*, 714–739.

Cudkowicz, M.E., Shefner, J.M., Schoenfeld, D.A., Zhang, H., Andreasson, K.I., Rothstein, J.D., and Drachman, D.B. (2006). Trial of celecoxib in amyotrophic lateral sclerosis. Ann. Neurol. *60*, 22–31.

Van Damme, P., Robberecht, W., and Van Den Bosch, L. (2017). Modelling amyotrophic lateral sclerosis: progress and possibilities. Dis. Model. Mech. *10*, 537–549.

David, S., López-Vales, R., and Wee Yong, V. (2012). Harmful and beneficial effects of inflammation after spinal cord injury. In Handbook of Clinical Neurology, pp. 485–502.

Davidson, B.L., and McCray, P.B. (2011). Current prospects for RNA interference-based therapies. Nat. Rev. Genet. *12*, 329–340.

Davies, M.R., Lee, L., Feeley, B.T., Kim, H.T., and Liu, X. (2017). Lysophosphatidic acid-induced RhoA signaling and prolonged macrophage infiltration worsens fibrosis and fatty infiltration following rotator cuff tears. J. Orthop. Res. *35*, 1539–1547.

DeJesus-Hernandez, M., Mackenzie, I.R., Boeve, B.F., Boxer, A.L., Baker, M., Rutherford, N.J., Nicholson, A.M., Finch, N.C.A., Flynn, H., Adamson, J., et al. (2011). Expanded GGGGCC Hexanucleotide Repeat in Noncoding Region of C9ORF72 Causes Chromosome 9p-Linked FTD and ALS. Neuron *72*, 245–256.

Deora, V., Lee, J.D., Albornoz, E.A., McAlary, L., Jagaraj, C.J., Robertson, A.A.B., Atkin, J.D., Cooper, M.A., Schroder, K., Yerbury, J.J., et al. (2019). The microglial NLRP3 inflammasome is activated by amyotrophic lateral sclerosis proteins. Glia.

Derave, W., Van Den Bosch, L., Lemmens, G., Eijnde, B.O., Robberecht, W., and Hespel, P. (2003a). Skeletal muscle properties in a transgenic mouse model for amyotrophic lateral sclerosis: effects of creatine treatment. Neurobiol. Dis. *13*, 264–272.

Derave, W., Van Den Bosch, L., Lemmens, G., Eijnde, B.O., Robberecht, W., and Hespel, P. (2003b). Skeletal muscle properties in a transgenic mouse model for amyotrophic lateral sclerosis: Effects of creatine treatment. Neurobiol. Dis. *13*, 264–272.

Deschenes, M.R. (2011). Motor unit and neuromuscular junction remodeling with aging. Curr. Aging Sci. *4*, 209–220.

DeVos, S.L., and Miller, T.M. (2013). Antisense Oligonucleotides: Treating Neurodegeneration at the Level of RNA. Neurotherapeutics *10*, 486–497.

Diaz, E., and Morales, H. (2016). Spinal Cord Anatomy and Clinical Syndromes. Semin. Ultrasound, CT MRI.

Dobrowolny, G., Aucello, M., Rizzuto, E., Beccafico, S., Mammucari, C., Boncompagni, S., Belia, S., Wannenes, F., Nicoletti, C., Del Prete, Z., et al. (2008). Skeletal Muscle Is a Primary Target of SOD1G93A-Mediated Toxicity. Cell Metab. *8*, 425–436.

Dodson, P.D., Billups, B., Rusznák, Z., Szucs, G., Barker, M.C., and Forsythe, I.D. (2003). Presynaptic Rat Kv1.2 Channels Suppress Synaptic Terminal Hyperexcitability Following Action Potential Invasion. J. Physiol. *550*, 27–33.

Dowdy, S.F. (2017). Overcoming cellular barriers for RNA therapeutics. Nat. Biotechnol. *35*, 222–229.

E Spohr, T.C.L. de S., Dezonne, R.S., Rehen, S.K., and Gomes, F.C.A. (2011). Astrocytes treated by lysophosphatidic acid induce axonal outgrowth of cortical progenitors through extracellular matrix protein and epidermal growth factor signaling pathway. J. Neurochem. *119*, 113–123.

Echaniz-Laguna, A., Zoll, J., Ponsot, E., N'guessan, B., Tranchant, C., Loeffler, J.-P., and Lampert, E. (2006). Muscular mitochondrial function in amyotrophic lateral sclerosis is progressively altered as the disease develops: a temporal study in man. Exp. Neurol. *198*, 25–30.

Edstrom, L., and Kugelberg, E. (1968). Histochemical composition, distribution of fibres and fatiguability of single motor units. J. Neurol. Neurosurg. Psychiatry *31*, 424–433.

Elamin, M., Bede, P., Montuschi, A., Pender, N., Chio, A., and Hardiman, O. (2015). Predicting prognosis in amyotrophic lateral sclerosis: a simple algorithm. J. Neurol. *262*, 1447–1454.

Elden, A.C., Kim, H.J., Hart, M.P., Chen-Plotkin, A.S., Johnson, B.S., Fang, X., Armakola, M., Geser, F., Greene, R., Lu, M.M., et al. (2010). Ataxin-2 intermediate-length polyglutamine expansions are associated with increased risk for ALS. Nature *466*, 1069–1075.

Engelhardt, J.I., Tajti, J., and Appel, S.H. (1993). Lymphocytic Infiltrates in the Spinal Cord in Amyotrophic Lateral Sclerosis. Arch. Neurol. *50*, 30–36.

Evers, M.M., Toonen, L.J.A., and van Roon-Mom, W.M.C. (2015). Antisense oligonucleotides in therapy for neurodegenerative disorders. Adv. Drug Deliv. Rev. *87*, 90–103.

Ferrante, R.J., Browne, S.E., Shinobu, L.A., Bowling, A.C., Baik, M.J., MacGarvey, U., Kowall, N.W., Brown, R.H., and Beal, M.F. (1997a). Evidence of increased oxidative damage in both sporadic and familial amyotrophic lateral sclerosis. J. Neurochem. *69*, 2064–2074.

Ferrante, R.J., Shinobu, L.A., Schulz, J.B., Matthews, R.T., Thomas, C.E., Kowall, N.W., Gurney, M.E., and Beal, M.F. (1997b). Increased 3-nitrotyrosine and oxidative damage in mice with a human copper/zinc superoxide dismutase mutation. Ann. Neurol. *42*, 326–334.

Ferrés-Coy, A., Galofré, M., Pilar-Cuéllar, F., Vidal, R., Paz, V., Ruiz-Bronchal, E., Campa, L., Pazos, Á., Caso, J.R., Leza, J.C., et al. (2016). Therapeutic antidepressant potential of a conjugated siRNA silencing the serotonin transporter after intranasal administration. Mol. Psychiatry *21*, 328–338.

Ferry, B., Gervasoni, D., and Vogt, C. (2014). Stereotaxic Neurosurgery in Laboratory Rodent.

Fischer, L.R., and Glass, J.D. (2007). Axonal degeneration in motor neuron disease. Neurodegener. Dis. *4*, 431–442.

Fischer, L.R., Culver, D.G., Tennant, P., Davis, A.A., Wang, M., Castellano-Sanchez, A., Khan, J., Polak, M.A., and Glass, J.D. (2004). Amyotrophic lateral sclerosis is a distal axonopathy: evidence in mice and man. Exp. Neurol. *185*, 232–240.

Floeter, M.K. (2010). The scientific basis of muscle disease Structure and function of muscle fibers and motor units. 1–10.

Forsberg, K., Jonsson, P.A., Andersen, P.M., Bergemalm, D., Graffmo, K.S., Hultdin, M., Jacobsson, J., Rosquist, R., Marklund, S.L., and Bränström, T. (2010). Novel antibodies reveal inclusions containing non-native SOD1 in sporadic ALS patients. PLoS One *5*, 1–9.

Frakes, A.E., Ferraiuolo, L., Haidet-Phillips, A.M., Schmelzer, L., Braun, L., Miranda, C.J., Ladner, K.J., Bevan, A.K., Foust, K.D., Godbout, J.P., et al. (2014). Microglia induce motor neuron death via the classical NF-κB pathway in amyotrophic lateral sclerosis. Neuron *81*, 1009–1023.

Fridovich, I. (1986). Superoxide dismutases. Adv. Enzymol. Relat. Areas Mol. Biol. *58*, 61–97.

Fukushima, N., Weiner, J.A., Kaushal, D., Contos, J.J.A., Rehen, S.K., Kingsbury, M.A., Kim, K.Y., and Chun, J. (2002). Lysophosphatidic Acid Influences the Morphology and Motility of Young, Postmitotic Cortical Neurons. Mol. Cell. Neurosci. *20*, 271–282.

Fullerton, J.N., and Gilroy, D.W. (2016). Resolution of inflammation: A new therapeutic frontier. Nat. Rev. Drug Discov. *15*, 551–567.

Gamez, J., Corbera-Bellalta, M., Nogales, G., Raguer, N., García-Arumí, E., Badia-Canto, M., Lladó-Carbó, E., and Álvarez-Sabín, J. (2006). Mutational analysis of the Cu/Zn superoxide dismutase gene in a Catalan ALS population: Should all sporadic ALS cases also be screened for SOD1? J. Neurol. Sci. *247*, 21–28.

García-Díaz, B., Riquelme, R., Varela-Nieto, I., Jiménez, A.J., de Diego, I., Gómez-Conde, A.I., Matas-Rico, E., Aguirre, J.Á., Chun, J., Pedraza, C., et al. (2015). Loss of lysophosphatidic acid receptor LPA1 alters oligodendrocyte differentiation and myelination in the mouse cerebral cortex. Brain Struct. Funct. *220*, 3701–3720.

Geary, R.S., Norris, D., Yu, R., and Bennett, C.F. (2015). Pharmacokinetics, biodistribution and cell uptake of antisense oligonucleotides. Adv. Drug Deliv. Rev.

Ghannam, J.Y., and Al Kharazi, K.A. (2019). Neuroanatomy, Cranial Meninges (StatPearls Publishing).

Gifondorwa, D.J., Robinson, M.B., Hayes, C.D., Taylor, A.R., Prevette, D.M., Oppenheim, R.W., Caress, J., and Milligan, C.E. (2007). Exogenous delivery of heat shock protein 70 increases lifespan in a mouse model of amyotrophic lateral sclerosis. J. Neurosci. *27*, 13173–13180.

Gill, C., Phelan, J.P., Hatzipetros, T., Kidd, J.D., Tassinari, V.R., Levine, B., Wang, M.Z., Moreno, A., Thompson, K., Maier, M., et al. (2019). SOD1-positive aggregate accumulation in the CNS predicts slower disease progression and increased longevity in a mutant SOD1 mouse model of ALS. Sci. Rep. *9*, 6724.

Ginhoux, F., Greter, M., Leboeuf, M., Nandi, S., See, P., Gokhan, S., Mehler, M.F., Conway, S.J., Ng, L.G., Stanley, E.R., et al. (2010). Fate mapping analysis

reveals that adult microglia derive from primitive macrophages. Science (80-.). *330*, 841–845.

Goetz, C.G. (2000). Amyotrophic lateral sclerosis: early contributions of Jean-Martin Charcot. Muscle Nerve *23*, 336–343.

Goldshmit, Y., Matteo, R., Sztal, T., Ellett, F., Frisca, F., Moreno, K., Crombie, D., Lieschke, G.J., Currie, P.D., Sabbadini, R.A., et al. (2012). Blockage of Lysophosphatidic Acid Signaling Improves Spinal Cord Injury Outcomes. Am. J. Pathol. *181*, 978–992.

Gotoh, L., Yamada, M., Hattori, K., Sasayama, D., Noda, T., Yoshida, S., Kunugi, H., and Yamada, M. (2019). Levels of lysophosphatidic acid in cerebrospinal fluid and plasma of patients with schizophrenia. Psychiatry Res. *273*, 331–335.

Gould, T.W. (2006). Complete Dissociation of Motor Neuron Death from Motor Dysfunction by Bax Deletion in a Mouse Model of ALS. J. Neurosci. *26*, 8774–8786.

Grad, L.I., Guest, W.C., Yanai, A., Pokrishevsky, E., O'Neill, M.A., Gibbs, E., Semenchenko, V., Yousefi, M., Wishart, D.S., Plotkin, S.S., et al. (2011). Intermolecular transmission of superoxide dismutase 1 misfolding in living cells. Proc. Natl. Acad. Sci. U. S. A. *108*, 16398–16403.

Grad, L.I., Pokrishevsky, E., Silverman, J.M., and Cashman, N.R. (2014a). Exosome-dependent and independent mechanisms are involved in prion-like transmission of propagated Cu/Zn superoxide dismutase misfolding. Prion *8*, 331–335.

Grad, L.I., Yerbury, J.J., Turner, B.J., Guest, W.C., Pokrishevsky, E., O'Neill, M.A., Yanai, A., Silverman, J.M., Zeineddine, R., Corcoran, L., et al. (2014b). Intercellular propagated misfolding of wild-type Cu/Zn superoxide dismutase occurs via exosome-dependent and -independent mechanisms. Proc. Natl. Acad. Sci. U. S. A. *111*, 3620–3625.

Granatiero, V., and Manfredi, G. (2019). Mitochondrial Transport and Turnover in the Pathogenesis of Amyotrophic Lateral Sclerosis. Biology (Basel). *8*, 36.

Gurney, M., Pu, H., Chiu, A., Dal Canto, M., Polchow, C., Alexander, D., Caliendo, J., Hentati, A., Kwon, Y., Deng, H., et al. (1994). Motor neuron degeneration in mice that express a human Cu,Zn superoxide dismutase mutation. Science (80-.). *264*, 1772–1775.

Halon, M., Kaczor, J.J., Ziolkowski, W., Flis, D.J., Borkowska, A., Popowska, U., Nyka, W., Wozniak, M., and Antosiewicz, J. (2014). Changes in skeletal muscle iron metabolism outpace amyotrophic lateral sclerosis onset in transgenic rats bearing the G93A hmSOD1 gene mutation. Free Radic. Res. *48*, 1363–1370.

Hardiman, O., Al-Chalabi, A., Chio, A., Corr, E.M., Logroscino, G., Robberecht, W., Shaw, P.J., Simmons, Z., and van den Berg, L.H. (2017). Amyotrophic lateral sclerosis. Nat. Rev. Disase Prim. *3*.

Hartmann, G., Krug, A., Waller-Fontaine, K., and Endres, S. (1996). Oligodeoxynucleotides enhance lipopolysaccharide-stimulated synthesis of tumor necrosis factor: dependence on phosphorothioate modification and

reversal by heparin. Mol. Med. *2*, 429–438.

Harvey, L. (2008). Background information. In Management of Spinal Cord Injuries, (Elsevier), pp. 3–33.

Hayward, L.J., Rodriguez, J.A., Kim, J.W., Tiwari, A., Goto, J.J., Cabelli, D.E., Valentine, J.S., and Brown, R.H. (2002a). Decreased Metallation and Activity in Subsets of Mutant Superoxide Dismutases Associated with Familial Amyotrophic Lateral Sclerosis. J. Biol. Chem. *277*, 15923–15931.

Hayward, L.J., Rodriguez, J.A., Kim, J.W., Tiwari, A., Goto, J.J., Cabelli, D.E., Valentine, J.S., and Brown, R.H. (2002b). Decreased metallation and activity in subsets of mutant superoxide dismutases associated with familial amyotrophic lateral sclerosis. J. Biol. Chem. *277*, 15923–15931.

Hecht, J.H., Weiner, J.A., Post, S.R., and Chun, J. (1996). Ventricular zone gene-1 (vzg-1) encodes a lysophosphatidic acid receptor expressed in neurogenic regions of the developing cerebral cortex. J. Cell Biol. *135*, 1071–1083.

Hensley, K., Abdel-Moaty, H., Hunter, J., Mhatre, M., Mou, S., Nguyen, K., Potapova, T., Pye, Q.N., Qi, M., Rice, H., et al. (2006). Primary glia expressing the G93A-SOD1 mutation present a neuroinflammatory phenotype and provide a cellular system for studies of glial inflammation. J. Neuroinflammation *3*, 2.

Hervias, I., Beal, M.F., and Manfredi, G. (2006). Mitochondrial dysfunction and amyotrophic lateral sclerosis. Muscle and Nerve *33*, 598–608.

Hirano, A., Donnenfeld, H., Sasaki, S., and Nakano, I. (1984). Fine structural observations of neurofilamentous changes in amyotrophic lateral sclerosis. J. Neuropathol. Exp. Neurol. *43*, 461–470.

Hirsch, N.P. (2007). Neuromuscular junction in health and disease. Br. J. Anaesth. *99*, 132–138.

Hothorn, T., and Jung, H.H. (2014). RandomForest4Life: A Random Forest for predicting ALS disease progression. Amyotroph. Lateral Scler. Front. Degener. *15*, 444–452.

Howland, D.S., Liu, J., She, Y., Goad, B., Maragakis, N.J., Kim, B., Erickson, J., Kulik, J., DeVito, L., Psaltis, G., et al. (2002). Focal loss of the glutamate transporter EAAT2 in a transgenic rat model of SOD1 mutant-mediated amyotrophic lateral sclerosis (ALS). Proc. Natl. Acad. Sci. *99*, 1604–1609.

Hughes, B.W., Kusner, L.L., and Kaminski, H.J. (2006). Molecular architecture of the neuromuscular junction. Muscle and Nerve *33*, 445–461.

Jaarsma, D., Haasdijk, E.D., Grashorn, J.A.C., Hawkins, R., van Duijn, W., Verspaget, H.W., London, J., and Holstege, J.C. (2000). Human Cu/Zn Superoxide Dismutase (SOD1) Overexpression in Mice Causes Mitochondrial Vacuolization, Axonal Degeneration, and Premature Motoneuron Death and Accelerates Motoneuron Disease in Mice Expressing a Familial Amyotrophic Lateral Sclerosis Mutant SOD1. Neurobiol. Dis. *7*, 623–643.

Jayant, R.D., Sosa, D., Kaushik, A., Atluri, V., Vashist, A., Tomitaka, A., and Nair, M. (2016). Current status of non-viral gene therapy for CNS disorders. Expert Opin. Drug Deliv. *13*, 1433–1445.

Jiang, J., Zhu, Q., Gendron, T.F., Saberi, S., McAlonis-Downes, M., Seelman, A., Stauffer, J.E., Jafar-nejad, P., Drenner, K., Schulte, D., et al. (2016). Gain of Toxicity from ALS/FTD-Linked Repeat Expansions in C9ORF72 Is Alleviated by Antisense Oligonucleotides Targeting GGGGCC-Containing RNAs. Neuron *90*, 535–550.

Juliano, R.L. (2016). The delivery of therapeutic oligonucleotides. Nucleic Acids Res. *44*, 6518–6548.

Kandel, Eric; Schwartz, James; Jessel, Thomas; Siegelbaum, S.A.H.A.J. (2013). Principles of neural science.

Kano, K., Arima, N., Ohgami, M., and Aoki, J. (2008). LPA and its Analogs-Attractive Tools for Elucidation of LPA Biology and Drug Development. Curr. Med. Chem. *15*, 2122–2131.

Katzberg, H.D. (2015). Neurogenic muscle cramps. J. Neurol. *262*, 1814–1821.

Kawahara, Y., Ito, K., Sun, H., Aizawa, H., Kanazawa, I., and Kwak, S. (2004). RNA editing and death of motor neurons. Nature *427*, 801–801.

Kawamata, T., Akiyama, H., Yamada, T., and McGeer, P.L. (1992). Immunologic reactions in amyotrophic lateral sclerosis brain and spinal cord tissue. Am. J. Pathol. *140*, 691–707.

Kiernan, M.C., Vucci, S., Cheah, B.C., Turner, M.R., Eisen, A., Hardiman, O., Burrell, J.R., and Zoing, M.C. (2011). Amyotrophic lateral sclerosis. Lancet *377*, 942–955.

Knibb, J.A., Keren, N., Kulka, A., Leigh, P.N., Martin, S., Shaw, C.E., Tsuda, M., and Al-Chalabi, A. (2016). A clinical tool for predicting survival in ALS. J. Neurol. Neurosurg. Psychiatry *87*, 1361–1367.

Kovacs, M., Trias, E., Varela, V., Ibarburu, S., Beckman, J.S., Moura, I.C., Hermine, O., King, P.H., Si, Y., Kwon, Y., et al. (2019). CD34 identifies a subset of proliferating microglial cells associated with degenerating motor neurons in ALS. Int. J. Mol. Sci. *20*.

Kreutzberg, G.W. (1996). Microglia: A sensor for pathological events in the CNS. Trends Neurosci. *19*, 312–318.

Lance, J.W. (1980). The control of muscle tone , reflexes , and movernenk Robert Wartenbeg Lecture.

LARSSON, L., MÜLLER, U., LI, X., and SCHIAFFINO, S. (1995). Thyroid hormone regulation of myosin heavy chain isoform composition in young and old rats, with special reference to IIX myosin. Acta Physiol. Scand. *153*, 109–116.

Lee, C.-W., Rivera, R., Gardell, S., Dubin, A.E., and Chun, J. (2006). GPR92 as a new G12/13- and Gq-coupled lysophosphatidic acid receptor that increases cAMP, LPA5. J. Biol. Chem. *281*, 23589–23597.

Lepore, A.C., Rauck, B., Dejea, C., Pardo, A.C., Rao, M.S., Rothstein, J.D., and Maragakis, N.J. (2008). Focal transplantation–based astrocyte replacement is neuroprotective in a model of motor neuron disease. Nat. Neurosci. *11*, 1294–1301.

Li, J. (2018). Muscle Atrophy.

Liang, X.-H., Sun, H., Nichols, J.G., and Crooke, S.T. (2017). RNase H1-Dependent Antisense Oligonucleotides Are Robustly Active in Directing RNA Cleavage in Both the Cytoplasm and the Nucleus. Mol. Ther. *25*, 2075–2092.

Liddell, E.G.T., and Sherrington, C.S. (1925). Recruitment and some other Features of Reflex Inhibition. Proc. R. Soc. B Biol. Sci. *97*, 488–518.

Lino, M.M., Schneider, C., and Caroni, P. (2002). Accumulation of SOD1 mutants in postnatal motoneurons does not cause motoneuron pathology or motoneuron disease. J. Neurosci. *22*, 4825–4832.

Linse, K., Aust, E., Joos, M., and Hermann, A. (2018). Communication Matters-Pitfalls and Promise of Hightech Communication Devices in Palliative Care of Severely Physically Disabled Patients With Amyotrophic Lateral Sclerosis. Front. Neurol. *9*, 603.

Liu, J., and Wang, F. (2017). Role of neuroinflammation in amyotrophic lateral sclerosis: Cellular mechanisms and therapeutic implications. Front. Immunol. *8*, 1–12.

Liu, H.N., Tjostheim, S., da Silva, K., Taylor, D., Zhao, B., Rakhit, R., Brown, M., Chakrabartty, A., McLaurin, J., and Robertson, J. (2012). Targeting of monomer/misfolded SOD1 as a therapeutic strategy for amyotrophic lateral sclerosis. J. Neurosci. *32*, 8791–8799.

Loeffler, J.P., Picchiarelli, G., Dupuis, L., and Gonzalez De Aguilar, J.L. (2016). The role of skeletal muscle in amyotrophic lateral sclerosis. In Brain Pathology, (Blackwell Publishing Ltd), pp. 227–236.

Logroscino, G., Traynor, B.J., Hardiman, O., Chio, A., Mitchell, D., Swingler, R.J., Millul, A., Benn, E., and Beghi, E. (2010). Incidence of amyotrophic lateral sclerosis in Europe. J. Neurol. Neurosurg. Psychiatry *81*, 385–390.

López-Serrano, C., Santos-Nogueira, E., Francos-Quijorna, I., Coll-Miró, M., Chun, J., and López-Vales, R. (2019). Lysophosphatidic acid receptor type 2 activation contributes to secondary damage after spinal cord injury in mice. Brain. Behav. Immun.

Lutz, C. (2018). Mouse models of ALS: Past, present and future. Brain Res. *1693*, 1–10.

Ma, J., Smith, B.P., Smith, T.L., Walker, F.O., Rosencrance, E. V., and Koman, L.A. (2002). Juvenile and adult rat neuromuscular junctions: Density, distribution, and morphology. Muscle Nerve *26*, 804–809.

Ma, L., Nagai, J., and Ueda, H. (2010). Microglial activation mediates de novo lysophosphatidic acid production in a model of neuropathic pain. J. Neurochem. *115*, 643–653.

Mancuso, R., and Navarro, X. (2015). Amyotrophic lateral sclerosis: Current perspectives from basic research to the clinic. Prog. Neurobiol. *133*, 1–26.

Mancuso, R., Osta, R., and Navarro, X. (2014a). Presymptomatic electrophysiological tests predict clinical onset and survival in SOD1 ^{G93A} ALS

mice. Muscle Nerve *50*, 943–949.

Mancuso, R., del Valle, J., Modol, L., Martinez, A., Granado-Serrano, A.B., Ramirez-Núñez, O., Pallás, M., Portero-Otin, M., Osta, R., and Navarro, X. (2014b). Resveratrol Improves Motoneuron Function and Extends Survival in SOD1G93A ALS Mice. Neurotherapeutics *11*, 419–432.

Mantovani, S., Garbelli, S., Pasini, A., Alimonti, D., Perotti, C., Melazzini, M., Bendotti, C., and Mora, G. (2009). Immune system alterations in sporadic amyotrophic lateral sclerosis patients suggest an ongoing neuroinflammatory process. J. Neuroimmunol. *210*, 73–79.

Marcuzzo, S., Zucca, I., Mastropietro, A., de Rosbo, N.K., Cavalcante, P., Tartari, S., Bonanno, S., Preite, L., Mantegazza, R., and Bernasconi, P. (2011). Hind limb muscle atrophy precedes cerebral neuronal degeneration in G93A-SOD1 mouse model of amyotrophic lateral sclerosis: A longitudinal MRI study. Exp. Neurol. *231*, 30–37.

Marin, B., Boumé diene, F., Logroscino, G., Couratier, P., Babron, M.C., Leutenegger, A.L., Copetti, M., Preux, P.M., and Beghi, E. (2017). Variation in world wide incidence of amyotrophic lateral sclerosis: A meta-analysis. Int. J. Epidemiol. *46*, 57–74.

Marshall, E. (1999). Gene therapy death prompts review of adenovirus vector. Science (80-.). *286*, 2244–2245.

Martínez-Muriana, A., Mancuso, R., Francos-Quijorna, I., Olmos-Alonso, A., Osta, R., Perry, V.H., Navarro, X., Gomez-Nicola, D., and López-Vales, R. (2016). CSF1R blockade slows the progression of amyotrophic lateral sclerosis by reducing microgliosis and invasion of macrophages into peripheral nerves. Sci. Rep. *6*, 25663.

Mathis, S., Couratier, P., Julian, A., Vallat, J.M., Corcia, P., and Le Masson, G. (2017). Management and therapeutic perspectives in amyotrophic lateral sclerosis. Expert Rev. Neurother. *17*, 263–276.

McCampbell, A., Cole, T., Wegener, A.J., Tomassy, G.S., Setnicka, A., Farley, B.J., Schoch, K.M., Hoye, M.L., Shabsovich, M., Sun, L., et al. (2018). Antisense oligonucleotides extend survival and reverse decrement in muscle response in ALS models. J. Clin. Invest. *128*, 3558–3567.

Meininger, V., Drory, V.E., Leigh, P.N., Ludolph, A., Robberecht, W., and Silani, V. (2009). Glatiramer acetate has no impact on disease progression in ALS at 40 mg/day: a double- blind, randomized, multicentre, placebo-controlled trial. Amyotroph. Lateral Scler. *10*, 378–383.

Michaelson, N., Facciponte, D., Bradley, W., and Stommel, E. (2017). Cytokine expression levels in ALS: A potential link between inflammation and BMAA-triggered protein misfolding. Cytokine Growth Factor Rev. *37*, 81–88.

Miller, C.M., Donner, A.J., Blank, E.E., Egger, A.W., Kellar, B.M., Østergaard, M.E., Seth, P.P., and Harris, E.N. (2016). Stabilin-1 and Stabilin-2 are specific receptors for the cellular internalization of phosphorothioate-modified antisense oligonucleotides (ASOs) in the liver. Nucleic Acids Res. *44*, 2782–2794.

Miller, T.M., Smith, R.A., Kordasiewicz, H., and Kaspar, B.K. (2008). Gene-targeted therapies for the central nervous system. Arch. Neurol. *65*, 447–451.

Miller, T.M., Pestronk, A., David, W., Rothstein, J., Simpson, E., Appel, S.H., Andres, P.L., Mahoney, K., Allred, P., Alexander, K., et al. (2013a). An antisense oligonucleotide against SOD1 delivered intrathecally for patients with SOD1 familial amyotrophic lateral sclerosis: A phase 1, randomised, first-in-man study. Lancet Neurol. *12*, 435–442.

Miller, T.M., Pestronk, A., David, W., Rothstein, J., Simpson, E., Appel, S.H., Andres, P.L., Mahoney, K., Allred, P., Alexander, K., et al. (2013b). An antisense oligonucleotide against SOD1 delivered intrathecally for patients with SOD1 familial amyotrophic lateral sclerosis: a phase 1, randomised, first-in-man study. Lancet. Neurol. *12*, 435–442.

Moloney, E.B., de Winter, F., and Verhaagen, J. (2014). ALS as a distal axonopathy: molecular mechanisms affecting neuromuscular junction stability in the presymptomatic stages of the disease. Front. Neurosci. *8*, 252.

Monias, B.P., Johnston, J.F., Eckers, D.J., Zounesn, M.A., and Freierq, S.M. (1992). Selective Inhibition of Mutant Ha-ras mRNA expression by antisense oligonucleotides. J. Biol. Chem. *267*, 1–9.

Münch, C., O'Brien, J., and Bertolotti, A. (2011). Prion-like propagation of mutant superoxide dismutase-1 misfolding in neuronal cells. Proc. Natl. Acad. Sci. U. S. A. *108*, 3548–3553.

Neumann, M., Sampathu, D.M., Kwong, L.K., Truax, A.C., Micsenyi, M.C., Chou, T.T., Bruce, J., Schuck, T., Grossman, M., Clark, C.M., et al. (2006). Ubiquitinated TDP-43 in frontotemporal lobar degeneration and amyotrophic lateral sclerosis. Science *314*, 130–133.

Newcombe, E.A., Camats-Perna, J., Silva, M.L., Valmas, N., Huat, T.J., and Medeiros, R. (2018). Inflammation: The link between comorbidities, genetics, and Alzheimer's disease 11 Medical and Health Sciences 1109 Neurosciences 11 Medical and Health Sciences 1107 Immunology. J. Neuroinflammation *15*.

Nishizawa, T., Yamashia, S., McGrath, K.F., Tamaki, H., Kasuga, N., and Takekura, H. (2006). Plasticity of neuromuscular junction architectures in rat slow and fast muscle fibers following temporary denervation and reinnervation processes. J. Muscle Res. Cell Motil. *27*, 607–615.

Noguchi, K., Ishii, S., and Shimizu, T. (2003). Identification of p2y9/GPR23 as a novel G protein-coupled receptor for lysophosphatidic acid, structurally distant from the Edg family. J. Biol. Chem. *278*, 25600–25606.

Noguchi, K., Herr, D., Mutoh, T., and Chun, J. (2009). Lysophosphatidic acid (LPA) and its receptors. Curr. Opin. Pharmacol. *9*, 15–23.

Nunes, F.M.F., Aleixo, A.C., Barchuk, A.R., Bomtorin, A.D., Grozinger, C.M., and Simões, Z.L.P. (2013). Non-target effects of green fluorescent protein (GFP)-derived double-stranded RNA (dsRNA-GFP) used in honey bee RNA interference (RNAi) assays. Insects *4*, 90–103.

Oakes, S.A., and Papa, F.R. (2015). The role of endoplasmic reticulum stress in

human pathology. Annu. Rev. Pathol. *10*, 173–194.

Oberstadt, M., Claßen, J., Arendt, T., and Holzer, M. (2018). TDP-43 and Cytoskeletal Proteins in ALS. Mol. Neurobiol. *55*, 3143–3151.

Onesti, E., Schettino, I., Gori, M.C., Frasca, V., Ceccanti, M., Cambieri, C., Ruoppolo, G., and Inghilleri, M. (2017). Dysphagia in Amyotrophic Lateral Sclerosis: Impact on Patient Behavior, Diet Adaptation, and Riluzole Management. Front. Neurol. *8*.

El Oussini, H., Scekic-Zahirovic, J., Vercruysse, P., Marques, C., Dirrig-Grosch, S., Dieterlé, S., Picchiarelli, G., Sinniger, J., Rouaux, C., and Dupuis, L. (2017). Degeneration of serotonin neurons triggers spasticity in amyotrophic lateral sclerosis. Ann. Neurol. *82*, 444–456.

Paganoni, S., Macklin, E.A., Lee, A., Murphy, A., Chang, J., Zipf, A., Cudkowicz, M., and Atassi, N. (2014). Diagnostic timelines and delays in diagnosing amyotrophic lateral sclerosis (ALS). Amyotroph. Lateral Scler. Front. Degener. *15*, 453–456.

Park, S.B., Kiernan, M.C., and Vucic, S. (2017). Axonal Excitability in Amyotrophic Lateral Sclerosis. Neurotherapeutics *14*, 78–90.

Pasinelli, P., Belford, M.E., Lennon, N., Bacskai, B.J., Hyman, B.T., Trotti, D., and Brown, R.H. (2004). Amyotrophic lateral sclerosis-associated SOD1 mutant proteins bind and aggregate with Bcl-2 in spinal cord mitochondria. Neuron *43*, 19–30.

Patel, P., Kriz, J., Gravel, M., Soucy, G., Bareil, C., Gravel, C., and Julien, J.-P. (2014). Adeno-associated virus-mediated delivery of a recombinant single-chain antibody against misfolded superoxide dismutase for treatment of amyotrophic lateral sclerosis. Mol. Ther. *22*, 498–510.

Paterson, D.S., and Darnall, R. (2009). 5-HT2A receptors are concentrated in regions of the human infant medulla involved in respiratory and autonomic control. Auton. Neurosci. *147*, 48–55.

Perretti, M., Leroy, X., Bland, E.J., and Montero-Melendez, T. (2015). Resolution Pharmacology: Opportunities for Therapeutic Innovation in Inflammation. Trends Pharmacol. Sci. *36*, 737–755.

Perrin, F.E., Gerber, Y.N., Teigell, M., Lonjon, N., Boniface, G., Bauchet, L., Rodriguez, J.J., Hugnot, J.P., and Privat, A.M. (2011). Anatomical study of serotonergic innervation and 5-HT(1A) receptor in the human spinal cord. Cell Death Dis. *2*, e218.

Petrov, D., Mansfield, C., Moussy, A., and Hermine, O. (2017). ALS clinical trials review: 20 years of failure. Are we any closer to registering a new treatment? Front. Aging Neurosci. *9*.

Philips, T., and Robberecht, W. (2011). Neuroinflammation in amyotrophic lateral sclerosis: Role of glial activation in motor neuron disease. Lancet Neurol. *10*, 253–263.

Pickles, S., Semmler, S., Broom, H.R., Destroismaisons, L., Legroux, L., Arbour, N., Meiering, E., Cashman, N.R., and Vande Velde, C. (2016). ALS-linked

misfolded SOD1 species have divergent impacts on mitochondria. Acta Neuropathol. Commun. *4*, 43.

Plastira, I., Bernhart, E., Goeritzer, M., DeVaney, T., Reicher, H., Hammer, A., Lohberger, B., Wintersperger, A., Zucol, B., Graier, W.F., et al. (2017). Lysophosphatidic acid via LPA-receptor 5/protein kinase D-dependent pathways induces a motile and pro-inflammatory microglial phenotype. J. Neuroinflammation *14*, 253.

Prakash, T.P., Graham, M.J., Yu, J., Carty, R., Low, A., Chappell, A., Schmidt, K., Zhao, C., Aghajan, M., Murray, H.F., et al. (2014). Targeted delivery of antisense oligonucleotides to hepatocytes using triantennary N-acetyl galactosamine improves potency 10-fold in mice. Nucleic Acids Res. *42*, 8796–8807.

Radák, Z. (2018). The physiology of physical training.

Ransohoff, R.M. (2016). How neuroinflammation contributes to neurodegeneration. Science (80-.). *353*, 777–783.

Ratovitski, T., Corson, L.B., Strain, J., Wong, P., Cleveland, D.W., Culotta, V.C., and Borchelt, D.R. (1999). Variation in the biochemical/biophysical properties of mutant superoxide dismutase 1 enzymes and the rate of disease progression in familial amyotrophic lateral sclerosis kindreds. Hum. Mol. Genet. *8*, 1451–1460.

Ravits, J.M., and La Spada, A.R. (2009). Als motor phenotype heterogeneity, focality, and spread: Deconstructing motor neuron degenerationsymbol. Neurology *73*, 805.

Reaume, A.G., Elliott, J.L., Hoffman, E.K., Kowa, N.W., Ferrante, R.J., Siwek, D.F., Wilcox, H.M., Flood, D.G., Beal, M.F., Jr, R.H.B., et al. (1996). Motor neurons in Cu/Zn superoxide dismutase-deficient mice develope normally but exhibit enhanced cell death after axonal injury. Nat. Genet. *13*, 43–47.

Rexed, B. (1952). The cytoarchitectonic organization of the spinal cord in the cat. J. Comp. Neurol. *96*, 414–495.

Rigo, F., Chun, S.J., Norris, D.A., Hung, G., Lee, S., Matson, J., Fey, R.A., Gaus, H., Hua, Y., Grundy, J.S., et al. (2014). Pharmacology of a central nervous system delivered 2'-O-methoxyethyl-modified survival of motor neuron splicing oligonucleotide in mice and nonhuman primates. J. Pharmacol. Exp. Ther. *350*, 46–55.

Rizzo, F., Riboldi, G., Salani, S., Nizzardo, M., Simone, C., Corti, S., and Hedlund, E. (2014). Cellular therapy to target neuroinflammation in amyotrophic lateral sclerosis. Cell. Mol. Life Sci. *71*, 999–1015.

Robberecht, W., Sapp, P., Viaene, M.K., Rosen, D., McKenna-Yasek, D., Haines, J., Horvitz, R., Theys, P., and Brown, R. (1994). Rapid Communication: Cu/Zn Superoxide Dismutase Activity in Familial and Sporadic Amyotrophic Lateral Sclerosis. J. Neurochem. *62*, 384–387.

Roberts, K., Zeineddine, R., Corcoran, L., Li, W., Campbell, I.L., and Yerbury, J.J. (2013). Extracellular aggregated Cu/Zn superoxide dismutase activates microglia to give a cytotoxic phenotype. Glia *61*, 409–419.

Rodríguez de Rivera, F.J., Oreja Guevara, C., Sanz Gallego, I., San José Valiente, B., Santiago Recuerda, A., Gómez Mendieta, M.A., Arpa, J., and Díez Tejedor, E. (2011). Evolución de pacientes con esclerosis lateral amiotrófica atendidos en una unidad multidisciplinar. Neurologia *26*, 455–460.

Roman, W., and Gomes, E.R. (2018). Nuclear positioning in skeletal muscle. Semin. Cell Dev. Biol. *82*, 51–56.

Rosen, D.R., Siddique, T., Patterson, D., Figlewicz, D.A., Sapp, P., Hentati, A., Donaldson, D., Goto, J., O'Regan, J.P., Deng, H.-X., et al. (1993a). Mutations in Cu/Zn superoxide dismutase gene are associated with familial amyotrophic lateral sclerosis. Nature *362*, 59–62.

Rosen, D.R., Siddique, T., Patterson, D., Figlewicz, D.A., Sapp, P., Hentati, A., Donaldson, D., Goto, J., O'Regan, J.P., Deng, H.-X., et al. (1993b). Mutations in Cu/Zn superoxide dismutase gene are associated with familial amyotrophic lateral sclerosis. Nature *362*, 59–62.

Ross, C.A., and Poirier, M.A. (2004). Protein aggregation and neurodegenerative disease. Nat. Med. *10 Suppl*, S10-7.

Rothstein, J.D., Van Kammen, M., Levey, A.I., Martin, L.J., and Kuncl, R.W. (1995). Selective loss of glial glutamate transporter GLT-1 in amyotrophic lateral sclerosis. Ann. Neurol. *38*, 73–84.

Rotunno, M.S., and Bosco, D.A. (2013). An emerging role for misfolded wild-type SOD1 in sporadic ALS pathogenesis. Front. Cell. Neurosci. *7*, 253.

Salameh, J.S., Brown, R.H., and Berry, J.D. (2015). Amyotrophic Lateral Sclerosi: Review. Semin Neurol *35*, 469–476.

Salloway, S., Sperling, R., Gilman, S., Fox, N.C., Blennow, K., Raskind, M., Sabbagh, M., Honig, L.S., Doody, R., Van Dyck, C.H., et al. (2009). A phase 2 multiple ascending dose trial of bapineuzumab in mild to moderate Alzheimer disease. Neurology *73*, 2061–2070.

Sano, T., Baker, D., Virag, T., Wada, A., Yatomi, Y., Kobayashi, T., Igarashi, Y., and Tigyi, G. (2002). Multiple mechanisms linked to platelet activation result in lysophosphatidic acid and sphingosine 1-phosphate generation in blood. J. Biol. Chem. *277*, 21197–21206.

Santos-Nogueira, E., López-Serrano, C., Hernández, J., Lago, N., Astudillo, A.M., Balsinde, J., Estivill-Torrús, G., de Fonseca, F.R., Chun, J., and López-Vales, R. (2015a). Activation of lysophosphatidic acid receptor type 1 contributes to pathophysiology of spinal cord injury. J. Neurosci. *35*, 10224–102035.

Santos-Nogueira, E., Lopez-Serrano, C., Hernandez, J., Lago, N., Astudillo, A.M., Balsinde, J., Estivill-Torrus, G., de Fonseca, F.R., Chun, J., and Lopez-Vales, R. (2015b). Activation of Lysophosphatidic Acid Receptor Type 1 Contributes to Pathophysiology of Spinal Cord Injury. J. Neurosci. *35*, 10224–10235.

Saxena, S., Cabuy, E., and Caroni, P. (2009). A role for motoneuron subtype–selective ER stress in disease manifestations of FALS mice. Nat. Neurosci. *12*, 627–636.

Scaggiante, B., Dapas, B., Farra, R., Grassi, M., Pozzato, G., Giansante, C., and Grassi, G. (2011). Improving siRNA Bio-Distribution and Minimizing Side Effects. Curr. Drug Metab. *12*, 11–23.

Schiaffino, S., and Reggiani, C. (2011). Fiber Types in Mammalian Skeletal Muscles. Physiol. Rev. *91*, 1447–1531.

Schiaffino, S., Gorza, L., Sartore, S., Saggin, L., Ausoni, S., Vianello, M., Gundersen, K., and LØmo, T. (1989). Three myosin heavy chain isoforms in type 2 skeletal muscle fibres. J. Muscle Res. Cell Motil. *10*, 197–205.

Schmidt, M.L., Carden, M.J., Lee, V.M., and Trojanowski, J.Q. (1987). Phosphate dependent and independent neurofilament epitopes in the axonal swellings of patients with motor neuron disease and controls. Lab. Invest. *56*, 282–294.

Schmitz, K., Brunkhorst, R., de Bruin, N., Mayer, C.A., Häussler, A., Ferreiros, N., Schiffmann, S., Parnham, M.J., Tunaru, S., Chun, J., et al. (2017). Dysregulation of lysophosphatidic acids in multiple sclerosis and autoimmune encephalomyelitis. Acta Neuropathol. Commun. *5*, 42.

Schnell, M.A., Zhang, Y., Tazelaar, J., Gao, G.P., Yu, Q.C., Qian, R., Chen, S.J., Varnavski, A.N., LeClair, C., Raper, S.E., et al. (2001). Activation of innate immunity in nonhuman primates following intraportal administration of adenoviral vectors. Mol. Ther. *3*, 708–722.

Schoch, K.M., and Miller, T.M. (2017). Antisense Oligonucleotides: Translation from Mouse Models to Human Neurodegenerative Diseases. Neuron *94*, 1056–1070.

Shaw, B.F., and Valentine, J.S. (2007). How do ALS-associated mutations in superoxide dismutase 1 promote aggregation of the protein? Trends Biochem. Sci. *32*, 78–85.

Shefner, J.M., Cudkowicz, M., and Brown, R.H. (2006). Motor unit number estimation predicts disease onset and survival in a transgenic mouse model of amyotrophic lateral sclerosis. Muscle Nerve *34*, 603–607.

Shibata, N., Hirano, A., Kobayashi, M., Sasaki, S., Takeo, K., Matsumoto, S., Shiozawa, Z., Komori, T., Ikemoto, A., Umahara, T., et al. (1994). CuZn superoxide dismutase-like immunoreactivity in Lewy body-like inclusions of sporadic amyotrophic lateral sclerosis. Neurosci. Lett. *179*, 149–152.

Sibilla, C., and Bertolotti, A. (2017). Prion properties of SOD1 in amyotrophic lateral sclerosis and potential therapy. Cold Spring Harb. Perspect. Biol. *9*.

Sieck, G.C., Fournier, M., Prakash, Y.S., and Blanco, C.E. (2017). Myosin phenotype and SDH enzyme variability among motor unit fibers. J. Appl. Physiol. *80*, 2179–2189.

Singh, S., and Joshi, N. (2017). Astrocytes: inexplicable cells in neurodegeneration. Int. J. Neurosci. *127*, 204–209.

Siu, L.T., and Gordon, T. (2003). Mechanisms controlling axonal sprouting at the neuromuscular junction. J. Neurocytol. *32*, 961–974.

Smith, B.N., Ticozzi, N., Fallini, C., Gkazi, A.S., Topp, S., Kenna, K.P., Scotter,

E.L., Kost, J., Keagle, P., Miller, J.W., et al. (2014). Exome-wide rare variant analysis identifies TUBA4A mutations associated with familial ALS. Neuron *84*, 324–331.

Smith, E.F., Shaw, P.J., and De Vos, K.J. (2017). The role of mitochondria in amyotrophic lateral sclerosis. Neurosci. Lett. 132933.

Smith, R.A., Miller, T.M., Yamanaka, K., Monia, B.P., Condon, T.P., Hung, G., Lobsiger, C.S., Ward, C.M., McAlonis-Downes, M., Wei, H., et al. (2006). Antisense oligonucleotide therapy for neurodegenerative disease. J. Clin. Invest. *116*, 2290–2296.

Solomon, J.N., Lewis, C.-A.B., Ajami, B., Corbel, S.Y., Rossi, F.M. V, and Krieger, C. (2006). Origin and distribution of bone marrow-derived cells in the central nervous system in a mouse model of amyotrophic lateral sclerosis. Glia *53*, 744–753.

Sorensen, S.D., Nicole, O., Peavy, R.D., Montoya, L.M., Lee, C.J., Murphy, T.J., Traynelis, S.F., and Hepler, J.R. (2003). Common signaling pathways link activation of murine PAR-1, LPA, and S1P receptors to proliferation of astrocytes. Mol. Pharmacol. *64*, 1199–1209.

Spreux-Varoquaux, O., Bensimon, G., Lacomblez, L., Salachas, F., Pradat, P.F., Le Forestier, N., Marouan, A., Dib, M., and Meininger, V. (2002). Glutamate levels in cerebrospinal fluid in amyotrophic lateral sclerosis: a reappraisal using a new HPLC method with coulometric detection in a large cohort of patients. J. Neurol. Sci. *193*, 73–78.

Stein, C.A., and Castanotto, D. (2017). FDA-Approved Oligonucleotide Therapies in 2017. Mol. Ther. *25*, 1069–1075.

Stephens, H.E., Joyce, N.C., and Oskarsson, B. (2017). National Study of Muscle Cramps in ALS in the USA. Amyotroph. Lateral Scler. Frontotemporal Degener. *18*, 32–36.

Sterling, L.E., Jawaid, A., Salamone, A.R., Murthy, S.B., Mosnik, D.M., McDowell, E., Wheaton, M., Strutt, A.M., Simpson, E., Appel, S., et al. (2010). Association between dysarthria and cognitive impairment in ALS: A prospective study. Amyotroph. Lateral Scler. *11*, 46–51.

Sugiura, T., Nakane, S., Kishimoto, S., Waku, K., Yoshioka, Y., and Tokumura, A. (2002). Lysophosphatidic acid, a growth factor-like lipid, in the saliva. J. Lipid Res. *43*, 2049–2055.

Tabuchi, S., Kume, K., Aihara, M., and Shimizu, T. (2000). Expression of lysophosphatidic acid receptor in rat astrocytes: mitogenic effect and expression of neurotrophic genes. Neurochem. Res. *25*, 573–582.

Talbott, E.O., Malek, A.M., and Lacomis, D. (2016). The epidemiology of amyotrophic lateral sclerosis. In Handbook of Clinical Neurology, pp. 225–238.

Tashiro, Y., Urushitani, M., Inoue, H., Koike, M., Uchiyama, Y., Komatsu, M., Tanaka, K., Yamazaki, M., Abe, M., Misawa, H., et al. (2012). Motor neuron-specific disruption of proteasomes, but not autophagy, replicates amyotrophic lateral sclerosis. J. Biol. Chem. *287*, 42984–42994.

Tateno, M., Kato, S., Sakurai, T., Nukina, N., Takahashi, R., and Araki, T. (2009). Mutant SOD1 impairs axonal transport of choline acetyltransferase and acetylcholine release by sequestering KAP3. Hum. Mol. Genet. *18*, 942–955.

Taylor, J.P., Brown, R.H., Cleveland, D.W., and Cleveland, D.W. (2016). Decoding ALS: from genes to mechanism. Nature *539*, 197–206.

Thakore, N.J., and Pioro, E.P. (2016). Depression in ALS in a large self-reporting cohort. Neurology *86*, 1031–1038.

Thomas, C.E., Ehrhardt, A., and Kay, M.A. (2003). Progress and problems with the use of viral vectors for gene therapy. Nat. Rev. Genet. *4*, 346–358.

Todd, A.J. (2010). Neuronal circuitry for pain processing in the dorsal horn. Nat. Rev. Neurosci. *11*, 823–836.

Trias, E., King, P.H., Si, Y., Kwon, Y., Varela, V., Ibarburu, S., Kovacs, M., Moura, I.C., Beckman, J.S., Hermine, O., et al. (2018). Mast cells and neutrophils mediate peripheral motor pathway degeneration in ALS. JCI Insight *3*.

Trias, E., Kovacs, M., King, P.H., Si, Y., Kwon, Y., Varela, V., Ibarburu, S., Moura, I.C., Hermine, O., Beckman, J.S., et al. (2019). Schwann cells orchestrate peripheral nerve inflammation through the expression of CSF1, IL-34, and SCF in amyotrophic lateral sclerosis. Glia glia.23768.

Trompetto, C., Marinelli, L., Mori, L., Pelosin, E., Currà, A., Molfetta, L., and Abbruzzese, G. (2014). Pathophysiology of spasticity: implications for neurorehabilitation. Biomed Res. Int. *2014*, 354906.

Turner, B.J., and Talbot, K. (2008). Transgenics, toxicity and therapeutics in rodent models of mutant SOD1-mediated familial ALS. Prog. Neurobiol. *85*, 94–134.

Turner, M.R., Cagnin, A., Turkheimer, F.E., Miller, C.C.J., Shaw, C.E., Brooks, D.J., Leigh, P.N., and Banati, R.B. (2004). Evidence of widespread cerebral microglial activation in amyotrophic lateral sclerosis: an [11C](R)-PK11195 positron emission tomography study. Neurobiol. Dis. *15*, 601–609.

Urushitani, M., Ezzi, S.A., and Julien, J.P. (2007). Therapeutic effects of immunization with mutant superoxide dismutase in mice models of amyotrophic lateral sclerosis. Proc. Natl. Acad. Sci. U. S. A. *104*, 2495–2500.

Valdés-Rives, S.A., and González-Arenas, A. (2017). Autotaxin-Lysophosphatidic Acid: From Inflammation to Cancer Development. Mediators Inflamm. *2017*.

Valera, E., and Masliah, E. (2013). Immunotherapy for neurodegenerative diseases: Focus on α- synucleinopathies. Pharmacol. Ther. *138*, 311–322.

Vance, C., Scotter, E.L., Nishimura, A.L., Troakes, C., Mitchell, J.C., Kathe, C., Urwin, H., Manser, C., Miller, C.C., Hortobágyi, T., et al. (2013). ALS mutant FUS disrupts nuclear localization and sequesters wild-type FUS within cytoplasmic stress granules. Hum. Mol. Genet. *22*, 2676–2688.

De Virgilio, A., Greco, A., Fabbrini, G., Inghilleri, M., Rizzo, M.I., Gallo, A., Conte, M., Rosato, C., Ciniglio Appiani, M., and de Vincentiis, M. (2016). Parkinson's

disease: Autoimmunity and neuroinflammation. Autoimmun. Rev. *15*, 1005–1011.

De Vos, K.J., Chapman, A.L., Tennant, M.E., Manser, C., Tudor, E.L., Lau, K.-F., Brownlees, J., Ackerley, S., Shaw, P.J., McLoughlin, D.M., et al. (2007). Familial amyotrophic lateral sclerosis-linked SOD1 mutants perturb fast axonal transport to reduce axonal mitochondria content. Hum. Mol. Genet. *16*, 2720–2728.

Vucic, S., and Kiernan, M.C. (2006). Axonal excitability properties in amyotrophic lateral sclerosis. Clin. Neurophysiol. *117*, 1458–1466.

Walsh, M.J., Cooper-Knock, J., Dodd, J.E., Stopford, M.J., Mihaylov, S.R., Kirby, J., Shaw, P.J., and Hautbergue, G.M. (2015). Invited review: decoding the pathophysiological mechanisms that underlie RNA dysregulation in neurodegenerative disorders: a review of the current state of the art. Neuropathol. Appl. Neurobiol. *41*, 109–134.

Wang, J., Xu, G., Gonzales, V., Coonfield, M., Fromholt, D., Copeland, N.G., Jenkins, N.A., and Borchelt, D.R. (2002). Fibrillar inclusions and motor neuron degeneration in transgenic mice expressing superoxide dismutase 1 with a disrupted copper-binding site. Neurobiol. Dis. *10*, 128–138.

Wang, J., Farr, G.W., Zeiss, C.J., Rodriguez-Gil, D.J., Wilson, J.H., Furtak, K., Rutkowski, D.T., Kaufman, R.J., Ruse, C.I., Yates Iii, J.R., et al. (2009). Progressive aggregation despite chaperone associations of a mutant SOD1-YFP in transgenic mice that develop ALS.

Wang, L., Gutmann, D.H., and Roos, R.P. (2011). Astrocyte loss of mutant SOD1 delays ALS disease onset and progression in G85R transgenic mice. Hum. Mol. Genet. *20*, 286–293.

Wang, L., Popko, B., and Roos, R.P. (2014). An enhanced integrated stress response ameliorates mutant SOD1-induced ALS. Hum. Mol. Genet. *23*, 2629–2638.

Watson, C., Paxinos, G., and Kayalioglu, G. (2009). The spinal cord.

Weiner, J.A., Fukushima, N., Contos, J.J.A., Scherer, S.S., and Chun, J. (2001). Regulation of Schwann cell morphology and adhesion by receptor-mediated lysophosphatidic acid signaling. J. Neurosci. *21*, 7069–7078.

Wherry, J., and Masopust, D. (2016). Viral pathogenesis.

De Winter, F., Vo, T., Stam, F.J., Wisman, L.A.B., Bär, P.R., Niclou, S.P., van Muiswinkel, F.L., and Verhaagen, J. (2006). The expression of the chemorepellent Semaphorin 3A is selectively induced in terminal Schwann cells of a subset of neuromuscular synapses that display limited anatomical plasticity and enhanced vulnerability in motor neuron disease. Mol. Cell. Neurosci. *32*, 102–117.

Wirth, T., Parker, N., and Ylä-Herttuala, S. (2013). History of gene therapy. Gene *525*, 162–169.

Wong, M., and Martin, L.J. (2010). Skeletal muscle-restricted expression of human SOD1 causes motor neuron degeneration in transgenic mice. Hum. Mol. Genet. *19*, 2284–2302.

Wong, P.C., Pardo, C.A., Borchelt, D.R., Lee, M.K., Copeland, N.G., Jenkins, N.A., Sisodia, S.S., Cleveland, D.W., and Price, D.L. (1995). An adverse property of a familial ALS-linked SOD1 mutation causes motor neuron disease characterized by vacuolar degeneration of mitochondria. Neuron *14*, 1105–1116.

Wu, C.-H., Fallini, C., Ticozzi, N., Keagle, P.J., Sapp, P.C., Piotrowska, K., Lowe, P., Koppers, M., McKenna-Yasek, D., Baron, D.M., et al. (2012). Mutations in the profilin 1 gene cause familial amyotrophic lateral sclerosis. Nature *488*, 499–503.

Xiao, Q., Zhao, W., Beers, D.R., Yen, A.A., Xie, W., Henkel, J.S., and Appel, S.H. (2007). Mutant SOD1G93A microglia are more neurotoxic relative to wild-type microglia. J. Neurochem. *102*, 2008–2019.

Yamanaka, K., Lobsiger, C.S., Copeland, N.G., Jenkins, N.A., Kassiotis, G., Kollias, G., Cleveland, D.W., and Boillée, S. (2006). Onset and Progression in Inherited ALS Determined by Motor Neurons and Microglia. Sci. *312*, 1389–1392.

Yanagida, K., Masago, K., Nakanishi, H., Kihara, Y., Hamano, F., Tajima, Y., Taguchi, R., Shimizu, T., and Ishii, S. (2009). Identification and characterization of a novel lysophosphatidic acid receptor, p2y5/LPA6. J. Biol. Chem. *284*, 17731–17741.

Yoo, Y.-E., and Ko, C.-P. (2012). Dihydrotestosterone ameliorates degeneration in muscle, axons and motoneurons and improves motor function in amyotrophic lateral sclerosis model mice. PLoS One *7*, e37258.

Yung, Y.C., Stoddard, N.C., and Chun, J. (2014). LPA receptor signaling: pharmacology, physiology, and pathophysiology. J. Lipid Res. *55*, 1192–1214.

Zhang, Y., Chen, K., Sloan, S.A., Bennett, M.L., Scholze, A.R., O'Keeffe, S., Phatnani, H.P., Guarnieri, P., Caneda, C., Ruderisch, N., et al. (2014). An RNA-sequencing transcriptome and splicing database of glia, neurons, and vascular cells of the cerebral cortex. J. Neurosci. *34*, 11929–11947.

van Zundert, B., and Brown, R.H. (2017a). Silencing strategies for therapy of SOD1-mediated ALS. Neurosci. Lett. *636*, 32–39.

van Zundert, B., and Brown, R.H. (2017b). Silencing strategies for therapy of SOD1-mediated ALS. Neurosci. Lett. *636*, 32–39.